The spin-$\frac{1}{2}$ Heisenberg antiferromagnet on a square lattice and its application to the cuprous oxides

Efstratios Manousakis

Department of Physics and Center for Materials Research and Technology, Florida State University, Tallahassee, Florida 32306-4052

The spin-$\frac{1}{2}$ antiferromagnetic Heisenberg model on a square lattice is used to describe the dynamics of the spin degrees of freedom of undoped copper oxides. Even though the model lacks an exact solution, a solid, accurate, and rather conventional picture emerges from a number of techniques—analytical (spin-wave theory, Schwinger boson mean-field theory, renormalization-group calculations), semianalytical (variational theory, series expansions), and numerical (quantum Monte Carlo, exact diagonalization, etc.). At zero temperature, the effect of the zero-point fluctuations is not strong enough to destroy the antiferromagnetic long-range order, despite the fact that we are dealing with a low-spin low-dimensional system. The corrections to the spin-wave theory, which treats perturbatively the effect of such fluctuations around the classical Néel ground state, appear to be small. At any nonzero temperature the order disappears and the correlation length at low temperature $T(k_B T/J \ll 1$, where J is the antiferromagnetic coupling) follows the singular form $\xi(T)=C\exp(\alpha J/k_B T)$. In the long-wavelength limit and at low T, the model has the same behavior as the quantum nonlinear σ model in two spatial dimensions and one Euclidean time dimension, which we also study with available analytical and Monte Carlo techniques. The quasiparticles of the theory are bosons; at low T and for wavelengths shorter than the correlation length they are well-defined spin-wave excitations. The spectrum of such excitations and the temperature-dependent correlation length have been determined by neutron and Raman scattering experiments done on La_2CuO_4. The good agreement of the experimental data with the predictions of this theory suggests that the magnetic state of the undoped materials is the conventional ordered state. We discuss, within a simple mean-field theory, the effect of weak three-dimensional antiferromagnetic coupling and the role of an antisymmetric term, introduced to explain a hidden ferromagnetic behavior of the uniform susceptibility. We find that understanding the copper-oxide antiferromagnetic insulator is only the first essential step towards the development of a theory of the superconductor created upon doping such materials.

CONTENTS

I. Introduction 1
A. History of the problem and experimental facts 1
B. Statement of the problem 5
II. Calculations at Zero Temperature. Analytical Approaches 6
A. Spin-wave theory 6
B. Beyond spin-wave theory 9
1. Perturbation theory and loop expansion 9
2. Paired-magnon analysis 11
C. Series expansions 13
D. Analogy with Bose fluids 14
III. Calculations at Zero Temperature. Computational Approaches 16
A. Exact diagonalizations 16
B. World-line Monte Carlo simulations 16
C. Projection methods. Random walks 17
D. Importance sampling 18
E. Variational calculations 19
F. Results and comparison 21
1. Energy 21
2. Staggered magnetization 22
3. Excitation spectrum 23
IV. Calculations at Finite Temperatures. Analytical Approaches 24
A. Path-integral formulation. Schwinger boson representation 25
B. Modified spin-wave theory 27
C. Low-T solution and correlation functions 27
D. Path-integral formulation. Fermion representation 30
E. Path-integral formulation. Nonlinear σ model 32
F. Renormalization-group calculations 34
G. Saddle-point approximation for the quantum nonlinear σ model 37
V. Calculations at Finite Temperatures. Numerical Results 41
A. Quantum Monte Carlo calculations on the Heisenberg model 41
B. Comparison of the results on the Heisenberg model 42
C. High-temperature series expansion for the correlation length 45
D. Simulation of the quantum nonlinear σ model 45
VI. Damping of Spin Waves 49
VII. Comparison with Experiments 50
A. Can the isotropic 2D Heisenberg model describe La_2CuO_4? 50
B. Correlation length 52
C. Spin-wave excitations 53
D. Uniform susceptibility 54
E. Staggered magnetization 56
VIII. Conclusions 56
Acknowledgments 57
Appendix: Calculation of Traces in Handscomb's Monte Carlo Method 57
References 58

I. INTRODUCTION

A. History of the problem and experimental facts

The discovery of copper-oxide superconductors with critical temperatures as high as 120 K (Bednorz and Müller, 1986; Chu *et al.*, 1987; Maeda *et al.*, 1988; Sheng and Hermann, 1988; for references see Sleight *et al.*, 1989) raised hopes that one day we may be able to manufacture materials that superconduct at room temperature. This discovery also raised doubts about the common belief that, due to the nature of the phonon-

mediated electron-electron interaction (Bardeen, Cooper, and Schrieffer, 1957), there are upper bounds on the critical temperatures much lower than those achieved with the copper oxides. In addition, the lack of a significant isotope effect with substitution of the oxygen sites seems to rule out the possibility that the phonon Debye frequency is the characteristic energy scale entering in the fundamental equations. Because of a number of peculiar properties of these materials, there is a growing suspicion that a different mechanism may be responsible for their superconductivity. Their phase diagram is rich because the superconducting phase occurs near a metal-insulator transition, an antiferromagnetic as well as a structural instability, and this fact has generated many ideas and proposals for new mechanisms. It is natural to imagine that such high temperatures and pairing energy scales may arise as low-energy scales of the interacting electronic degrees of freedom in specific lattice structures of appropriate stoichiometry, where the lattice dynamics do not play the key role. Anderson's original suggestion (Anderson, 1987; Anderson *et al.*, 1987) that novel quantum spin fluctuations in the CuO_2 planes, common in all these materials, may be responsible for the superconductivity has received significant attention. Interesting magnetic properties revealed by neutron-scattering experiments provide further support for this idea. The $La_2CuO_{4\pm y}$ material has a susceptibility anomaly at a three-dimensional (3D) Néel temperature T_N that is sensitive to the value of y (Yamada *et al.*, 1987). Furthermore, the instantaneous two-dimensional (2D) antiferromagnetic correlations exceed 1000 Å for $T\sim 200$ K, with no average staggered magnetization (Shirane *et al.*, 1987; Endoh *et al.*., 1988). It was conjectured that such fluctuations might destroy the antiferromagnetic long-range order in the ground state, giving rise to a new state of the spin system, a quantum "spin-liquid" state (Anderson, 1987). The superconductivity in these materials was then conjectured to arise from the behavior of a novel quantum fluid created out of a highly correlated set of electronic degrees of freedom.

The Hubbard model, one of the simplest models to go beyond the independent electron approximation, was designed to study effects of electron correlations in such narrow-band systems and in Anderson-Mott insulators. Anderson argued that the appropriate model is the two-dimensional single-band Hubbard model in its strong on-site Coulomb repulsion limit. In this model the fermion creation operators create electrons at the outer $d_{x^2-y^2}$ orbital of the Cu atoms, which is hybridized in an antibonding symmetry with the p_x and p_y orbitals of the two oxygen atoms in the CuO_2 cell. This is valid if the atomic energy for the creation of an additional Cu hole is lower than the atomic energy for an additional O hole and if the energy difference is larger than the Coulomb repulsion U on the Cu site. Let us momentarily accept this assumption for pedagogical purposes. Standard strong-coupling perturbation treatment of the single-band Hubbard Hamiltonian produces the following effective Hamiltonian (Harris and Lange, 1967;[1] Brinkman and Rice, 1970):

$$H_{\rm eff}=H_1+H_2\ , \tag{1.1a}$$

$$H_1=-t\sum_{\langle i,j\rangle,\sigma}(c^\dagger_{i,\sigma}c_{j,\sigma}+\text{H.c.})\ , \tag{1.1b}$$

$$H_2=-\frac{J}{2}\sum_{\langle i,j\rangle,\sigma}(c^\dagger_{j,\sigma}c_{i,\sigma}n_{i,-\sigma}c^\dagger_{i,\sigma}c_{j,\sigma}+c^\dagger_{j,-\sigma}c_{i,-\sigma}c^\dagger_{i,\sigma}c_{j,\sigma})\ , \tag{1.1c}$$

where $n_{i,\sigma}=c^\dagger_{i\sigma}c_{i\sigma}$, t is the hopping matrix element, and $J=4t^2/U$. The first term (H_1) produces the constrained hole hopping which avoids double occupancy. The second term (H_2) is obtained from the Hubbard model by integrating out virtual processes in which the electron hops momentarily to a neighboring site occupied by an electron of opposite spin and then, in the final state, the two electrons return either to the original configuration or to one with spins exchanged. In this reduction scheme, a three-site interaction term emerges that, for simplicity, has not been included in the above expression; this paper deals with the undoped case in which both H_1 and the three-site interaction are inactive. At half-filling, H_2, apart from a constant, is equivalent to the spin-$\frac{1}{2}$ antiferromagnetic Heisenberg model on a square lattice with

$$H=J\sum_{\langle ij\rangle}\mathbf{S}_i\cdot\mathbf{S}_j\ . \tag{1.2}$$

The Heisenberg Hamiltonian (1.2) is assumed to describe the antiferromagnetic undoped insulator La_2CuO_4 or the oxygen-deficient YBa_2CuO_6 or other undoped copper-oxide materials. Doping the insulator La_2CuO_4 to create, for example, $La_{2-x}Sr_xCuO_4$ introduces holes on the CuO_2 planes. Increasing the oxygen content in the YBa_2CuO_{6+x} controls the electron filling factor of the 2D CuO_2 planes in a less obvious way because of the presence of the CuO chains. The doped CuO_2 planes in this rather simple formulation may be described by Eqs. (1.1) where holes are introduced. Ignoring the three-site interaction term, this effective Hamiltonian is now known as the *t-J* model.

The *t-J* Hamiltonian is an interesting model on its own, and its derivation from the single-band Hubbard model may serve as an illustration only. This model can be obtained in the strong-coupling limit from a more realistic model that takes into account the more detailed orbital structure of the CuO_2 cell even when the holes created by doping sit primarily on the oxygen sites (Zhang and Rice, 1988). In this case the Cu—O hybridization binds the added hole on each square of O atoms to the central

[1]See also Hirsch, 1985 and, for a simple derivation, Huang and Manousakis, 1987.

Cu^{2+} ion to form a local singlet. The motion of this hole from one CuO_2 unit cell to the next can be described by the effective Hamiltonian (1.1). More importantly, the spin-$\frac{1}{2}$ Heisenberg antiferromagnet on a square lattice, which is the subject of this paper, can be obtained under even more general assumptions. Furthermore, there are phenomenological reasons to believe that Eq. (1.2) is an appropriate model to describe the 2D spin fluctuations in the insulator and, when supplied with a hole-hopping term, could be an appropriate model to describe the doped materials. For example, the neutron- and Raman-scattering results from the undoped insulator La_2CuO_4 can be understood in terms of Eq. (1.2) as discussed in this paper. Furthermore, it has been argued (Mila and Rice, 1989; Millis *et al.*, 1990; Monien, Monthoux, and Pines, 1990; Monien, Pines, and Slichter, 1990; Monien, Pines, and Takigawa, 1990; Pines, 1990) that the results of NMR measurements (Walstedt *et al.*, 1988; Hammel *et al.*, 1989) are consistent with a single-component quantum fluid with an intimate coupling between charge and antiferromagnetically correlated spin degrees of freedom. In addition, it seems plausible that the *t-J* model may be the relevant reduction of the complex problem of copper oxides to a low-energy set of variables (see also Shastry, 1989). Pairing in the Hamiltonian (1.1) has been studied by several authors using mean-field theory (Baskaran, Zou, and Anderson, 1987; Ruckenstein, Hirschfeld, and Appel, 1987, Affleck, 1988; Kotliar, 1988), variational theory (Gros *et al.*, 1987; Gros, 1988; Yokoyama and Shiba, 1988) and exact diagonalization of finite-size systems (Kaxiras and Manousakis, 1988; Riera and Young, 1989). These studies indicate that pairing between holes in the model may be energetically favorable in a certain range of t/U. Motion of a single hole in the *t-J* model has also been studied by several authors using analytical (for example, Schmitt-Rink *et al.*, 1988; Shraiman and Siggia, 1988; Kane *et al.*, 1989) or numerical techniques (Dagotto *et al.*, 1990; Dagotto and Poilblanc, 1990).

The Hamiltonian (1.2) can be thought of as a simple and rather general model to describe the copper-copper superexchange antiferromagnetic interaction (Anderson, 1959) mediated by the intervening oxygen ions via virtual hopping processes involving doubly occupied Cu sites. The problem of quantum antiferromagnets is rather old and longstanding; however, a number of questions arose following the discovery of copper-oxide superconductors. The goals of this paper are to review calculations performed on the spin-$\frac{1}{2}$ quantum antiferromagnetic Heisenberg model (1.2), draw conclusions about its $T=0$ and low-temperature properties, and connect it with the phenomenology of the undoped antiferromagnetic insulator La_2CuO_4. We first review the properties of the model (Secs. II–VI) and then attempt to establish its relevance to the physics of the pure La_2CuO_4 and compare the calculated magnetic properties and excitations to those observed (Sec. VII).

The spin-wave theory was developed by Anderson (1952) and Kubo (1952) to study the ground state of antiferromagnets with large spin S. Spin-wave theory is an expansion in powers of $1/(zS)$, z being the coordination number, and it is based on two assumptions: (a) that antiferromagnetic long-range order exists in the ground state and (b) that the amplitude of quantum fluctuations about the classical Néel state is small. It is, therefore, natural to raise doubts about the convergence of this expansion for low-spin and low-dimensional (low-z) systems. Anderson (1973), for instance, conjectured that the ground state of the 2D spin-$\frac{1}{2}$ antiferromagnet, the lowest spin case, might be disordered and postulated the resonating valence bond state as a possible lowest-energy state. More recently, these questions received significant attention due to their relevance to the copper-oxide superconductors. Even though there is no exact theorem that proves it, we shall present significant evidence that strongly supports the hypothesis that the ground state of the spin-$\frac{1}{2}$ antiferromagnetic Heisenberg model on a square lattice is characterized by antiferromagnetic long-range order. The role of the zero-point quantum fluctuations is to reduce the value of the staggered magnetization from its classical value by about 40%.

The idea that the 2D spin-$\frac{1}{2}$ antiferromagnetic Heisenberg model may be relevant for the physics behind these materials is supported by a comparison of the correlation length $\xi(T)$ obtained from this model or the equivalent quantum nonlinear σ model with that inferred by neutron scattering experiments. Due to practical difficulties in creating large single crystals of $YBa_2Cu_3O_{7-x}$, systematic neutron studies have been performed only on the La_2CuO_4. The results of the numerical calculations are consistent with the neutron scattering data when a value of the antiferromagnetic coupling J is chosen $\simeq 1500$ K. This value is close to that estimated by high-energy neutron (Aeppli *et al.*, 1989) and Raman scattering experiments (Lyons *et al.*, 1988; Singh *et al.*, 1989b).

Chakravarty, Halperin, and Nelson (1988, 1989) used the renormalization-group approach to study the quantum nonlinear σ model in two spatial dimensions and one Euclidean time dimension (which is equivalent to the 2D antiferromagnetic Heisenberg model). They calculated the correlation length at low temperatures with the β function calculated in one- and two-loop order. Their one-loop calculation suggests that $\xi(T\rightarrow 0) = \lambda\hbar c/Te^{2\pi\rho_s/T}$ in the ordered phase; Chakravarty *et al.* show that in the renormalized classical regime, where the model maps to a 2D nonlinear σ model with a renormalized spin-stiffness constant, they can use the β function for the classical nonlinear σ model calculated up to two-loop order. This improved calculation suggests a different prefactor, namely, $\xi(T)=Ce^{2\pi\rho_s/T}$. Chakravarty *et al.* (1988, 1989) adjust the parameters (with values for the spin-wave velocity c and spin-stiffness constant ρ_s not far from those expected on microscopic grounds) and provide a good fit to the correlation length $\xi(T)$ obtained by neutron scattering experiments with both expressions.

The Schwinger boson mean-field theory of Arovas and Auerbach (1988) and Takahashi's calculation (1989) suggest the form calculated by Chakravarty *et al.* in one-loop order. Manousakis and Salvador (1988) have shown that the expression obtained in one-loop order does not fit the $\xi(T)$ calculated with quantum Monte Carlo simulations of the spin-$\frac{1}{2}$ antiferromagnetic Heisenberg model. The improved form, obtained in two-loop order by Chakravarty *et al.*, has been shown to agree with the results of the quantum Monte Carlo simulations of the spin-$\frac{1}{2}$ antiferromagnetic Heisenberg model on a square lattice (Gomez-Santos *et al.*, 1989; Manousakis and Salvador, 1989b, 1989c). Direct simulation of the quantum nonlinear σ model (Manousakis and Salvador, 1989b, 1989c) shows that the correlation length at low T and in the regime controlled by the ordered phase can be approximated by the form calculated by Chakravarty *et al.* in two-loop order, which also agrees with the $\xi(T)$ obtained from the quantum Monte Carlo study. Furthermore, the $\xi(T)$ agrees reasonably well with the neutron scattering data obtained on different single crystals of La_2CuO_4 using values of J close to that estimated by neutron and Raman scattering experiments. Therefore the undoped material La_2CuO_4 can be described by a spin-$\frac{1}{2}$ antiferromagnetic Heisenberg model on a square lattice whose behavior is controlled by the spin-wave excitations around a state characterized by long-range order.

The spin excitations have been observed by neutron-scattering (Shirane *et al.*, 1987; Endoh *et al.*, 1988; Aeppli *et al.*, 1989) and Raman-scattering experiments (Lyons *et al.*, 1987, 1988). At any nonzero temperature, the long-range order of the 2D Heisenberg model should be destroyed by thermal fluctuations (Mermin and Wagner, 1966). At low $T(k_BT/J \ll 1)$, where the correlation length $\xi(T)$ is exponentially large, the spin-wave excitations are well defined for wavelengths significantly smaller than $\xi(T)$. An appropriately extended spin-wave theory for low T (described in Sec. IV) can account for the observed peaks in the neutron scattering data within experimental resolution. These experiments determine the spin-wave velocity, from which an estimate for the antiferromagnetic coupling $J \simeq 1500$ K is found. High-frequency peaks (at about 3000 cm^{-1}) seen in the Raman scattering intensity can be explained as mainly two-magnon excitations from near the Brillouin-zone boundary and traveling with almost opposite momenta. With approximate corrections for magnon-magnon interaction effects, the value of J has also been estimated from these measurements. This value of J is in reasonable agreement with those found either from the correlation length or from neutron scattering.

The interplanar coupling J' is of the order of $10^{-5}J$ as estimated by Chakravarty, Halperin, and Nelson (1989). This small J' has a small effect on the 2D spin correlations above the 3D Néel ordering temperature. Furthermore, the zero-temperature properties calculated for an isolated CuO_2 plane are only weakly affected by such a small value of J'. Thio *et al.* (1988) have examined the role of possible Ising-like anisotropies, by considering different values for couplings J_x, J_y, J_z, i.e.,

$$H = \sum_{\langle ij \rangle} (J_x S_i^x S_j^x + J_y S_i^y S_j^y + J_z S_i^z S_j^z) , \tag{1.3}$$

and they found that such anisotropies are weak. Clearly, on-site Ising anisotropy of the form $\sum_i (S_i^z)^2$ plays no role for spin 1/2. They discovered, however, that an antisymmetric term is needed to explain hidden ferromagnetism manifesting itself below T_N; this ferromagnetism cants the spins away from the direction of the staggered magnetization (which lies in the $\hat{a}$-$\hat{c}$ plane, the copper-oxygen plane) towards the $\hat{b}$ axis (the axis perpendicular to the copper-oxygen plane) by a small angle. This term is also small compared to the antiferromagnetic coupling $J(|J^{bc}|/J \sim 10^{-3})$.

The first part of this paper (Secs. II–III) deals with results for the ground state of Eq. (1.2) obtained with several analytical, semianalytical, and numerical techniques. The model (1.2) provides one of the simplest quantum-mechanical Hamiltonians to test our analytical and computational techniques. For this reason we give a brief overview of the techniques applied to this problem and we compare and discuss the results obtained. We conclude that there is solid evidence that the picture suggested by spin-wave theory is qualitatively correct. Despite quantum fluctuations, giving rise to a rather large contribution to the ground-state expectation values (for example, the staggered magnetization is reduced by 40%), the ground state of the model for spin-$\frac{1}{2}$ on a square lattice is characterized by antiferromagnetic long-range order. At $T=0$, the staggered magnetization, the spin-wave excitation spectrum, and certain response functions of the model (1.2) are consistent with those predicted by spin-wave theory. It is interesting to note that Schrieffer *et al.* (1989), starting from the itinerant picture, have reached a similar conclusion by including corrections to the mean-field theory due to fluctuation effects.

The second part (Secs. IV–V) reviews the low-temperature behavior of the Hamiltonian (1.2) on a square lattice, as found by a modified spin-wave theory (Takahashi, 1989a), by mean-field theory (Arovas and Auerbach, 1988; Affleck and Marston, 1988), and by quantum Monte Carlo calculations. We also review the renormalization-group approach of Chakravarty *et al.* and the saddle-point calculation for the quantum nonlinear σ model. We find that all these calculations agree in the exponential behavior of the correlation length, namely $\xi(T) \sim e^{b/T}$; the low-order analytical calculations, however, disagree in the prefactor. The results of the quantum Monte Carlo calculations on the spin-$\frac{1}{2}$ Heisenberg antiferromagnet on a square lattice and those on the quantum nonlinear σ model agree with the two-loop calculation of Chakravarty *et al.*, which gives a constant prefactor. In Sec. VI, we briefly discuss results on the lifetime of the magnon excitation at low temperatures.

In the last part of this paper (Sec. VII), a direct com-

parison is attempted between the theoretically calculated magnetic properties of the La_2CuO_4 and those observed. We discuss whether or not the model (1.2) can describe the physics of the La_2CuO_4 and we compare the calculated correlation length, staggered magnetization, spin-wave velocity, and uniform susceptibility with the experimental data. The behavior of the uniform susceptibility and the staggered magnetization have been studied by introducing a weak 3D antiferromagnetic coupling and the antisymmetric coupling only within the mean-field theory introduced by Thio *et al.* (1988). We find it interesting that such a basic model can give a good quantitative description of the spin dynamics in such complex materials.

B. Statement of the problem

Here we give some of the preliminaries and we define the problem to be studied. We consider an $L \times L$ square lattice of lattice spacing a and $N = L^2$ sites. The degrees of freedom are vector spin operators $\mathbf{S}_\mathbf{r}$ attached to the site at $\mathbf{r}$ and obey the usual commutation relations

$$[S_\mathbf{r}^\alpha, S_{\mathbf{r}'}^\beta] = iS_\mathbf{r}^\gamma \delta_{\mathbf{r},\mathbf{r}'} , \tag{1.4}$$

where the superscripts α, β, and γ stand for the x, y, and z components or any cyclic permutation of them. We consider periodic boundary conditions and, at the end of the calculation, take the thermodynamic limit.

The dynamics of the degrees of freedom are controlled by the spin-$\frac{1}{2}$ antiferromagnetic Heisenberg Hamiltonian which, for convenience, we express as

$$H = \sum_{\langle \mathbf{r},\mathbf{r}' \rangle} \left[JS_\mathbf{r}^z S_{\mathbf{r}'}^z + \frac{J_{xy}}{2} (S_\mathbf{r}^+ S_{\mathbf{r}'}^- + S_\mathbf{r}^- S_{\mathbf{r}'}^+) \right] , \tag{1.5}$$

where $S^+ = S^x + iS^y$ and $S^- = S^x - iS^y$ and $J_{xy} = J$. Allowing J_{xy} to be not necessarily equal to J, we obtain a more general model with anisotropic coupling between the three components of the spin operator. When $J_{xy} = J$, the Hamiltonian (1.5) reduces to the isotropic Heisenberg model, which is invariant under rotations of the internal (spin) space. (Notice that in our units $\hbar = 1$ and the lattice spacing $a = 1$.)

We wish to find the eigenstates and eigenvalues of Eq. (1.5). Although we are interested in the spin-$\frac{1}{2}$ antiferromagnet, some of the techniques and statements are valid for the general spin-S case. Let $|S_\mathbf{r}^z\rangle$ denote the eigenstates of the operator $\hat{S}_\mathbf{r}^z$ with eigenvalue $S_\mathbf{r}^z$. The Hilbert space in which the Hamiltonian (1.5) operates is spanned by the basis

$$|\{S_\mathbf{r}^z\}\rangle \equiv \prod_\mathbf{r} |S_\mathbf{r}^z\rangle . \tag{1.6}$$

Since the Hamiltonian commutes with the operators of total spin and the z component of the total spin, namely,

$$\hat{S}_{\text{tot}}^2 \equiv \left| \sum_\mathbf{r} S_\mathbf{r} \right|^2 , \tag{1.7}$$

$$\hat{S}_{\text{tot}}^z \equiv \sum_\mathbf{r} \hat{S}_\mathbf{r}^z , \tag{1.8}$$

we may choose to work in a subspace with well-defined eigenvalues of $\hat{S}_{\text{tot}}$ and $\hat{S}_{\text{tot}}^z$. Specifically, Marshall (1955) proved that the ground state of the antiferromagnetic Heisenberg model on a bipartite lattice is characterized by $S_{\text{tot}} = 0$.

In order to define the ground-state staggered magnetization, we add a field h to the Hamiltonian (1.5), which couples to the spins of the two sublattices differently,

$$H' = H + h \sum_\mathbf{r} (-1)^{\|\mathbf{r}\|} S_\mathbf{r}^z , \tag{1.9}$$

where $\|\mathbf{r}\| \equiv x + y$ and x, y are the two components of the vector $\mathbf{r}$. Then, we define

$$\hat{m}_z^\dagger \equiv \frac{1}{N} \sum_\mathbf{r} (-1)^{\|\mathbf{r}\|} \hat{S}_\mathbf{r}^z , \tag{1.10a}$$

$$m^\dagger \equiv \lim_{h \to 0} \lim_{N \to \infty} \langle 0 | \hat{m}_z^\dagger | 0 \rangle . \tag{1.10b}$$

Provided that we take the thermodynamic limit before we set the external sublattice field h to zero, if the ground-state expectation value $m^\dagger$ remains finite we shall say that the ground state is characterized by antiferromagnetic long-range order. In other words, even though in the limit of $h \to 0$ the symmetries of the Hamiltonian [the translational invariance and, if $J_{xy} = J$, the internal space $O(3)$ invariance] are restored, the ground state can spontaneously break them.

One-dimensional antiferromagnetic spin chains described by the Hamiltonian (1.5) have a ground state with no long-range order. The ground-state energy of the spin-$\frac{1}{2}$ antiferromagnetic Heisenberg chain can be calculated exactly using the Bethe ansatz (Bethe, 1931; see also Orbach, 1958). However, for chains of spins higher than $\frac{1}{2}$ there is no exact solution. The excitation spectrum of such spin chains may exhibit interesting properties. More specifically, it follows from the Bethe ansatz that the correlation function decays following a power law, and it has been conjectured (Haldane, 1983a, 1983b) that when $J \leq J_{xy}$ half-integer spin chains have a gapless excitation spectrum. For integer spin chains, however, there may be a finite gap, and the spin-correlation function decays exponentially with distance.

Beyond one dimension, the exact solution for the ground-state energy or wave function of the Hamiltonian (1.5) on an infinite lattice is unknown. There are some rigorous proofs regarding the nature of the ground state, however. It has been shown that the ground state of the three-dimensional antiferromagnetic Heisenberg model for spin $S \geq 1$ (Dyson, Lieb, and Simon, 1978) and quite recently for $S = \frac{1}{2}$ (Kennedy, Lieb, and Shastry, 1988) is characterized by antiferromagnetic long-range order. The long-range order disappears at some finite critical temperature in 3D. In two space dimensions (2D), the

Heisenberg model cannot exhibit long-range order for any spin at finite temperature (Mermin and Wagner, 1966). The situation may be quite different for the ground state ($T=0$) of these models. It has been shown that antiferromagnetic long-range order exists in the ground state of the isotropic antiferromagnetic Heisenberg model on a square lattice (Neves and Perez, 1986) and on a hexagonal lattice (Affleck *et al.*, 1988) for any $S \geq 1$. More general rigorous statements have been obtained for J_{xy} not necessarily equal to J. There is proof (Kubo and Kishi, 1988; see also Nishimori *et al.*, 1989 and Kubo, 1988) that antiferromagnetic long-range order exists in the ground state of Eq. (1.5) on a square lattice for any $S \geq 1$ and arbitrary J/J_{xy}, and for spin $\frac{1}{2}$ when $0 \leq J/J_{xy} < 0.13$ and $J/J_{xy} > 1.78$. So far, no rigorous proof is available for the existence or nonexistence of antiferromagnetic long-range order in the ground state of the isotropic spin-$\frac{1}{2}$ antiferromagnetic Heisenberg model on a square lattice, which is the model of our interest.

We wish to study the ground-state properties of the Hamiltonian (1.2) on a square lattice in the isotropic case. In particular, we shall examine whether the ground state of the model possesses antiferromagnetic long-range order and calculate the ground-state energy and wave function, the staggered magnetization, the structure factor, and the elementary excitations above the ground state. We shall also study this model at finite temperature and calculate certain thermodynamic functions and correlation functions. For instance, although there is no long-ranger order at any $T \neq 0$, the temperature dependence of the correlation length is an interesting quantity. Since there are no exact results for the case of our interest, we need to employ several techniques available for studying systems with many degrees of freedom and examine whether a consistent picture emerges from a variety of different studies.

II. CALCULATIONS AT ZERO TEMPERATURE. ANALYTICAL APPROACHES

Anderson (1952) extended the spin-wave theory introduced by Holstein and Primakoff (1940) for ferromagnets to the study of the ground state of antiferromagnets with large spin S. Following Anderson, during the same year, Kubo (1952) using the Holstein-Primakoff transformation and an expansion in powers of $1/S$, derived Anderson's results. The foundation of spin-wave theory is the assumption that antiferromagnetic long-range order exists in the ground state and that the amplitude of zero-point motion of quantum fluctuations about the classical Néel state is small. Initially, this approach was thought to be an expansion in powers of $1/S$. Since the role of quantum fluctuations becomes more important for small S, it is natural to question the speed of convergence of this approach for the smallest possible spin case, the spin-$\frac{1}{2}$ antiferromagnet, which is the case of our interest. Later, however, it became clear that the result of spin-wave theory is the leading order in a perturbation-theory expansion in the number of loops, which is also an expansion in powers of $1/z$, z being the coordination number. Still, this expansion is strictly valid for higher-dimensional lattices, where z is large and the fluctuations are suppressed.

In more recent years it was argued (Anderson, 1973) that large-amplitude quantum fluctuations in the two-dimensional spin-$\frac{1}{2}$ case might give rise to a new state. It was speculated that such a state might be characterized by short-range order, in which a "spin liquid" could be formed; this state would be a superposition of states in which the spins are locally bonded to one another, forming a resonating valence bond state (Anderson, 1987). According to the original resonating valence bond theory, superconductivity arises when such a state is doped and hole hopping leads to motion of the preexisting pairs. The validity of this as a superconductivity theory does not depend critically on the existence of antiferromagnetic long-range order at half-filling because we expect the long-range order to be destroyed with a small amount of doping. Liang *et al.* (1988) show that the energy of such a resonating valence bond state is very close to the exact ground-state energy of the spin-$\frac{1}{2}$ antiferromagnetic Heisenberg model. This paper, however, presents strong evidence that the square-lattice spin-$\frac{1}{2}$ antiferromagnetic Heisenberg model possesses antiferromagnetic long-range order in its ground state. Therefore, such a resonating valence bond state could be an appropriate approximation of the ground state far enough from half-filling where there is no antiferromagnetic long-range order.

It is important to make gradual steps towards the full understanding of the problem based on sound techniques and conclusions. It is therefore useful to clarify the situation at half-filling. In Sec. III we shall review computational methods that have been recently used to study the nature of the ground state of the spin-$\frac{1}{2}$ antiferromagnetic Heseinberg model on a square lattice. We shall conclude that the picture suggested by spin-wave theory is qualitatively correct. Even though the spin-wave theory is standard and can be found either in the original papers (Anderson, 1952; Kubo, 1952; see also Oguchi, 1960) or in standard books (e.g., Marshall and Lovesey, 1971; Mattis, 1982), it is useful for easy reference first to review the main results of spin-wave and related theories in some detail.

A. Spin-wave theory

First, we introduce the Holstein-Primakoff transformation as implemented for antiferromagnets. Since it does not entail any loss of simplicity, we derive the results of spin-wave theory for a general hypercubic d-dimensional lattice. An equivalent representation to that obtained using the basis (1.6) is obtained by labeling the basis states by the eigenvalues of the "spin-deviation" operator

$$\hat{n}_{\mathbf{r}} \equiv S - \hat{S}^{z}_{\mathbf{r}} , \tag{2.1a}$$

when the site $\mathbf{r}$ is on one sublattice, say A, and

$$\hat{n}_{\mathbf{r}} \equiv S + \hat{S}^z_{\mathbf{r}} , \tag{2.1b}$$

for a site $\mathbf{r}$ on the other sublattice B. In this representation the Hilbert space is spanned by

$$|\{n_{\mathbf{r}}\}\rangle \equiv \prod_{\mathbf{r}} |n_{\mathbf{r}}\rangle , \tag{2.2}$$

and the eigenvalues of $n_{\mathbf{r}}$ are $0,1,\ldots,2S$. A general state can be expressed as

$$|\psi\rangle = \sum_{\{n_{\mathbf{r}}\}} C(\{n_{\mathbf{r}}\})|\{n_{\mathbf{r}}\}\rangle . \tag{2.3}$$

The operator $\hat{S}^z$ is diagonal in this representation, while $S^+_{\mathbf{r}}$ and $S^-_{\mathbf{r}}$ when $\mathbf{r}$ is on the A sublattice have the following properties:

$$S^+_{\mathbf{r}}|n_{\mathbf{r}}\rangle = \left[2S\left[1-\frac{n_{\mathbf{r}}-1}{2S}\right]n_{\mathbf{r}}\right]^{1/2}|n_{\mathbf{r}}-1\rangle , \tag{2.4a}$$

$$S^-_{\mathbf{r}}|n_{\mathbf{r}}\rangle = \left[2S(n_{\mathbf{r}}+1)\left[1-\frac{n_{\mathbf{r}}}{2S}\right]\right]^{1/2}|n_{\mathbf{r}}+1\rangle . \tag{2.4b}$$

When the site r is on the B sublattice, the action of the above two operators is interchanged. It is a convenient bookkeeeping device to introduce the operators

$$a^\dagger_{\mathbf{r}}|n_{\mathbf{r}}\rangle \equiv \sqrt{n_{\mathbf{r}}+1}|n_{\mathbf{r}}+1\rangle , \tag{2.5a}$$

$$a_{\mathbf{r}}|n_{\mathbf{r}}\rangle \equiv \sqrt{n_{\mathbf{r}}}|n_{\mathbf{r}}-1\rangle , \tag{2.5b}$$

and similarly $b^\dagger_{\mathbf{r}}$ and $b_{\mathbf{r}}$ when $\mathbf{r}$ is on the B sublattice. The operators $a^\dagger_{\mathbf{r}}, a_{\mathbf{r}}$, and $b^\dagger_{\mathbf{r}}, b_{\mathbf{r}}$ obey the usual commutation relations for a two-component system of bosons,

$$[a_{\mathbf{r}}, a^\dagger_{\mathbf{r}'}] = [b_{\mathbf{r}}, b^\dagger_{\mathbf{r}'}] = \delta_{\mathbf{r},\mathbf{r}'} , \tag{2.6a}$$

$$[a_{\mathbf{r}}, a_{\mathbf{r}'}] = [a^\dagger_{\mathbf{r}}, a^\dagger_{\mathbf{r}'}] = [b_{\mathbf{r}}, b_{\mathbf{r}'}] = [b^\dagger_{\mathbf{r}}, b^\dagger_{\mathbf{r}'}] = 0 , \tag{2.6b}$$

$$[a_{\mathbf{r}}, b_{\mathbf{r}'}] = [a^\dagger_{\mathbf{r}}, b^\dagger_{\mathbf{r}'}] = [a_{\mathbf{r}}, b^\dagger_{\mathbf{r}'}] = [a^\dagger_{\mathbf{r}}, b_{\mathbf{r}'}] = 0 . \tag{2.6c}$$

These equations can be obtained by applying the operators to a general state (2.3) and using the definitions (2.5). We find

$$S^+_{\mathbf{r}} = \sqrt{2S} f_S(\hat{n}_{\mathbf{r}}) a_{\mathbf{r}} , \tag{2.7a}$$

$$S^-_{\mathbf{r}} = \sqrt{2S}\, a^\dagger_{\mathbf{r}} f_S(\hat{n}_{\mathbf{r}}) , \tag{2.7b}$$

$$\hat{S}^z_{\mathbf{r}} = S - \hat{n}_{\mathbf{r}} , \tag{2.7c}$$

$$\hat{n}_{\mathbf{r}} = a^\dagger_{\mathbf{r}} a_{\mathbf{r}} , \tag{2.7d}$$

$$f_S(\hat{n}_{\mathbf{r}}) \equiv \left[1-\frac{\hat{n}_{\mathbf{r}}}{2S}\right]^{1/2} , \tag{2.7e}$$

for $\mathbf{r}$ on the A sublattice and

$$S^+_{\mathbf{r}} = \sqrt{2S}\, b^\dagger_{\mathbf{r}} f_S(\hat{n}_{\mathbf{r}}) , \tag{2.8a}$$

$$S^-_{\mathbf{r}} = \sqrt{2S} f_S(\hat{n}_{\mathbf{r}}) b_{\mathbf{r}} , \tag{2.8b}$$

$$\hat{S}^z_{\mathbf{r}} = -S + \hat{n}_{\mathbf{r}} , \tag{2.8c}$$

$$\hat{n}_{\mathbf{r}} = b^\dagger_{\mathbf{r}} b_{\mathbf{r}} , \tag{2.8d}$$

when $\mathbf{r}$ is on the B sublattice.

In Eqs. (2.5) the eigenvalue $n_{\mathbf{r}}$ is free to take any value from 0 to ∞ rather than from 0 to $2S$. There is no discrepancy, since the sector of states with $0 \le n_{\mathbf{r}} \le 2S$ will not be connected to states with $n_{\mathbf{r}} > 2S$ because $|n_{\mathbf{r}} = 2S\rangle$ is annihilated by $S^-_{\mathbf{r}}$ ($S^+_{\mathbf{r}}$) when $\mathbf{r}$ is on A (B) sublattice:

$$S^-_{\mathbf{r}}|n_{\mathbf{r}} = 2S\rangle = 0 . \tag{2.9}$$

The Hamiltonian (1.5) can be expressed in terms of a, $a^\dagger$, b, and $b^\dagger$ operators using the expressions for S^z, S^+, and S^-, and therefore the spin problem is transformed to an equivalent problem of interacting bosons:

$$H = -NdJS^2 + 2dJS\sum_{\mathbf{r}} \hat{n}_{\mathbf{r}} + J_{xy}S\sum_{\langle \mathbf{r},\mathbf{r}'\rangle}[f_S(\hat{n}_{\mathbf{r}})a_{\mathbf{r}} f_S(\hat{n}_{\mathbf{r}'})b_{\mathbf{r}'} + a^\dagger_{\mathbf{r}} f_S(\hat{n}_{\mathbf{r}}) b^\dagger_{\mathbf{r}'} f_S(\hat{n}_{\mathbf{r}'})] - J\sum_{\langle \mathbf{r},\mathbf{r}'\rangle} \hat{n}_{\mathbf{r}}\hat{n}_{\mathbf{r}'} . \tag{2.10}$$

The operator $f_S(\hat{n}_{\mathbf{r}})$, if we allow $\hat{n}_{\mathbf{r}}$ to take values from 0 to ∞, can be expanded as

$$f_S(\hat{n}_{\mathbf{r}}) = 1 - \frac{\hat{n}_{\mathbf{r}}}{4S} - \frac{\hat{n}^2_{\mathbf{r}}}{32S^2} - \cdots . \tag{2.11a}$$

We emphasize that if we truncate this expansion at any order, condition (2.9), which decouples the physical from the unphysical states, is no longer satisfied. If, on the other hand, we restrict ourselves in the physical subspace of $2S+1$ dimensions, then this operator can be written as

$$f_S(\hat{n}_{\mathbf{r}}) = \sum_{m=0}^{2S} d_m(S)\hat{n}^m_{\mathbf{r}} . \tag{2.11b}$$

In the linear spin-wave approximation introduced by Anderson (1952) for antiferromagnets, one retains in Eqs. (2.10) terms up to quadratic in the boson operators. This means that $f_S(\hat{n}_{\mathbf{r}})$ is approximated by 1 and the last term of Eq. (2.10) is neglected, i.e.,

$$H_{LSW} = -NdJS^2 + 2dJS\sum_{\mathbf{r}} \hat{n}_{\mathbf{r}} + J_{xy}S\sum_{\langle \mathbf{r},\mathbf{r}'\rangle}(a_{\mathbf{r}}b_{\mathbf{r}'} + a^\dagger_{\mathbf{r}} b^\dagger_{\mathbf{r}'}) . \tag{2.12}$$

This Hamiltonian connects the physical states with $0 \le n_{\mathbf{r}} \le 2S$ with states having $n_{\mathbf{r}} > 2S$. If the ground-state expectation value of $n_{\mathbf{r}}$ is small compared to $2S$ (1 for spin-$\frac{1}{2}$), this approximation makes sense. This condition can be checked once the spectrum of (2.12) is found.

A quadratic Hamiltonian such as (2.12) can always be diagonalized. We introduce the Fourier transforms of these operators as

$$a_{\mathbf{k}} = \sqrt{2/N}\sum_{\mathbf{r}\in A} e^{i\mathbf{k}\cdot\mathbf{r}} a_{\mathbf{r}} , \tag{2.13a}$$

$$b_{\mathbf{k}} = \sqrt{2/N}\sum_{\mathbf{r}\in B} e^{-i\mathbf{k}\cdot\mathbf{r}} b_{\mathbf{r}} , \tag{2.13b}$$

where the wave vectors $\mathbf{k}$ correspond to the reciprocal space of sublattice A or B. We perform a canonical transformation to new operators $\alpha_{\mathbf{k}}$, $\alpha_{\mathbf{k}}^{\dagger}$, $\beta_{\mathbf{k}}$, and $\beta_{\mathbf{k}}^{\dagger}$, which also obey boson commutation relations,

$$\alpha_{\mathbf{k}}=\cosh\theta_{\mathbf{k}}a_{\mathbf{k}}+\sinh\theta_{\mathbf{k}}b_{\mathbf{k}}^{\dagger}\ , \tag{2.14a}$$

$$\beta_{\mathbf{k}}=\sinh\theta_{\mathbf{k}}a_{\mathbf{k}}^{\dagger}+\cosh\theta_{\mathbf{k}}b_{\mathbf{k}}\ . \tag{2.14b}$$

We invert the transformation (2.14) by expressing $a_{\mathbf{k}}, a_{\mathbf{k}}^{\dagger}$ and $b_{\mathbf{k}}, b_{\mathbf{k}}^{\dagger}$ in terms of $\alpha_{\mathbf{k}}$, $\alpha_{\mathbf{k}}^{\dagger}$, $\beta_{\mathbf{k}}$, and $\beta_{\mathbf{k}}^{\dagger}$ and substitute these in (2.12). The function $\theta_{\mathbf{k}}$ is determined so that the coefficient of $\alpha_{\mathbf{k}}^{\dagger}\beta_{\mathbf{k}}^{\dagger}, \alpha_{\mathbf{k}}\beta_{\mathbf{k}}$ is zero. We obtain

$$\tanh(2\theta_{\mathbf{k}})=\lambda\gamma_{\mathbf{k}} \tag{2.15a}$$

where $\lambda\equiv J_{xy}/J$,

$$\gamma_{\mathbf{k}}\equiv\frac{1}{d}\sum_{\mu}\cos(\mathbf{k}\cdot\hat{e}_{\mu})\ , \tag{2.15b}$$

where $\hat{e}_{\mu}$ is the unit vector in the μ direction, and

$$H_{LSW}=E_0^0+\sum_{\mathbf{k}}\omega_0(k)(n_{\mathbf{k}}^{\alpha}+n_{\mathbf{k}}^{\beta})\ , \tag{2.16a}$$

where

$$n_{\mathbf{k}}^{\alpha}=\alpha_{\mathbf{k}}^{\dagger}\alpha_{\mathbf{k}},\quad n_{\mathbf{k}}^{\beta}=\beta_{\mathbf{k}}^{\dagger}\beta_{\mathbf{k}}\ , \tag{2.16b}$$

$$E_0^0=-dJSN(S+\zeta)\ , \tag{2.16c}$$

$$\zeta\equiv\frac{2}{N}\sum_{\mathbf{k}}\left[1-\sqrt{1-\lambda^2\gamma_{\mathbf{k}}^2}\right]\ , \tag{2.16d}$$

$$\omega_0(\mathbf{k})=2dJS\sqrt{1-\lambda^2\gamma_{\mathbf{k}}^2}\ . \tag{2.16e}$$

The ground state $|\psi_0\rangle$ is defined by the conditions $\alpha_{\mathbf{k}}|\psi_0\rangle=0$ and $\beta_{\mathbf{k}}|\psi_0\rangle=0$ for all $\mathbf{k}$ in the Brillouin zone. For the square lattice and the isotropic case ($\lambda=1$), $\zeta\simeq0.158$ and the ground-state energy per site in the linear spin-wave approximation is -0.658. Keeping terms up to order $1/S$ in the expansion (2.11a), we find that the diagonal terms of the Hamiltonian have the form

$$\begin{aligned}H=&E_0+\sum_{\mathbf{k}}\omega(k)(n_{\mathbf{k}}^{\alpha}+n_{\mathbf{k}}^{\beta})\\&+\frac{dJ}{N}\sum_{\mathbf{k}_1,\mathbf{k}_2}[(1-C_{12})(n_{\mathbf{k}_1}^{\alpha}n_{\mathbf{k}_2}^{\alpha}+n_{\mathbf{k}_1}^{\beta}n_{\mathbf{k}_2}^{\beta})\\&-2(1+C_{12})n_{\mathbf{k}_1}^{\alpha}n_{\mathbf{k}_2}^{\beta}]+\cdots\ ,\end{aligned} \tag{2.17}$$

where

$$E_0=-dJS^2N\left[1+\frac{\zeta}{2S}\right]^2\ , \tag{2.18a}$$

$$\omega(\mathbf{k})=\omega_0(\mathbf{k})\left[1+\frac{\zeta}{2S}\right]\ , \tag{2.18b}$$

$$C_{12}\equiv\sqrt{1-\lambda^2\gamma_{\mathbf{k}_1}^2}\sqrt{1-\lambda^2\gamma_{\mathbf{k}_2}^2}\ . \tag{2.18c}$$

The ground-state energy per site in this approximation for the spin-$\frac{1}{2}$ isotropic model on a square lattice is $E_0/JN=-0.6705$. Since the energy of the Néel state is -0.5 and in the linear spin-wave approximation is -0.658, and the next correction in the $1/S$ expansion is small, one might conclude that there is an apparent convergence in the case of the ground-state energy. It is very different, however, to justify an expansion in powers of $1/S$ for $S=\frac{1}{2}$. After a more careful consideration of Eq. (2.11a) we might agree that the expansion is in powers of $\hat{n}_{\mathbf{r}}/2S$ and therefore the expansion parameter for $S=\frac{1}{2}$ is really the expectation value of $\hat{n}_{\mathbf{r}}$. That is to say, the ground state of Eq. (1.2) is in a linear superposition of states (2.2) with very small amplitude for those with large $n_{\mathbf{r}}$. Therefore the convergence of the expansion could be explained if

$$\epsilon\equiv\frac{1}{N}\sum_{\mathbf{k}}\langle n_{\mathbf{k}}\rangle\ll1\ . \tag{2.19a}$$

We obtain

$$\epsilon=\frac{1}{2N}\sum_{\mathbf{k}}\left[\frac{1}{\sqrt{1-\gamma_{\mathbf{k}}^2}}-1\right]\ , \tag{2.19b}$$

and, for a square lattice, $\epsilon\simeq0.197$, which is a rather small number.

The elementary excitations above the ground state are spin waves of two flavors (due to the two sublattices) and are created by $\alpha_{\mathbf{k}}^{\dagger}$ and $\beta_{\mathbf{k}}^{\dagger}$ acting on the ground state. The energy of these states is given by $\omega(k)$ [Eq. (2.18b)] and, in the long-wavelength limit, and for $\lambda=1$ (isotropic limit) $\omega(k\rightarrow0)=ck$. We define

$$Z_c\equiv c/c_0\ , \tag{2.20}$$

where c_0 is the "bare" spin-wave velocity obtained in the linear spin-wave approximation, namely, $c_0\equiv\sqrt{2}Ja$. For the isotropic spin-$\frac{1}{2}$ antiferromagnet on a square lattice in the above approximation the ratio $Z_c=1+\zeta=1.158$.

The ground-state expectation value of the staggered magnetization operator, as defined by Eq. (1.10), for $S=\frac{1}{2}$ is obtained as

$$m^{\dagger}=\tfrac{1}{2}-\epsilon\ , \tag{2.21}$$

and for a square lattice $m^{\dagger}\simeq0.303$. Hence spin-wave theory predicts an ordered ground state with finite staggered magnetization approximately 61% of its classical value. In one dimension the integral in Eq. (2.19b) diverges logarithmically due to the long-wavelength modes. This instability can be attributed to the fact that the ground state fails to develop long-range order in one dimension. The fact that the integral (2.19b) diverges also means that there is no small expansion parameter, and that the perturbative expansion around an ordered state is incorrect for spin chains.

We wish to add to the Hamiltonian (1.9) a term of the form $H_{\perp}\sum_i\hat{S}_i^x$. The perpendicular susceptibility is defined as $\chi_{\perp}\equiv\partial\langle M_{\perp}\rangle/\partial H_{\perp}$, where $\langle M_{\perp}\rangle$ is the ground-

state expectation value of $1/N\sum_i \hat{S}_i^x$. $\chi_\perp$ describes the response to an external magnetic field in a direction perpendicular to the staggered magnetization. We define

$$Z_\chi \equiv \frac{\chi_\perp}{\chi_{\perp,0}} , \tag{2.22}$$

where $\chi_{\perp,0}\equiv 1/(4dJ)$. Including the next correction in the $1/S$ expansion, we obtain the value $Z_\chi = 1-\zeta-2\epsilon = 0.448$ for an isotropic spin-$\frac{1}{2}$ square-lattice antiferromagnet.

The cross section for inelastic neutron scattering from an antiferromagnet with staggered magnetization in the z direction contains the response functions $\langle 0|S^x_{-\mathbf{q}}(t)S^x_{\mathbf{q}}(0)|0\rangle$ and $\langle 0|S^y_{\mathbf{q}}(t)S^y_{\mathbf{q}}(0)|0\rangle$. The $\langle 0|S^z_{\mathbf{q}}(t)S^z_{\mathbf{q}}(0)|0\rangle$ part leads to elastic scattering; since the Heisenberg Hamiltonian commutes with the total S_z, terms of the form S^-S^- or S^+S^+ are not contained in the total cross section (for details see Marshall and Lovesey 1971; Lovesey, 1984). It is straightforward to calculate the response function

$$S_\perp(\mathbf{q},\omega) \equiv \sum_n |\langle n|S^x_{\mathbf{q}}|0\rangle|^2 \delta(\omega-\omega_{n0}) \tag{2.23a}$$

using linear spin-wave theory. Here $|n\rangle$ are the eigenstates of the Hamiltonian and $\hbar\omega_{n0}=E_n=E_0$, with E_n the corresponding eigenvalues. In this approximation only one-magnon excitation contributes, giving

$$S_\perp(\mathbf{q},\omega) = S_{LSW}(\mathbf{q})\delta(\omega-\omega_{\mathbf{q}}) , \tag{2.23b}$$

$$S_{LSW}(\mathbf{q}) = \frac{1}{4}\frac{1-\gamma_{\mathbf{q}}}{\sqrt{1-\gamma_{\mathbf{q}}^2}} . \tag{2.23c}$$

Clearly, when one goes beyond the simple linear spin-wave theory some strength will be removed from the single spin-wave excitation and will be shifted to two-magnon or multimagnon excitations neglected in this single-mode model. At low temperature the single-magnon peak will broaden due to its scattering from thermally excited magnon excitations, as discussed in Secs. V and VI.

The Hamiltonian (2.17) can be used to calculate finite-temperature properties of Eq. (1.2) in 3D. In the case of 2D, this theory needs to be properly modified, however, since at any $T\neq 0$ the staggered magnetization is zero due to the Mermin-Wagner theorem. We discuss the finite-temperature properties of Eq. (1.2) in Sec. IV. Next we study the ground state further, using other methods that support the picture suggested by spin-wave theory.

B. Beyond spin-wave theory

One of the criticisms of spin-wave theory is that the truncation of the series (2.11) to a finite order may lead to a spectrum that has admixtures of unphysical states with quanta of spin deviations $n_{\mathbf{r}} > 2S$. This problem was first addressed by Dyson (1956) for the ferromagnetic case. In this section we discuss two different attempts to eliminate this problem for the antiferromagnetic case. First, in Sec. II.B.1, we outline the perturbation expansion in the number of loops. In this approach, instead of the boson operators (2.5), the spin operators are used, and so the constraint is taken into account by their commutation rules. For the perturbation expansion a Wick's theorem appropriate for spin operators will be used. Second, in Sec. II.B.2, the method known from the theory of quantum fluids as "paired-phonon" analysis (Feenberg, 1969) is generalized to the case of quantum antiferromagnets to take into account the nonorthogonality of spin waves. In this method one starts from a correlated basis which takes into account the short-range correlations due to the constraint. Another technique for dealing with this problem is a series expansion method that considers the Ising part of the Hamiltonian (1.2) as unperturbed and the x-y part as a perturbation. This approach will be discussed in Sec. II.C.

1. Perturbation theory and loop expansion

Significant effort has been invested in ordinary perturbation-expansion treatment of the Hamiltonian (1.2) in the original spin-operator representation. Again this treatment is based on the assumption that there is antiferromagnetic long-range order in the direction of the external staggered field (z direction). In this section we discuss this formulation of the perturbation expansion, which leads to a systematic loop expansion.

For a spin-$\frac{1}{2}$ system, we write

$$S^z_{\mathbf{r}} = -\tfrac{1}{2} + S^+_{\mathbf{r}}S^-_{\mathbf{r}} , \quad \mathbf{r}\in A , \tag{2.24a}$$

$$S^z_{\mathbf{r}} = \tfrac{1}{2} - S^-_{\mathbf{r}}S^+_{\mathbf{r}} , \quad \mathbf{r}\in B , \tag{2.24b}$$

and the Hamiltonian (1.9) is separated into two parts

$$H' = H_0 + H_I , \tag{2.25a}$$

$$H_0 = -dS^2JN + \omega_A \sum_{\mathbf{r}\in A} S^+_{\mathbf{r}}S^-_{\mathbf{r}} + \omega_B \sum_{\mathbf{r}\in B} T^+_{\mathbf{r}}T^-_{\mathbf{r}} , \tag{2.25b}$$

$$H_I = J\sum_{\langle \mathbf{r},\mathbf{r}'\rangle} S^+_{\mathbf{r}}S^-_{\mathbf{r}}T^+_{\mathbf{r}'}T^-_{\mathbf{r}'} + \frac{J_{xy}}{2}\sum_{\langle \mathbf{r},\mathbf{r}'\rangle}(S^+_{\mathbf{r}}T^+_{\mathbf{r}'} + T^-_{\mathbf{r}'}S^-_{\mathbf{r}}) , \tag{2.25c}$$

where we have defined $\omega_A = dJ + h$, $\omega_B = dJ - h$, and $T^+_{\mathbf{r}} \equiv S^-_{\mathbf{r}}$ and $T^-_{\mathbf{r}} \equiv S^+_{\mathbf{r}}$ when $\mathbf{r}$ is on the B sublattice; h is the sublattice field introduced in Eq. (1.9). The ground state $|0\rangle$ of H_0 is the state with no spin deviations (i.e., the Néel state), which is annihilated by both $S^-_{\mathbf{r}}$ for $\mathbf{r}$ on the A sublattice and $T^-_{\mathbf{r}}$ for $\mathbf{r}$ on the B sublattice.

In the present formalism the Ising term has been divided into one-body and two-body terms, and the latter generates the so called "longitudinal" spin-wave interaction and has been regarded, together with the transverse part (J_{xy}), as a perturbation. The terms arising from the transverse interaction alone, in this approach, can be

summed up to infinite order. Although J and J_{xy} appearing in the perturbation cannot both be assumed to be small, we shall develop a formal perturbation expansion in powers of them. The terms of the expansion will be classified according to the order in H' and according to the number of loops. The terms can be summed up to infinite order for a given number of loops, leading to an expansion in powers of $1/z$, where z is the number of nearest neighbors (Wang *et al.*, 1966).

The usual time-dependent perturbation expansion is implemented with the use of Green's functions for the propagation of a spin deviation defined as

$$G_A(\mathbf{r}'-\mathbf{r},t'-t)\equiv -i\langle\psi_0|P\tilde{S}^-_{\mathbf{r}'}(t')\tilde{S}^+_{\mathbf{r}}(t)|\psi_0\rangle\ , \quad (2.26a)$$

$$G_B(\mathbf{r}'-\mathbf{r},t'-t)\equiv -i\langle\psi_0|P\tilde{T}^-_{\mathbf{r}'}(t')\tilde{T}^+_{\mathbf{r}}(t)|\psi_0\rangle\ , \quad (2.26b)$$

where $|\psi_0\rangle$ is the ground state of H'. The time dependence of the spin operators arises by expressing the operators in the Heisenberg representation, e.g., $\tilde{S}^+_{\mathbf{r}}(t)=e^{iH't}S^+_{\mathbf{r}}e^{-iH't}$. In the zeroth order, the Green's functions are defined as

$$G^0_A(\mathbf{r}'-\mathbf{r},t'-t)\equiv -i\langle 0|PS^-_{\mathbf{r}'}(t')S^+_{\mathbf{r}}(t)|0\rangle$$
$$=-ie^{-i\omega_A(t'-t)}\theta(t'-t)\delta_{\mathbf{r},\mathbf{r}'}\ , \quad (2.27)$$

and similarly for G^0_B. The operators are in the interaction representation $S^+_{\mathbf{r}}(t)=e^{iH_0t}S^+_{\mathbf{r}}e^{-iH_0t}$. Then, utilizing the Gell-Mann and Low theorem and the standard strategy of performing a Feynman perturbation expansion, we obtain

$$G_A(\mathbf{r}'-\mathbf{r},t'-t)=-i\frac{\langle 0|PS^-_{\mathbf{r}'}(t')S^+_{\mathbf{r}}(t)U(\infty)|0\rangle}{\langle 0|U(\infty)|0\rangle}\ , \quad (2.28)$$

and G_B is given by a similar expression. Here $U(t)=P\exp[-i\int^t_{-\infty}H_I(t')dt']$. We have assumed one-to-one correspondence between the eigenstates of H_0 and those of H' (adiabatic turning-on of the interaction). The unperturbed part commutes with the staggered magnetization $m^\dagger_z$ defined by Eq. (1.10), and the full H' does not; hence $m^\dagger_z$ is a constant of motion for the dynamics controlled by H_0 but not for that controlled by H'. Therefore the above theorem and the applicability of the expansion make sense if the expectation value of the staggered magnetization behaves like a classical vector in the thermodynamic limit.

We may then proceed to expand the evolution operator $U(\infty)$ in both the numerator and the denominator of (2.28) as a power series of time integrals of the perturbation H_I. The terms are conveniently represented by diagrams (Fig. 1) with the following rules. A directed horizontal solid line joining the external or an internal point $(\mathbf{r}_1,t_1)$ with an internal or the external point $(\mathbf{r}_1,t_2)$ represents a factor $G^0_A(0,t_2-t_1)$ given by Eq. (2.27). Similarly the directed horizontal dashed line denotes the other Green's function G^0_B. There are two types of interaction lines denoted by vertical wavy lines connecting

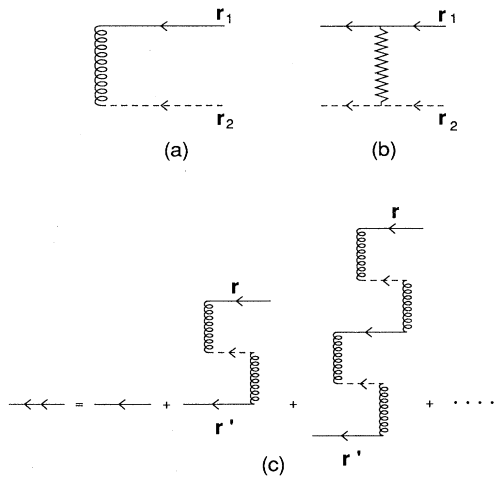

FIG. 1. (a) Diagrammatic representation of the longitudinal interaction line. (b) Diagrammatic representation of the transverse interaction line. (c) All the zero-loop diagrams (the chain diagrams).

the propagation lines. A transverse interaction line connects the terminal point of G^0_A with the terminal point of G^0_B or the initial point of G^0_A with the initial point of G^0_B [see, for example, Fig. 1(a)]. It gives a contribution $J_{xy}(r_{12})$, which, in our case, is nonzero only for nearest neighbors given by $J_{xy}/2$. A longitudinal nearest-neighbor interaction line connecting two incoming and two outgoing Green's functions, as shown in Fig. 1(b) gives a contribution $-iJ$. We must sum over all internal sites and integrate over all internal times. The final contribution needs to be divided by the usual symmetry factor of the diagram, which gives the number of ways in which the diagram can be rotated or reflected onto itself. Lastly, we need to determine the appropriate sign of the diagram. For $S=\frac{1}{2}$, terms in which a string of operators like $S^+_{\mathbf{r}_1}(t_2)\cdots S^+_{\mathbf{r}_1}(t_1)$ acts on $|0\rangle$, and in which no $S^-_{\mathbf{r}_1}$ is encountered in between the time t_1 and time t_2, will vanish. Similar conclusions are obtained for the case of S^- and T^+ and T^- operators. Therefore the fact that each site has only two possible states introduces constraints in the summation over the internal points and times. It is more convenient to release the constraints and subtract the diagrams in which the Green's functions overlap. This introduces spurious diagrams which occur with a negative sign. More precisely, the sign of the diagram is $(-1)^Q$ where Q is the number of "half-overlapping" pairs of Green's function in the diagram. For example, the diagrams of Fig. 2(a) have a minus sign and can be thought of as spurious contributions which have to be subtracted, since the case $\mathbf{r}'=\mathbf{r}$ has not been excluded from the diagram of Fig. 1(c).

Finally, Goldstone's theorem is valid in this case also; it states that the disconnected diagrams of the numerator cancel the denominator, and therefore the ratio of the expectation values (2.28) can be written as a sum of only the connected numerator diagrams.

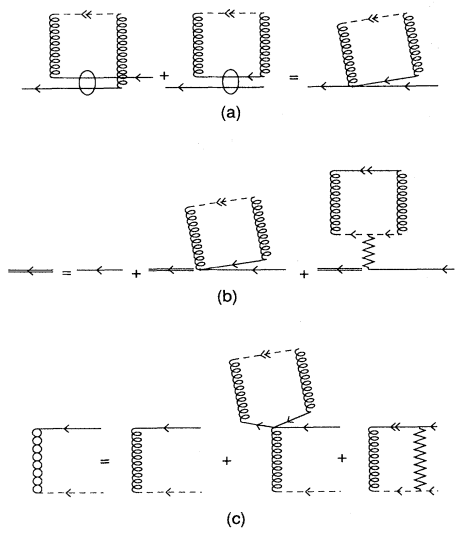

FIG. 2. (a) Example of spurious contributions which have to be subtracted, since the case $\mathbf{r}'=\mathbf{r}$ has not been excluded from the diagram of Fig. 1(c). (b) Diagrammatic representation of Dyson's equation to sum up the one-loop contribution to the self-energy. (c) Diagrammatic representation of Dyson's equation to sum up the one-loop contribution to the interaction vertices. The line with the double arrow is the sum of the chain diagrams shown in Fig. 1(c).

The terms of this series can be classified either by the order in perturbation theory (power of J or J_{xy}, i.e., number of interaction lines) or by the number of loops. The loop expansion is an expansion in power of $1/z$ where z is the number of neighbors and therefore a meaningful expansion in the large-z limit. Furthermore, the significance of higher-loop diagrams decreases due to phase-space limitations.

All the zero-loop diagrams are the chain diagrams shown in Fig. 1(c), and they can be summed to infinite order to give

$$G_A(\mathbf{k},\omega)=G_A^0(\omega)+G_A^0(\omega)J(\mathbf{k})G_B^0(-\omega)J(\mathbf{k})G_A^0(\omega)+\cdots$$
$$=\frac{1}{[G_A^0(\omega)]^{-1}-G_B^0(-\omega)J^2(\mathbf{k})} \tag{2.29}$$

where $G_A^0(\omega)$ and $G_B^0(\omega)$ are the Fourier transforms of Eq. (2.26), i.e.,

$$G_{A,B}^0(\omega)=\frac{1}{\omega-\omega_{A,B}+i\delta}\ , \tag{2.30}$$

and where $\delta\to 0$. Taking the limit $h\to 0$, we obtain

$$G_A(\omega,\mathbf{k})=\frac{A_+(\mathbf{k})}{\omega-\omega_0(\mathbf{k})+i\delta_1}+\frac{A_-(\mathbf{k})}{\omega+\omega_0(\mathbf{k})-i\delta_2}\ , \tag{2.31a}$$

where $\omega_0(\mathbf{k})$ is the same as Eq. (2.16) obtained in linear spin-wave theory and

$$A_\pm(\mathbf{k})\equiv\tfrac{1}{2}\left[1\pm\frac{1}{\sqrt{1-\gamma_{\mathbf{k}}^2}}\right]\ . \tag{2.31b}$$

The sublattice magnetization is obtained as

$$\langle\psi_0|S_{\mathbf{r}}^z|\psi_0\rangle=-\tfrac{1}{2}+\langle\psi_0|S_{\mathbf{r}}^+S_{\mathbf{r}}^-|\psi_0\rangle$$
$$=-\tfrac{1}{2}+i\lim_{t\to 0}\frac{1}{2\pi N}\sum_{\mathbf{k}}\int d\omega\, G_A(\omega,\mathbf{k})e^{-i\omega t}\ . \tag{2.32}$$

Using the approximation (2.31a) for G_A and closing the integration contour in the upper half-plane, we obtain the same expression for the staggered magnetization as Eq. (2.21) obtained in spin-wave theory. The above diagrams include all contributions to order $1/z^0$.

The next correction to order $1/z$ is the sum of all the one-loop diagrams. One can still use Dyson's equation to sum up to infinite order in J and J_{xy} and obtain the one-loop contribution to the self-energy and interaction vertices as shown diagrammatically in Fig. 2(b)–2(c). Equations for the Green's function corresponding to the B sublattice can be obtained by interchanging the dashed and solid lines. The diagram with the "triple point" is a notation for the sum of the two "lock diagrams" shown in Fig. 2(a). The results in this approximation are identical to the results of Anderson, Kubo, and Oguchi obtained in the next correction in their $1/S$ expansion, i.e., in the nonlinear spin-wave theory. The pole of the Green's function is renormalized by a factor $1+\zeta$ where ζ is given by Eq. (2.16e), and hence the spin-wave energies are given by $\omega(k)$ of Eq. (2.18b). There are no one-loop corrections to the staggered magnetization.

Two-loop contributions have also been calculated with the Green's function formalism (Pikalev *et al.*, 1968; Solyom, 1968; Stinchcombe *et al.*, 1971). The corrections to the ground state, staggered magnetization, and spin-wave velocity are negligible, which provides certain justification for the validity of the spin-wave approximation.

2. Paired-magnon analysis

In this section we outline a different method that deals with the single-occupancy constraint directly. We shall define a basis set of multimagnon states which respects short-range pair correlations arising from such constraints.

We start by defining a set of "multimagnon" states as follows:

$$|\cdots n(k)\cdots\rangle\equiv\prod_{\mathbf{k}}(\sigma_{\mathbf{k}}^z)^{n(k)}|\phi\rangle\ , \tag{2.33a}$$

$$\sigma_{\mathbf{k}}^z=\frac{1}{\sqrt{N}}\sum_{\mathbf{r}}e^{i\mathbf{k}\cdot\mathbf{r}}\sigma_{\mathbf{r}}^z \tag{2.33b}$$

where $n(k)=0,1,2,\ldots,N$ and $\sigma_{\mathbf{r}}^z\equiv 2\hat{S}_{\mathbf{r}}^z$

$$|\phi\rangle\equiv\frac{1}{\sqrt{2^N}}\sum_c(-1)^{L(c)}|c\rangle\ , \tag{2.33c}$$

and the sum is over all possible spin configurations c of

spins on the lattice, and $L(c)$ is the number of up spins in one sublattice contained in the configuration c. Another way of writing the state $|\phi\rangle$ is

$$|\phi\rangle = \prod_{\mathbf{r}\in A} |\mathbf{r}\rangle_+ \prod_{\mathbf{r}\in B} |\mathbf{r}\rangle_- , \tag{2.34a}$$

$$|\mathbf{r}\rangle_\pm \equiv \frac{1}{\sqrt{2}}(|+\rangle \pm |-\rangle) , \tag{2.34b}$$

where $|+\rangle$ and $|-\rangle$ are eigenstates of $\sigma_{\mathbf{r}}^z$ with eigenvalues $+1$ and -1, respectively. Since the states $|\mathbf{r}\rangle_+$ and $|\mathbf{r}\rangle_-$ form a complete basis of the Hilbert space of the electrons at $\mathbf{r}$, all possible states of the Hilbert space for N spins can be obtained by acting on $|\phi\rangle$ by all products of $\sigma_{\mathbf{r}_1}^z \cdots \sigma_{\mathbf{r}_l}^z$ for any l different sites. The state (2.33c) or (2.34a) has zero staggered magnetization in the z and y directions and has full staggered magnetization in the x direction. If we rotate the Néel state with staggered order in the z direction around the y axis by $\pi/2$ we obtain the state (2.33c).

The set of states defined by Eq. (2.33) form a nonorthogonal basis and therefore we need to orthonormalize them. We first define states having m and n "magnons" at states with momentum $\mathbf{k}$ and $-\mathbf{k}$, respectively, as

$$|m,n\rangle \equiv C \sum_{\{\mathbf{r}_i\}} \exp[i\mathbf{k}\cdot(\mathbf{r}_1 + \cdots + \mathbf{r}_m - \mathbf{r}_{m+1} - \cdots - \mathbf{r}_{m+n})] \prod_{i<j} f_{ij} \sigma_{\mathbf{r}_1}^z \cdots \sigma_{\mathbf{r}_m}^z \sigma_{\mathbf{r}_{m+1}}^z \cdots \sigma_{\mathbf{r}_{m+n}}^z |\phi\rangle , \tag{2.35}$$

with $\mathbf{k}\neq 0$ and $C \equiv \{[N-(m+n)]!/m!n!N!\}^{1/2}$. Here, $f_{ij}=0$ if $\mathbf{r}_i=\mathbf{r}_j$, and $f_{ij}=1$ otherwise. This definition of multimagnon states takes into account the constraint that no two spin deviations can be at the same site. These states are orthogonal, but they do not form a complete set. The entire Hilbert space is spanned by

$$|\cdots m_{\mathbf{k}}, m_{-\mathbf{k}} \cdots\rangle \equiv \prod_{\mathbf{k},k_x>0} \left[C_{\mathbf{k}} \sum_{\{\mathbf{r}_i\}} \exp[i\mathbf{k}\cdot(\mathbf{r}_1 + \cdots + \mathbf{r}_{m_{\mathbf{k}}} - \mathbf{r}_{m_{\mathbf{k}}+1} - \cdots - \mathbf{r}_{m_{\mathbf{k}}+m_{-\mathbf{k}}})] \times \prod_{i<j} f_{ij} \sigma_{\mathbf{r}_1}^z \cdots \sigma_{\mathbf{r}_{m_{\mathbf{k}}}}^z \sigma_{\mathbf{r}_{m_{\mathbf{k}}+1}}^z \cdots \sigma_{\mathbf{r}_{m_{\mathbf{k}}+m_{-\mathbf{k}}}}^z \right] |\phi\rangle , \tag{2.36}$$

where $m_{\mathbf{k}}$ and $m_{-\mathbf{k}}$ are the number of magnons in the momentum states $\mathbf{k}$ and $-\mathbf{k}$, respectively. These paired multimagnon states are nonorthogonal. We can proceed further by introducing a separability approximation in the calculation of the matrix elements of the unit operator and the Hamiltonian. This approximation was introduced in the theory of quantum fluids (Feenberg, 1969) in the context of "paired-phonon analysis" of strongly correlated Bose liquids. Next we shall extend the method of "paired-phonon analysis" to a "paired-magnon analysis" to study the spin-$\frac{1}{2}$ Heisenberg antiferromagnet. The separability approximation neglects the coupling of paired multimagnon states, and so we obtain

$$\langle \cdots m'_{\mathbf{k}}, m'_{-\mathbf{k}} \cdots | \cdots m_{\mathbf{k}}, m_{-\mathbf{k}} \cdots \rangle \rightarrow \prod_{\mathbf{k},k_x>0} \langle m'_{\mathbf{k}}, m'_{-\mathbf{k}} | m_{\mathbf{k}}, m_{-\mathbf{k}} \rangle = \prod_{\mathbf{k},k_x>0} \delta_{m'_{\mathbf{k}}, m_{\mathbf{k}}} \delta_{m'_{-\mathbf{k}}, m_{-\mathbf{k}}} \tag{2.37a}$$

and

$$\langle \cdots m'_{\mathbf{k}}, m'_{-\mathbf{k}} \cdots | H - E_\phi | \cdots m_{\mathbf{k}}, m_{-\mathbf{k}} \cdots \rangle \rightarrow \sum_{\mathbf{q},q_x>0} \langle m'_{\mathbf{q}}, m'_{-\mathbf{q}} | H - E_\phi | m_{\mathbf{q}}, m_{-\mathbf{q}} \rangle \prod_{\mathbf{k}\neq\mathbf{q},k_x>0} \langle m'_{\mathbf{k}}, m'_{-\mathbf{k}} | m_{\mathbf{k}}, m_{-\mathbf{k}} \rangle , \tag{2.37b}$$

where $E_\phi = \langle\phi|H|\phi\rangle = -dN/4$. Since we have orthogonalized the states (2.35) for all $\mathbf{k}$, within the separability approximation the states (2.36) are orthogonal. This approximation makes sense only in a limited function space characterized by $\sum_{\mathbf{k}} m_{\mathbf{k}} \ll N$.

The matrix elements of Eq. (1.2) can be calculated in the separability approximation analytically. In this approximation, the ground-state wave function can be written as

$$|\psi_0\rangle = \prod_{\mathbf{k},k_z>0} F_{\mathbf{k}} |\phi\rangle . \tag{2.38}$$

The state $F_{\mathbf{k}}|\phi\rangle$ can be written as a linear superposition of states (2.35) with $m=n$, namely, $F_{\mathbf{k}}|\phi\rangle = \sum_{m=0}^{\infty} C_m |m,m\rangle$. The eigenvalue problem can be solved analytically for the ground state and, after some algebra (Manousakis, 1989), we find the same energy as in linear spin-wave theory and the ground-state wave function

$$|\psi_0\rangle = \Lambda \exp\left[-\tfrac{1}{2} \sum_{i<j} u_{ij} \sigma_i^z \sigma_j^z \right] |\phi\rangle , \tag{2.39a}$$

where

$$u_{ij} \equiv \frac{1}{N} \sum_{\mathbf{k}} \left[\left(\frac{1+\gamma(k)}{1-\gamma(k)} \right)^{1/2} - 1 \right] e^{i\mathbf{k}\cdot(\mathbf{r}_i - \mathbf{r}_j)} . \tag{2.39b}$$

The expectation value of the staggered magnetization operator in the paired-magnon analysis is identical to that obtained from spin-wave theory.

The average number of virtually excited magnons in

the interacting ground state for an infinite square lattice is small compared to the number of sites. We find that this fraction is $\langle 1/N \sum_{\mathbf{k}} m_{\mathbf{k}} \rangle = 0.197$. Hence this criterion for the validity of the separability approximation may be reasonably satisfied.

In analogy with other interacting Bose systems, the "momentum distribution" of the spin degrees of freedom in the interacting ground state is given in this approximation by

$$\langle \psi_0 | a_{\mathbf{k}}^{\dagger} a_{\mathbf{k}} | \psi_0 \rangle = \frac{1}{2} \left[\frac{1}{\sqrt{1-\gamma_{\mathbf{k}}^2}} - 1 \right] . \tag{2.40}$$

The condensate fraction, i.e., the fraction of degrees of freedom occupying the zero-momentum state for a square lattice, is $m_0 = 1 - (1/N) \sum_{\mathbf{k}} m_k = 0.803$. That is, there is a significant fraction of degrees of freedom at $\mathbf{k}=0$, even in the interacting ground state. We can conclude that the square-lattice spin-$\frac{1}{2}$ antiferromagnetic Heisenberg model relative to helium is not as strongly interacting a system. In the former, the "condensate" fraction is $\sim 80\%$, whereas in helium the strong interactions leave only $\sim 9\%$ of the atoms in the condensate (Manousakis *et al.*, 1985).

As a next step one can imagine performing perturbation theory in a basis of correlated multimagnon states defined by using the correlation operator $G \equiv \exp(-\frac{1}{2} \sum_{i<j} u_{ij} \hat{\sigma}_i^z \hat{\sigma}_j^z)$. Such a perturbation expansion can be expected to converge quite rapidly because, for example, the ground state in zeroth order is given by the expectation value of H with the state (2.39), which is, as we shall see, close to the exact value, and therefore the perturbative corrections are small. Such a technique has been used to calculate the excitation spectrum of liquid ^{4}He giving accurate results (Manousakis and Pandharipande, 1984).

C. Series expansions

There are series expansions in which one considers the Ising part of Eq. (1.5) as the unperturbed part and the J_{xy} as a perturbation (Parrinello and Arai, 1974, and references therein). This is an expansion in powers of $\lambda \equiv J_{xy}/J$, and we need to extrapolate to the $\lambda = 1$ limit. The coefficients of the expansions are known (Singh, 1989; Singh and Huse, 1989) up to the tenth order for the ground-state energy per site ϵ_0, the staggered magnetization $m^{\dagger}$,

$$m^{\dagger} = \tfrac{1}{2} - \tfrac{1}{9}\lambda^2 - \frac{4}{225}\lambda^4 - 0.009\,471\,3\lambda^6 - 0.007\,442\,9\lambda^8 - 0.004\,376\,91\lambda^{10} - \cdots \tag{2.41a}$$

$$4\epsilon_0/J = -2 - \tfrac{2}{3}\lambda^2 + 0.0037\lambda^4 - 0.006\,326\,28\lambda^6 - 0.003\,300\,85\lambda^8 - 0.001\,247\,40\lambda^{10} - \cdots , \tag{2.41b}$$

and the perpendicular susceptibility $\chi_{\perp}$,

$$\tfrac{1}{2}\chi_{\perp} J = \tfrac{1}{8} - \tfrac{1}{6}\lambda + 0.177\,083\lambda^2 - 0.189\,814\,8\lambda^3 + 0.191\,761\lambda^4 - 0.196\,579\lambda^5 + 0.197\,934\lambda^6 - 0.201\,447\lambda^7 + \cdots , \tag{2.41c}$$

where λ must be smaller than unity for convergence. There is no small parameter (for the isotropic Heisenberg model $\lambda = 1$), and therefore one needs a justified extrapolation scheme.

Huse (1988) changed variables from λ to δ such that $1 - \delta = \sqrt{1-\lambda^2}$, so that the singularities of $m^{\dagger}$ or ϵ_0 at $\lambda = 1$, expected from spin-wave theory, were removed. He performed an extrapolation to the $\delta = 1$, limit, using the series (2.41a), which at that time was available up to sixth order only, and found rapid convergence of the staggered magnetization series. Singh (1989), using the series up to tenth order, noticed that when the variable λ was changed to δ, $m^{\dagger}$ took the form

$$m^{\dagger} = \tfrac{1}{2} - \tfrac{2}{9}\delta + 0.08\delta^2 - 0.009\,319\delta^3 - 0.046\,42\delta^4 + 0.082\,57\delta^5 + \cdots \tag{2.42}$$

and the contribution of the last term was larger than all other terms except the first two, a fact that raised doubts about the convergence of the series at $\delta = 1$. The transformation from λ to δ can bring other unphysical singularities inside the circle of unit radius in the δ plane; in such cases, the physical singularity at $\delta = 1$ would not be the closest one to the origin about which the expansion is performed, and this limits the radius of convergence to $\delta < 1$. Thus a series may be divergent at $\delta = 1$ and the apparent convergence found by Huse (1988) could be spurious.

Singh (1989) used a different method for summing the series (2.41). He considered the sequence of the partial sums S_n of the series (2.41) truncated at the nth order; in the limit $n \to \infty$ the convergence is controlled by the physical singularity. Using the formula $S_n \simeq S_{\infty} + C/(n+\alpha)^{\mu}$, with $\mu = \frac{1}{2}$, and determining α and C by fitting the five points $S_{n=2,\ldots,10}$ he found that the extrapolated value for $n \to \infty$ lays between $m^{\dagger} = 0.305$ and 0.312. Extrapolation along these lines gives $\epsilon_0 = -0.6696 \pm 0.000\,25$ for the ground-state energy per site. For the case of the perpendicular susceptibility, Singh changed variables from λ to $z = 2\lambda/(1+\lambda)$ to remove the simple pole at $\lambda = -1$ that corresponds to the staggered perpendicular susceptibility. Then, using certain constraints in his extrapolation procedure (see Singh, 1989), he found that both the sequence S_n and the series expressed in the δ variable gave similar values; he estimated $Z_{\chi} = 0.52 \pm 0.03$ and, by similar analysis, $Z_c = 1.18 \pm 0.02$. This technique has been also used (Singh *et al.*, 1989) to calculate the moments of the Raman-scattering intensity and extract the value of the antiferromagnetic coupling J. We shall discuss this work in Sec. VII, where we compare the theory with experiment.

D. Analogy with Bose fluids

Next, we shall outline another useful representation in which an interesting analogy with the physics of Bose fluids is pointed out. The similarity of hard-core Bose fluids and spin systems was pointed out by Matsubara and Matsuba (1956), who have shown that liquid ^{4}He when approximated as a quantum lattice gas model is equivalent to the ferromagnetic spin-$\frac{1}{2}$ Heisenberg model. Using a unitary transformation of the basis (Marshall, 1955), we make use of this analogy for quantum antiferromagnets. The eigenstates of the spin-$\frac{1}{2}$ antiferromagnetic Heisenberg model can be expressed as

$$|\Psi\rangle=\sum_{\mathbf{r}_1,\mathbf{r}_2,\ldots,\mathbf{r}_{N_u}}\psi(\mathbf{r}_1,\mathbf{r}_2,\ldots,\mathbf{r}_{N_u})(-1)^{L(c)}\times|\mathbf{r}_1,\mathbf{r}_2,\ldots,\mathbf{r}_{N_u}\rangle\ , \tag{2.43}$$

where the configuration $|c\rangle$ is labeled by the location of one kind of spins (say, the up-spins, in which case N_u is the number of up-spins) on the lattice and the function $\psi(\mathbf{r}_1,\mathbf{r}_2,\ldots,\mathbf{r}_{N_u})$ gives the amplitude of that configuration in the state $|\psi\rangle$. The phase $(-1)^{L(c)}$ has been defined earlier [after Eq. (2.33(c)] and is separated from the amplitude ψ in order to have a non-negative ψ for any ground-state configuration (Marshall, 1955). In this representation, it is straightforward to show that the eigenvalue problem, $H|\Psi\rangle=E|\Psi\rangle$, reduces to a difference equation for the amplitude $\psi(\mathbf{r}_1,\mathbf{r}_2,\ldots,\mathbf{r}_{N_u})$, identical to the many-particle Schrödinger equation on a square lattice:

$$-\frac{J_{xy}}{4}\sum_{i=1}^{N_u}\tilde{\nabla}_i^2\psi(\mathbf{r}_1,\mathbf{r}_2,\ldots,\mathbf{r}_{N_u})+\sum_{i<j}V_{ij}\psi(\mathbf{r}_1,\mathbf{r}_2,\ldots,\mathbf{r}_{N_u})=\epsilon\psi(\mathbf{r}_1,\mathbf{r}_2,\ldots,\mathbf{r}_{N_u})\ , \tag{2.44}$$

where $\tilde{\nabla}_i^2\psi(\mathbf{r}_1,\ldots,\mathbf{r}_i,\ldots,\mathbf{r}_{N_u})\equiv\sum_\delta(\psi(\mathbf{r}_1,\ldots,\mathbf{r}_i+\boldsymbol{\delta},\ldots,\mathbf{r}_{N_u})-\psi(\mathbf{r}_1,\ldots,\mathbf{r}_i,\ldots,\mathbf{r}_{N_u}))$ is the Laplacian operator on the discrete square lattice and $\boldsymbol{\delta}$ is a vector of unit length that connects the site located at $\mathbf{r}_i$ with each of the four nearest neighbors. Here $\epsilon=E-NJ/2+2N_uJ+N_uJ_{xy}$, with E being the ground-state energy eigenvalue of Eq. (1.2). The "particles" correspond to up-spins, and the wave function ψ is symmetric with respect to "particle" permutations; hence this is a quantum lattice gas of bosons with "mass" $m=2/J_{xy}$ (we use units where $a=1$ and $\hbar=1$) and the particles interact via a pair potential V_{ij} having an infinite on-site repulsion. If ij are nearest neighbors $V_{ij}=J$, otherwise $V_{ij}=0$.

This is a useful representation because our knowledge about the system of Bose particles can be used for the magnetic system as well. Depending on the relative magnitude of J_{xy} and J, Eq. (2.44) has different consequences. For $J_{xy}\ll J$, the "potential" energy term dominates, and the particles prefer to stay predominantly at the configuration that minimizes the Ising interaction, thus creating a quantum solid, which for "particle" density $\rho=\frac{1}{2}(S^z_{\rm tot}=0)$ corresponds to an antiferromagnetic ordered state in the z direction. When $J_{xy}\gg J$, the "kinetic" energy dominates, and the system behaves as a quantum liquid. The ground state of the system, in this case, has a condensate that corresponds to off-diagonal long-range order in the one-body density matrix and $\langle\psi|b_0^\dagger|\psi\rangle=n_c\neq0$ where $b_0^\dagger$ creates a "particle" at the zero-momentum state and n_c is the condensate fraction. Going back to the spin variables, this means that $\langle\Psi|m_x^\dagger|\Psi\rangle=\langle\Psi|m_y^\dagger|\Psi\rangle=n_c$ where $m_{x,y}^\dagger$ are the components of the staggered magnetization. Therefore, in this case, the magnetic system is characterized by antiferromagnetic long-range order in the x-y plane. In the isotropic case $J_{xy}=J$ there is spherical symmetry and hence, by a rotation in the spin space, the "potential" and the "kinetic" energy terms can be interchanged; thus, assuming for a moment that the system prefers to be a quantum liquid instead of being a quantum solid, this can be changed to the opposite by such a rotation. The ground state, however, can spontaneously break such symmetry by choosing a given direction to develop staggered magnetization aided by the presence of an external staggered field, which will be removed after we take the thermodynamic limit.

The simplest nontrivial ground-state wave function of a Bose fluid that takes into account short-range correlations due to the existence of the hard core [$V(\mathbf{r}=0)=\infty$] is the Jastrow (1955) wave function,

$$\psi_0(\mathbf{r}_1,\mathbf{r}_2,\ldots,\mathbf{r}_{N_u})=\prod_{i<j}f_{ij}\ , \tag{2.45a}$$

where $f_{ij}=0$ for $i=j$ and $f_{ij}>0$ for $i\neq j$. It is customary to write

$$f_{ij}=e^{-U_{ij}/2}\ . \tag{2.45b}$$

The state (2.45) is known to have a broken symmetry associated with the Bose condensate. Inserting Eq. (2.45) in (2.43) and going back to the spin variables by replacing $\rho_i=S_i^z+\frac{1}{2}$ [where $\rho_i=1$ or 0 depending on whether there is a "particle" (up-spin) at site i or not], we find the Marshall state

$$|\psi_0\rangle=\sum_c(-1)^{L(c)}\exp\left[-\tfrac{1}{2}\sum_{i<j}U_{ij}\hat{S}_i^z\hat{S}_j^z\right]|c\rangle\ , \tag{2.46a}$$

where the sum now runs over all lattice sites with $u_{ij}=4U_{ij}$. If we extend the sum not only over those configurations with N_u up-spins but over all possible configurations, this state takes the form

$$|\psi_0\rangle=\exp\left[-\tfrac{1}{2}\sum_{i<j}u_{ij}\hat{S}_i^z\hat{S}_j^z\right]|\phi\rangle\ , \tag{2.46b}$$

where $|\phi\rangle$ is the Néel state with antiferromagnetic order in the x direction defined by Eq. (2.34). The variational state (2.46b) is characterized by reduced antiferromagnet-

ic order, with $\langle \hat{S}_i^y \rangle = \langle \hat{S}_i^z \rangle = 0$ and $\langle \hat{S}_i^x \rangle = \pm m^\dagger$. If we restrict the sum in (2.46a) over configurations with zero z component of the net spin, we find that $\langle \hat{S}_i^x \rangle = \langle \hat{S}_i^y \rangle = \langle \hat{S}_i^z \rangle = 0$; however, each of the two correlation functions, $\langle \hat{S}_i^x \hat{S}_j^x \rangle$ and $\langle \hat{S}_i^y \hat{S}_j^y \rangle$, at large distances approaches the value $\frac{1}{2}(-1)^{i+j} m^{\dagger 2}$, while $\langle \hat{S}_i^z \hat{S}_j^z \rangle$ approaches zero.

The elementary excitations in the Bose fluid are density fluctuations (phonons in the long-wavelength limit), which in the magnetic system correspond to spin waves. In the Bose system they are created by the density operator $\rho_{\mathbf{q}}$ acting on the interacting ground state (Bijl, 1940; Feynman, 1954), while in the spin system they are created by the $\sigma_{\mathbf{q}}^z$ operator. Chester and Reatto (1966) have shown that the zero-point motion of the long-wavelength modes (zero-sound) of the Bose system gives rise to a long-range tail in the Jastrow wave function. For a 2D system, we obtain

$$u(r \to \infty) = \tfrac{1}{4} U(r \to \infty) = \frac{mc}{4\rho_0 \pi r} , \tag{2.47}$$

where, for the spin-$\frac{1}{2}$ system, c is the spin-wave velocity and $m = 2/J$ (when $J_{xy} = J$). The ground state of the Heisenberg antiferromagnet has zero total S_z, and the number of up-spins is exactly equal to half the total number of sites, giving $\rho_0 = \frac{1}{2}$.

Using Eq. (2.39b) for u_{ij}, we find

$$u(r \to \infty) = \frac{\sqrt{2}}{\pi r} . \tag{2.48}$$

Comparing the tails (2.47) and (2.48), we find $c = \sqrt{2} Ja$, which is the value found by linear spin-wave theory.

The Jastrow wave function (2.45) possesses antiferromagnetic long-range order with the staggered magnetization in the x-y plane, and therefore the dynamic structure function defined by Eq. (2.23a) corresponds to

$$S(\mathbf{q},\omega) \equiv \sum_{n \neq 0} |\langle n | \hat{S}_{\mathbf{q}}^z | 0 \rangle|^2 \delta(\omega - \omega_{n0}) . \tag{2.49}$$

Notice that $S(\mathbf{q},\omega)$ defined by this equation in the equivalent hard-core Bose representation corresponds to the density-density correlation function.

The ω moments of the dynamic structure factor, known as "sum rules", are useful because $S(\mathbf{q},\omega)$ is not directly accessible to simulations of quantum systems and its calculation from exact diagonalization is restricted to systems of small sizes (Chen and Schüttler, 1989).

The structure factor is obtained as

$$S(\mathbf{q}) \equiv \langle 0 | \hat{S}_{-\mathbf{q}}^z \hat{S}_{\mathbf{q}}^z | 0 \rangle = \int_0^\infty d\omega \, S(\mathbf{q},\omega) . \tag{2.50}$$

The ω moment of $S(\mathbf{q},\omega)$ can be obtained as the double commutator $\langle 0 | [\hat{S}_{-\mathbf{q}}^z, [H, \hat{S}_{\mathbf{q}}^z]] | 0 \rangle$, which gives

$$\int_0^\infty d\omega \, \omega S(\mathbf{q},\omega) = 2df(1 - \gamma_{\mathbf{q}}) , \tag{2.51a}$$

where

$$f \equiv \frac{J}{4} \langle 0 | S_i^+ S_{i+\delta}^- + S_i^- S_{i+\delta}^+ | 0 \rangle . \tag{2.51b}$$

A third sum rule can be derived (Liu and Manousakis, 1989) by studying the response of the spin system to an external magnetic field in the z direction. This is analogous to the compressibility sum rule known in the theory of quantum fluids and in this case is translated to the "magnetic susceptibility sum rule." We obtain

$$\frac{1}{2\epsilon''} = \lim_{q \to 0} \int_0^\infty \frac{S(\mathbf{q},\omega)}{\omega} d\omega = \lim_{q \to 0} \sum_{n \neq 0} \frac{|\langle n | \hat{S}_q^z | 0 \rangle|^2}{E_n - E_0} , \tag{2.52}$$

where ϵ'' is the second derivative of the ground-state energy per site $\epsilon(M)$ as a function of the magnetization $M = 1/N \langle 0 | \sum_i S_i^z | 0 \rangle$. $\chi_\perp = 1/\epsilon''$ is the perpendicular susceptibility in units of $g\mu_B = 1$, where μ_B and g are the Bohr magneton and g factor of the electron.

Feynman's assumption (Feynman, 1954; Feynman and Cohen, 1966), introduced for the elementary excitations of liquid ^{4}He, states that in the long-wavelength limit a single-phonon (in this case, single-magnon) excitation dominates the dynamical structure function. This is equivalent to the statement that only excitations created by the $\hat{S}_{\mathbf{q}}^z$ acting on the interacting ground state dominate in this limit. This leads to the following approximation for the spin-dynamical structure function (Pines and Nozières, 1966; Hohenberg and Brinkman, 1974)

$$\lim_{q \to 0} S(\mathbf{q},\omega) = Z_{\mathbf{q}} \delta(\omega - \omega_{\mathbf{q}}) , \tag{2.53}$$

and from the sum rule (2.50) we find that $Z_{\mathbf{q}} = S(\mathbf{q})$, and the combination of (2.51) and (2.53) gives

$$\omega_{\mathbf{q}} = \frac{2df(1 - \gamma_{\mathbf{q}})}{S(\mathbf{q})} . \tag{2.54a}$$

Furthermore, $\lim_{q \to 0} \int_0^\infty \omega S(\mathbf{q},\omega) d\omega = d/2 f q^2$, and $\omega(q \to 0) = cq$ and the spin-wave velocity for $d = 2$ is given by

$$c = \frac{f}{s} , \tag{2.54b}$$

where s is the slope of $S(\mathbf{q})$ in the long-wavelength limit, i.e., $S(q \to 0) = sq$. Using the sum rule (2.52) and Eqs. (2.53) and (2.54b), we find that

$$c = \sqrt{2f\epsilon''} . \tag{2.55}$$

Equation (2.55) is a microscopic derivation of the equivalent expression

$$c^2 = \rho_s / \chi_\perp , \tag{2.56}$$

derived by Halperin and Hohenberg (1969) looking at the problem from a somewhat different angle. The spin-stiffness constant in the approach explained above can be identified as $\rho_s = 2f$. Halperin and Hohenberg used the analogy between the spin system and liquid helium and the hydrodynamics of the two-fluid model. The present derivation allows identification of the phenomenological parameters and furthermore their evaluation from the microscopic Hamiltonian.

III. CALCULATIONS AT ZERO TEMPERATURE. COMPUTATIONAL APPROACHES

In this section we review results obtained for the ground-state properties and elementary excitations of the spin-$\frac{1}{2}$ antiferromagnetic Heisenberg model on a square-lattice by means of exact numerical diagonalization techniques or stochastic methods such as "world-line" Monte Carlo, projector Monte Carlo, Green's function Monte Carlo, or variational methods. We start by briefly reviewing the methods.

A. Exact diagonalizations

The Hamiltonian (1.2) for systems with a finite number of spins can be expressed in a basis such as Eq. (1.6) and then diagonalized exactly to obtain all the eigenvalues and eigenstates. The applicability of this approach is limited to small-size systems, since the dimensionality of the Hilbert space increases exponentially with the size of the lattice—for a lattice with N sites, the total number of possible states is 2^N. Considering the global symmetries of H, we can restrict ourselves to working inside invariant subspaces with reduced dimensionality, since these subspaces are not coupled by the Hamiltonian. We can work in subspaces characterized by definite eigenvalues of $\hat{S}^z_{\rm tot}$ and $S^2_{\rm tot}$. In practice, the $[H,S^z_{\rm tot}]$ symmetry that leads to reduction in an invariant subspace of well defined $S^z_{\rm tot}$ and the translational symmetry that leads to a subspace with well defined momentum can be easily taken into account. If the Hamiltonian is a small-size matrix inside the invariant subspaces, it can be diagonalized using standard diagonalization routines; otherwise iterative schemes known as Lanczos algorithms are generally used.

The first such diagonalizations for the spin-$\frac{1}{2}$ antiferromagnetic Heisenberg model on a square lattice containing up to 16 spins were performed by Oitmaa and Betts (1978). Recently, Dagotto and Moreo (1988), Kikuchi and Okabe (1989), and Tang and Hirsch (1989) have extended these calculations to lattices with up to 24 and 26 spins. The results of the numerical exact diagonalizations published by the above authors for the finite-size lattices studied are all correct; however, finite-size analysis to obtain infinite-size values in certain calculations was carried out using a different extrapolation formula from that predicted by spin-wave theory. The results of all the numerical calculations are carefully analyzed in Sec. III.F, where an extrapolation formula that can be theoretically supported is used. The conclusions of these calculations support the picture that the ground state of the spin-$\frac{1}{2}$ antiferromagnetic Heisenberg model has long-range order with an extrapolated value for the staggered magnetization not too far from the prediction of spin-wave theory. Their results are also consistent with a gapless excitation spectrum in the thermodynamic limit. These results will be compared to the other numerical results obtained by Monte Carlo and variational Monte Carlo calculations at the end of this section.

B. World-line Monte Carlo simulations

The "world-line" Monte Carlo method introduced by Suzuki (1976) has been applied to spin systems by several authors, and the reader is referred to two reviews, by Suzuki (1986) and de Raedt and Lagendijk (1985), for further details. This approach has been applied in low-dimensional fermion and spin systems by Hirsch, Scalapino, and collaborators (see Hirsch *et al.*, 1981, 1982; Loh *et al.* 1985; Scalettar *et al.*, 1985); recently, it has been applied to the square-lattice spin-$\frac{1}{2}$ antiferromagnetic Heisenberg model by Miyashita (1988), Okabe and Kikuchi (1988, 1990), Reger and Young (1988), and other authors.

In this technique, the Hamiltonian (1.2) is broken up into components H_1 and H_2, arranged in a checkerboard pattern as shown in Fig. 3(a). The $H_1(H_2)$ involves only the bonds in the dark-(light-) shaded squares. While such separation is convenient because H_1 or H_2 separately contain noninteracting squares, $[H_1,H_2]\neq 0$. This method uses the Trotter formula (Trotter, 1959) for the operator,

$$e^{-\beta(H_1+H_2)}=\lim_{m\to\infty}(e^{-\beta H_1/m}e^{-\beta H_2/m})^m , \qquad (3.1)$$

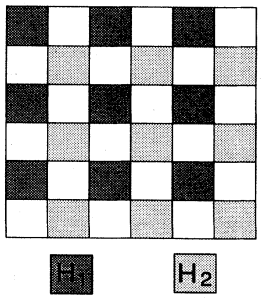

(a)

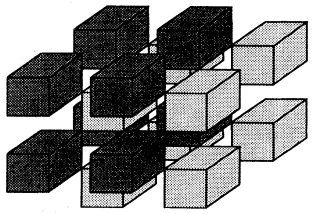

(b)

FIG. 3. (a) The checkerboard breakup of the Hamiltonian in the world-line Monte Carlo method. The piece $H_1(H_2)$ involves only the bonds in the dark-(light-) shaded squares. (b) The checkerboard evolution after the Trotter "time" dimension is introduced.

in the calculation of the trace in the thermodynamic average of an operator $\hat{O}$, i.e.,

$$\langle \hat{O} \rangle_{TD} \equiv \frac{\mathrm{tr}(\hat{O} e^{-\beta \hat{H}})}{\mathrm{tr}(e^{-\beta \hat{H}})} . \tag{3.2}$$

Inserting the resolution of the identity operator using the complete set of states (1.6) between the different factors of Eq. (3.1), one transforms the original quantum spin system into an equivalent system of classical spins which involves an additional dimension with $2m$ (Euclidean) "imaginary time" slices. The expectation value of an operator is expressed as a classical ensemble average over configurations of Ising-like variables $s_{\mathbf{r}}(\tau)$, which live on an $L \times L \times 2m$ cubic lattice shown in Fig. 3(B) and $1 \leq \tau \leq 2m$. We have to impose periodic boundary conditions at the boundaries in the "time" direction because of the trace, i.e., $s_{\mathbf{r}}(2m+1) = s_{\mathbf{r}}(1)$. The Boltzmann weight $P(c)$ for a configuration c is the product $\prod_i M_i$ of the matrix elements $M_i = \langle \alpha' | e^{-\Delta\tau H_{\mathrm{SQ}}} | \alpha \rangle$ for the ith shaded cube of Fig. 3(b), where H_{SQ} is the Hamiltonian of the light- and dark-shaded squares and $\Delta\tau = \beta/m$ and $|\alpha\rangle$, $|\alpha'\rangle$ are the spin configurations at the base and top of the shaded cube.

In the Monte Carlo simulation the thermodynamic average of the operator $\hat{O}$ is obtained as

$$\langle \hat{O} \rangle = \frac{\sum_c O(c)}{N_c} , \tag{3.3}$$

where the sum is over N_c configurations c distributed according to the Boltzmann weight $P(c)$. When we are interested in the ground state, we can restrict ourselves to the subspace with $S^z_{\mathrm{tot}} = 0$, and we need to take the limits $m \to \infty$ and $\beta \to \infty$. The elementary local move that conserves S^z_{tot} is to take an unshaded cube having shaded cubes above and below it and replace the common configuration of the top and bottom squares with a new configuration. The move is accepted with probability $R/(1+R)$, where R is the ratio of Boltzmann weights for the new and old configurations.

The local moves, however, do not cover the entire sample space. Each configuration is characterized by the following two "winding numbers" (see, for example, Marcu, 1987):

$$n_{w_1} = \sum_{x,\tau} (-1)^{y+\tau} s_{\mathbf{r}}(\tau) , \tag{3.4a}$$

$$n_{w_2} = \sum_{y,\tau} (-1)^{x+\tau} s_{\mathbf{r}}(\tau) , \tag{3.4b}$$

where x and y are the components of $\mathbf{r}$. Here n_{w_1} is independent of y, and n_{w_2} independent of x. The local moves do not sample configurations with different winding numbers and configurations in which the world lines of two like spins twist around each other. Sampling of these configurations allows the system to explore parts of the configuration space close to local minima of the energy. These could cause transitions to phases with topological order; for example, this is believed to be the case for $J^{\perp} > J$. One way of producing twists is to offer changes of the spins at the corners of the same noninteracting cube. The winding number n_{w_1} of the configuration $\{s_{\mathbf{r}}(\tau)\}$ can be changed by making global moves along the x direction $s_{\mathbf{r}}(\tau) \to s_{\mathbf{r}}(\tau) + (-1)^{x+\tau}$ and similarly for n_{w_2}. When one adds the twists, and the above global moves, to the local moves, one obtains an ergodic Markov process for this model.

C. Projection methods. Random walks

A method, first used by Metropolis and Ulam (1949), in which the ground state is projected out from a trial state will be the subject of our discussion in this section. This method can be improved significantly by guiding the random walk using the "importance sampling" approach of Kalos (1962, 1966), which will be explained in Sec. III.D. In its first simplest formulation, the method uses a trial state $|\psi_T\rangle$ which has nonzero overlap with the true ground state $|\psi_0\rangle$; applying the imaginary "time" evolution operator $e^{-\tau \hat{H}}$ to the trial state, we obtain the ground state asymptotically:

$$|\psi_0\rangle = C \lim_{\tau \to \infty} e^{-\tau \hat{H}} |\psi_T\rangle . \tag{3.5}$$

This can be shown by expanding the trial state in the complete set of the eigenstates of $\hat{H}$. After a long enough time, $\tau \Delta E \gg 1$, where ΔE is the energy gap from the ground state to the first excited state of the system, the evolution operator filters $|\psi_0\rangle$ from $|\psi_T\rangle$ apart from a constant C. The constant $C = e^{\tau E_0} / \langle \psi_0 | \psi_T \rangle$, where E_0 is the true ground-state energy. More generally, these equations can be cast in iterative form,

$$|\psi_0^n\rangle = \hat{G}(\hat{H}) |\psi_0^{n-1}\rangle \tag{3.6}$$

where, for the case (3.5), $\hat{G}(\hat{H}) = e^{-\Delta\tau \hat{H}}$, $|\psi_0^0\rangle = |\psi_T\rangle$, and Eq. (3.6) needs to be iterated until convergence is achieved. The operator $e^{-\tau \hat{H}}$ is chosen because Eq. (3.5) is the formal infinite-time solution to the imaginary-time Schrödinger equation. Several other choices for $\hat{G}(\hat{H})$ can be made in order to isolate the lowest-energy state; for instance, the resolvent operator $\hat{G}(\hat{H}) = E - z/\hat{H} - z$, with $z < E_0$, has been used in certain of the Green's function Monte Carlo studies from which the name originates. For the case of a Hamiltonian with spectrum bounded from above and below, such as the Heisenberg model on a finite lattice, the following operator has recently been used (Gross, Sánchez-Velasco, and Siggia, 1989a; Trivedi and Ceperley, 1989):

$$\hat{G}(\hat{H}) = 1 - \Delta\tau(\hat{H} - W) . \tag{3.7}$$

Here $\Delta\tau \leq 2/(E_{\max} - W)$, where $E_{\max} = NJ/2$ is the maximum energy eigenvalue for the Heisenberg model. The largest eigenvalue of G must be equal to unity, which im-

plies that $W \simeq E_0$. This choice of $\hat{G}$ is advantageous since it does not require a small $\Delta\tau$ in the evaluation of its matrix elements.

There are several choices of $\hat{G}$ depending on the author and the physical problem; here, we restrict ourselves to a specific choice to illustrate the method. First, we discuss how a stochastic method can be used to sample the projection operator. Consider the spin-$\frac{1}{2}$ antiferromagnetic Heisenberg model and the basis $|c\rangle$ defined by multiplying the basis (1.6) by the phase factor $(-1)^{L(c)}$, where $L(c)$ is the number of down-spins in one sublattice, as discussed in Sec. II. In this basis Eq. (3.6) takes the form

$$\psi_0^n(\mathbf{R}) = \sum_{\mathbf{R}'} G(\mathbf{R},\mathbf{R}')\psi_0^{n-1}(\mathbf{R}') , \tag{3.8}$$

where $\mathbf{R}=(\mathbf{r}_1,\mathbf{r}_2,\ldots,\mathbf{r}_{N_u})$, as introduced in the boson representation in Sec. II.D and $G(\mathbf{R},\mathbf{R}') = \langle \mathbf{R}|\hat{G}(\hat{H})|\mathbf{R}'\rangle$. With the choice (3.7) for $\hat{G}$ we obtain

$$\psi_0^n(\mathbf{R}) = \left[1-\Delta\tau\left[\sum_{i<j} V_{ij} - W\right]\right]\psi_0^{n-1}(\mathbf{R}) + \Delta\tau\frac{J^{\perp}}{4}\sum_{i,\delta}\psi_0^{n-1}(\mathbf{r}_1,\ldots,\mathbf{r}_i+\boldsymbol{\delta},\ldots,\mathbf{r}_{N_u}) , \tag{3.9}$$

where V_{ij} is defined in Sec. II.D. Equation (3.9) can be thought of as an equation describing the motion of random walkers that are initially distributed according to ψ_0^{n-1} and remain either in their position $\mathbf{R}$ or move to another configuration $\mathbf{R}'=(\mathbf{r}_1,\ldots,\mathbf{r}_i+\boldsymbol{\delta},\ldots,\mathbf{r}_{N_u})$, with relative probabilities $P_r = 1-\Delta\tau(\sum_{i<j} V_{ij} - W)$ and $P_m = \Delta\tau(J^{\perp}/4)$, respectively. Therefore we can define a stochastic process that produces the distribution $\psi_0^n(\mathbf{R})$ starting from $\psi_0^{n-1}(\mathbf{R})$. We begin with a population of configurations distributed according to $\psi_0^0(\mathbf{R})=\psi_T(\mathbf{R})$. Each random walker moves in an N_u-dimensional space. In the nth iteration, i.e., after "time" $\tau = n\Delta\tau$, the nth generation of random walkers should be distributed according to $\psi_0^n(\mathbf{R})$. The random walkers from $\mathbf{R}$ either move to $\mathbf{R}'$ or remain in their original positions with relative probability P_m or P_r, respectively.

The energy can be obtained as

$$E_0 = \frac{\langle\psi_0|H|\psi_T\rangle}{\langle\psi_0|\psi_T\rangle} . \tag{3.10}$$

The true ground-state energy is obtained by applying the Hamiltonian to the left, on $|\psi_0\rangle$. Therefore the ground-state energy can be obtained as ratio of averages,

$$E_0 = \frac{\sum_{\mathbf{R}} H\psi_T(\mathbf{R})}{\sum_{\mathbf{R}}\psi_T(\mathbf{R})} , \tag{3.11}$$

where the sum is over configurations $\mathbf{R}$ distributed according to $\psi_0(\mathbf{R})$, which is the output distribution of the iterative stochastic process (3.9). The expectation value of operators that do not share eigenstates with the Hamiltonian, i.e.,

$$\langle\hat{O}\rangle = \frac{\langle\psi_0|\hat{O}|\psi_0\rangle}{\langle\psi_0|\psi_0\rangle} = \lim_{n\to\infty}\frac{\langle\psi_T|G^n H G^n|\psi_T\rangle}{\langle\psi_T|G^{2n}|\psi_T\rangle} , \tag{3.12}$$

requires forward walking for another set of N generations, where one keeps track of the progenitors of the final population of configurations that were born at the nth generation (see Chin *et al.*, 1984).

D. Importance sampling

The projection operator moves each particle to each neighboring site with the same probability. The procedure of obtaining configurations distributed according to the ground-state wave function becomes very efficient if the walkers are guided in their moves by a reasonable guiding wave function ψ_G. This method is called "importance sampling" or, more commonly, the Green's function Monte Carlo method. The former term is also used for a different meaning in the field theory literature, we shall use the latter for any projection method that uses a guiding function, as explained below. The method, an important step forward in treating the ground state of quantum many-body systems using a trial wave function, was originally developed by Kalos (1962, 1966, 1970). It has been successfully applied to several continuum systems, including liquid helium (Kalos *et al.*, 1974; Whitlock *et al.*, 1979; Kalos *et al.*, 1981), helium droplets (Pandharipande *et al.*, 1983, 1986), molecular physics (Anderson, 1975, 1981; Moskowitz *et al.*, 1982; Reynolds *et al.*, 1982; Schmidt and Kalos, 1984), electron gas (Ceperley and Adler, 1980), liquid and solid hydrogen (Ceperley and Adler, 1981), nuclear physics (Koonin, 1981; Zabolitzky and Kalos, 1981; Negele, 1982), and lattice models, including lattice gauge theories (Heys and Stump, 1983; Chin *et al.*, 1984, 1988); recently it has been applied to the spin-$\frac{1}{2}$ antiferromagnetic Heisenberg model (Carlson, 1989; Trivedi and Ceperley, 1989).

The guiding action of the wave function reduces the statistical fluctuations, and this allows simulation of much larger systems. To see how this works, we multiply both sides of Eq. (3.8) by the guiding function $\psi_T(\mathbf{R})$ and we rewrite Eq. (3.8) as

$$\phi^n(\mathbf{R}) = \sum_{\mathbf{R}'} G_M(\mathbf{R},\mathbf{R}')\phi^{n-1}(\mathbf{R}') , \tag{3.13}$$

where $\phi^n(\mathbf{R})=\psi_0^n(\mathbf{R})\psi_T(\mathbf{R})$ and $G_M(\mathbf{R},\mathbf{R}') = \psi_T(\mathbf{R})G(\mathbf{R},\mathbf{R}')/\psi_T(\mathbf{R}')$. In the case of the spin-$\frac{1}{2}$ antiferromagnetic Heisenberg model, Eq. (3.9) takes the form

$$\phi^n(\mathbf{R}) = \left[1-\Delta\tau\left[\sum_{i<j} V_{ij} - W\right]\right]\phi^{n-1}(\mathbf{R}) + \Delta\tau\frac{J^{\perp}}{4}\sum_{i,\delta}\frac{\psi_T(\ldots,\mathbf{r}_i,\ldots)}{\psi_T(\ldots,\mathbf{r}_i+\boldsymbol{\delta},\ldots)} \times\phi^{n-1}(\ldots,\mathbf{r}_i+\boldsymbol{\delta},\ldots) . \tag{3.14}$$

Hence the random walks are biased and [because of the ratio $\psi_T(\mathbf{R})/\psi_T(\mathbf{R}')$] certain regions of the configuration space are sampled more often. The price we have to pay is that the limiting distribution of the walkers, as $n\to\infty$, is $\phi(\mathbf{R})=\psi_0(\mathbf{R})\psi_T(\mathbf{R})$. The ground-state energy can be easily calculated by rewriting Eq. (3.10) as

$$E_0=\frac{\sum_{\mathbf{R}}\psi_0(\mathbf{R})\psi_T(\mathbf{R})\dfrac{H\psi_T(\mathbf{R})}{\psi_T(\mathbf{R})}}{\sum_{\mathbf{R}}\psi_0(\mathbf{R})\psi_T(\mathbf{R})}=\frac{\sum_{\mathbf{R}}\phi(\mathbf{R})\dfrac{H\psi_T(\mathbf{R})}{\psi_T(\mathbf{R})}}{\sum_{\mathbf{R}}\phi(\mathbf{R})}, \tag{3.15}$$

where the second sum is over all configurations. Therefore the expectation value (3.15) can be calculated as the average of $H\psi_T(\mathbf{R})/\psi_T(\mathbf{R})$ over configurations $\mathbf{R}$ generated by Eq. (3.14) after a long enough time. However, there is a problem in obtaining expectation values of operators that do not share eigenstates with $\hat{H}$. In this case only the mixed estimate $\langle O\rangle_M$ is given by Eq. (3.10) or (3.15) when we replace $\hat{H}$ with the operator $\hat{O}$. The mixed estimate can be corrected to give a true extrapolated estimate by assuming that the difference between the true and the trial state is small. The extrapolated estimate is obtained as $\langle\hat{O}\rangle\simeq 2\langle O\rangle_M-\langle O\rangle_T$, where $\langle O\rangle_T$ is the expectation value of $\hat{O}$ with the guiding (or variational) wave function. The correction to the extrapolated estimate is of order $(\psi_0-\psi_T)^2$ and therefore small, provided that ψ_T is close to the exact ψ_0.

E. Variational calculations

In the "importance sampling" technique, it is very important to have accurate variational wave functions. In systems where the Green's function Monte Carlo method has been applied with success there was a prior or parallel search for accurate variational wave functions. Expectation values of operators that do not commute with the Hamiltonian need to be calculated using an extrapolated estimate that assumes that the trial state is accurate. Inversely, having a trial wave function and using the Green's function Monte Carlo approach, we can determine the accuracy of this wave function. Furthermore, an accurate wave function gives us a useful insight into the dominant physical processes, which are important in a determination of the properties of the system. Following this line of reasoning, it is highly desirable to obtain accurate ground-state wave functions for the antiferromagnetic ground state and the excited states. The use of these wave functions may not be limited to the undoped antiferromagnet, since they may be modified to include hole hopping and hole-hole pairing when hopping terms are present in the Hamiltonian.

In this case the calculation part is straightforward; the expectation value of the Hamiltonian can be written as

$$E_T=\frac{\sum_{\mathbf{R}}|\psi_T(\mathbf{R})|^2\dfrac{H\psi_T(\mathbf{R})}{\psi_T(\mathbf{R})}}{\sum_{\mathbf{R}}|\psi_T(\mathbf{R})|^2}=\frac{1}{N_c}\sum_{\mathbf{R}\in\psi_T^2}\frac{H\psi_T(\mathbf{R})}{\psi_T(\mathbf{R})}. \tag{3.16}$$

The sum in the second part of the equation is over N_c configurations $\mathbf{R}$ distributed according to $|\psi_T(\mathbf{R})|^2$, which can be treated as a probability distribution generated by the Metropolis algorithm.

The nontrivial part is the construction of forms of variational wave functions which emphasize the correlations and configurations that are energetically important and suppress those that give a large positive contribution to the energy expectation value. Next, we give some simple wave functions that have been used for the spin-$\frac{1}{2}$ antiferromagnetic Heisenberg model.

In Sec. II.D we discussed the analogy with the hard-core Bose fluids and showed that the wave function (2.39) is the Jastrow ansatz, which, for the amplitude $\psi_0(\mathbf{R})$, is expressed by Eq. (2.45). Variational wave functions of the form (2.39a) have been studied by Hulthén (1938), Kastelijn (1952), Marshall (1955), Taketa and Nakamura (1956), Bartkowski (1972), and Suzuki and Miyashita (1978). More recently this wave function was studied by Horsch and von der Linden (1988), Huse and Elser (1988), Liu and Manousakis (1989), and Manousakis (1989) using the variational Monte Carlo approach. Huse and Elser took $u(1)=u_1$ and $u(r)=a/r^b$ for $r>1$, where $r=|\mathbf{R}_i-\mathbf{R}_j|$, and treated u_1, a, and b as variational parameters. They obtained $\sim -0.664J$ for the ground-state energy per site for $u_1\sim 0.65$, $a\sim 0.475$, and $b\sim 0.7$. Horsch and von der Linden (1988), using only $u(1)$ as a variational parameter [and $u(r>1)=0$], found $-0.644J$ for the ground-state energy. The function u in general is not a function of the distance r between two points on the lattice, but rather a function of the two components x and y of the vector $\mathbf{R}_{ij}$. In Fig. 4, we plot

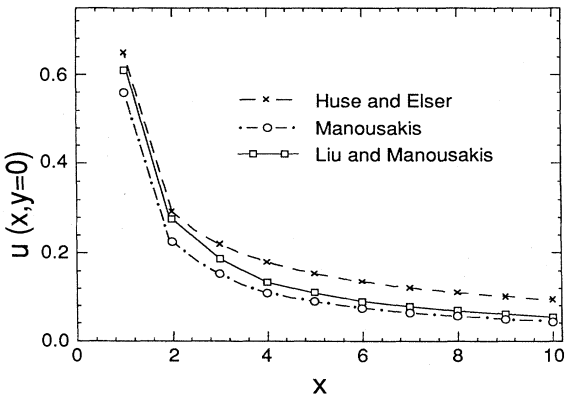

FIG. 4. Comparison of $u(x,y=0)$ obtained by Huse and Elser (crosses), Manousakis (open circles), and Liu and Manousakis (open squares). The dash-dotted line for $x\geq 2$ is the asymptotic tail [Eq. (2.48)]. The other lines are to guide the eye.

$u(x,y=0)$ (open circles) obtained by numerical evaluation of the sum (2.39) and compare it with the results of Huse and Elser (crosses). The function (2.39b) has a long-distance behavior given by Eq. (2.48), which is consistent with the existence of long-wavelength spin-wave excitations. The form (2.48) is shown by the dash-dotted line for $x \geq 2$ in Fig. 4; notice that the asymptotic form agrees very well with the numerically evaluated sum (2.39b) for essentially $x \geq 2$. The rest of the lines are drawn as guides to the eye. Monte Carlo evaluation of the ground-state energy with the parameter-free wave function (2.39b) gives the same energy within error bars as that obtained with the Huse-Elser wave function. The advantage of Eq. (2.39a–b), however, is its simple physical origin and the fact that it is a parameter-free wave function. The wave function (2.39a) has been optimized further by Liu and Manousakis (1989). It is well known that the ground-state energy is not very sensitive to the exact long-range tail of the wave function. Liu and Manousakis have performed a variational Monte Carlo calculation which determines the wave function by requiring it to be consistent with the sum rules of the spin-dynamic structure factor and long-wavelength excitations. It is discussed next.

Liu and Manousakis (1989) used the Jastrow-Marshall form (2.39a), including in the sum (2.33c) only states with zero magnetization, and took $u(1)$ and $u(\sqrt{2})$ as variational parameters and

$$u(\mathbf{r})=\alpha u_{\mathrm{LR}}(\mathbf{r}) \text{ for } \sqrt{x^2+y^2} \geq 2 , \tag{3.17}$$

where $u_{\mathrm{LR}}(\mathbf{r})$ is given by Eq. (2.39b) [and can be approximated by (2.48)] and α is a parameter of order 1. The tail $u(r \rightarrow \infty)$ of Eq. (3.17) is given by the Chester and Reatto relation (2.47) with $c=\alpha c_0$, where $c_0=\sqrt{2}Ja$. This value of c and that obtained from Eq. (2.55), by calculating f and ϵ'' using the same variational wave function, must agree. Therefore $u(1)$ and $u(\sqrt{2})$ are determined by minimizing the ground-state energy, while the parameter α can be determined self-consistently: given a value of α, the spin-wave velocity c is obtained by calculating f and the curvature of $\epsilon(M)$. A new value of α is then obtained via $\alpha=c/c_0$. This is iterated until the input and the output value of α are the same. The wave function obtained with this approach is shown in Fig. 4 by open squares and the solid line is used as a guide to the eye. The extrapolated values to the infinite system for the ground-state energy, staggered magnetization, spin-wave velocity, and perpendicular susceptibility are accurate; they will be presented and compared with the other calculations below.

A somewhat related class of wave functions is obtained using the Gutzwiller (1963, 1964) projection operator acting on a Hartree-Fock-type wave function,

$$|\Psi\rangle=\prod_i (1-n_{i\uparrow}n_{i\downarrow})|\Phi(\Delta)\rangle , \tag{3.17a}$$

where $\Phi(\Delta)$ is a Hartree-Fock wave function to describe antiferromagnetic long-range order,

$$|\Phi(\Delta)\rangle=\prod_{\mathbf{k}} \alpha^{\dagger}_{\mathbf{k}\uparrow} \prod_{\mathbf{k}} \alpha^{\dagger}_{\mathbf{k}\downarrow}|0\rangle , \tag{3.17b}$$

where

$$\alpha^{\dagger}_{\mathbf{k}\sigma}=u^{-}_{\mathbf{k}} c^{\dagger}_{\mathbf{k}\sigma}+\mathrm{sgn}(\sigma)u^{+}_{\mathbf{k}} c^{\dagger}_{\mathbf{k}+\pi\sigma} \tag{3.17c}$$

and

$$u^{\pm}_{\mathbf{k}}=\left[\frac{1}{2}\left[1\pm\frac{\gamma_{\mathbf{k}}}{\sqrt{\gamma^2_{\mathbf{k}}+\Delta^2}}\right]\right]^{1/2} . \tag{3.17d}$$

Here $c_{\mathbf{k}\sigma}$ is the Fourier transform of $c_{i\sigma}$ and $\mathrm{sgn}(\sigma)$ is $+1$ or -1 for $\sigma=\uparrow$ or $\sigma=\downarrow$ and $\pi=(\pi,\pi)$. The states with doubly occupied sites in the Hartree-Fock state are eliminated using the Gutzwiller projection operator. In this variational wave function, Δ is the only variational parameter, and its optimal value controls the antiferromagnetic order parameter. Yokoyama and Shiba (1987), using Eq. (3.17), have calculated the expectation value of Eq. (1.2). Their extrapolated value for the ground-state energy and staggered magnetization for the infinite square lattice are higher (-0.642 and 0.43, respectively) than those obtained with Marshall-Jastrow-type wave functions. It is clear that this wave function only accounts for the on-site constraint and does not describe the short-range correlations. That is, two particles are only statistically correlated if they are at neighboring sites and there are no dynamical correlation factors in the wave function induced by the hard core. Wave functions for which the Gutzwiller projection operator acts on BCS or other mean-field-type wave functions have been used by Gros *et al.* (1987) and Gros (1988) to study superconducting instabilities in the strong-coupling Hubbard model. These states may be energetically favorable when the antiferromagnetic order is destroyed by introducing holes into the system.

There is another class of wave functions closely related to the resonating valence bond theory of superconductivity. Generally speaking, these are states that can be written as linear superposition of states in which all possible spin pairs are paired in a singlet state. Following Anderson's suggestion (1987), several studies of such wave functions have been published. For instance, Liang, Doucot, and Anderson (1988) considered only short-range bonds and found an estimate for the ground-state energy of -0.604 ± 0.0004, while including long-range bonds they found -0.6682 ± 0.0004, which is very close to the best estimate of -0.6692 obtained with the Green's function Monte Carlo method. However, such states have no long-range order, which contradicts the picture suggested by quantum Monte Carlo simulations of the model. The latter picture agrees with the idea of an ordered state suggested by spin-wave theory, both in the qualitative sense (finite-size scaling of the observables) and in the quantitative sense as discussed next. Such resonating valence bond states may be relevant in the case where mobile holes are introduced which destroy the antiferromagnetic long-range order. In this paper, however, we restrict ourselves to the half-filled case. A

TABLE I. Comparison of the ground-state energy per site extrapolated to the infinite-size lattice (in units of J) calculated with various methods.

Method	Energy per site
Linear Spin-Wave Theory	−0.658
Spin-Wave Theory	−0.6705
Series expansions (Singh, 1989)	−0.6696±0.0003
Green's function Monte Carlo (Trivedi-Ceperley, 1989)	−0.6692±0.0002
Green's function Monte Carlo (Carlson, 1989)	−0.6692±0.0002
Variational Monte Carlo (Yokoyama-Shiba, 1987)	−0.642
Variational Monte Carlo (Liang *et al.*, 1988)	−0.6682±0.0004
Variational Monte Carlo (Huse-Elser, 1988)	−0.6638
Variational Monte Carlo (Horsch-Linden, 1988)	−0.644
Variational Monte Carlo (Manousakis, 1989)	−0.6635±0.0002
Variational Monte Carlo (Liu-Manousakis, 1989)	−0.6637±0.0002
World-line Monte Carlo (Reger-Young, 1988)	−0.670±0.001
Projector Monte Carlo (Gross *et al.*, 1989)	−0.6661±0.0002
Projector Monte Carlo (Barnes *et al.*, 1989)	−0.669±0.001
Projection technique (Becker *et al.*, 1989)	−0.6674
Exact diagonalization (Dagotto-Moreo, 1988)	−0.675±0.01
Exact diagonalization (Tang-Hirsch, 1989)	−0.672±0.001

broad class of resonating valence bond wave functions has recently been studied (see, for instance, Zivkovic *et al.*, 1990, and references therein) and should be reviewed in a different context and a different angle from that of the present paper.

F. Results and comparison

1. Energy

The inclusion of the zero-point motion of all massless excitations in two space dimensions, suggested by spin-wave theory, leads to the following leading L dependence of the ground-state energy per site for a square lattice of size L^2:

$$\epsilon_0(L)=\epsilon_0(\infty)+\lambda L^{-3}+\cdots \tag{3.18}$$

More detailed finite-size scaling arguments based on the nonlinear σ model have been given by Gross, Sánchez-Velasco, and Siggia (1989a) and by Neuberger and Ziman (1989). Table I summarizes the results for the ground-state energy per site in units of J obtained with the above-mentioned techniques, and in Fig. 5 we compare them. To show the finite-size scaling (3.18), we plot the energy per site versus L^{-3}. The results of the Green's function Monte Carlo calculations of Carlson (1989) are shown by open squares and those of Trivedi and Ceperley (1989) by crosses. The results of the variational calculations of Liu and Manousakis (1989) are shown by solid squares. The solid lines joining the data points are straight-line fits, as suggested by Eq. (3.18). The dashed line is obtained with the parameter-free wave function (2.39). Both Carlson's and Trivedi and Ceperley's calculations, carried out with apparently different projection and guiding functions, give the same result of $\epsilon_0(\infty)=-0.6692$. Notice that the scaling agrees with the expectations. The variational result obtained with the "best" two-spin correlation factor, explained in Sec. III. E, is about 1% higher than the Green's function Monte Carlo result (which we believe to be the most accurate). We believe that this difference can be removed only if one includes higher-spin correlation factors in the variational wave function. We also show the result obtained in linear spin-wave theory (-0.658) for an infinite square lattice. Including the $1/S$ correction, the ground-state energy per site obtained in spin-wave theory is -0.6705, which is very close to the Green's function Monte Carlo results. Higher-order corrections in $1/S$ have been approximately considered (Solyom, 1968; Stinchcombe *et al.*, 1971; Nishimori and Miyake, 1985) and give negligible contributions. There are reports on the ground-state energy per site based on the unguided random walk Monte Carlo method (Barnes and Swanson, 1988; Gross *et al.* 1989) explained in Sec. III. C. The result reported by Gross *et al.* (1989) is about 0.003 below

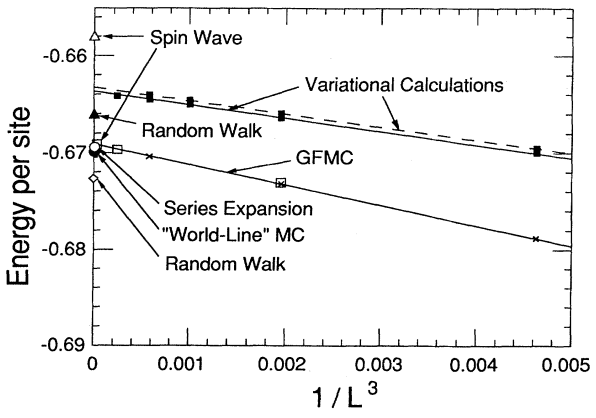

FIG. 5. Comparison of the results for the ground-state energy obtained with various calculations. See text for details.

the Green's function Monte Carlo result, while that reported by Barnes (1988) and by Barnes and Swanson (1988) lies above the Green's function Monte Carlo value by roughly the same amount. A more recent report by Barnes *et al.* (1989) gives -0.669 ± 0.001. The result of the "world-pline" Monte Carlo study (Reger and Young, 1988) has a much larger error bar; it is, however, very close to that obtained by series expansion about the Ising limit (Singh, 1989) and quite close to the Green's function Monte Carlo value. These results are very close to a value of -0.6674 calculated by Becker *et al.* (1989) using a recently developed projection technique for the ground-state energy. The differences, however, between the results of all the ground-state energy calculations given here are rather small (all are in $<2\%$ agreement with the Green's function Monte Carlo result).

It is worth mentioning that a variational Monte Carlo calculation with a quite different wave function, performed by Liang, Doucot, and Anderson (1988), which does not assume antiferromagnetic long-range order, gives an accurate ground-state energy. This wave function with the inclusion of long-range resonating valence bonds gives an energy of -0.6688 ± 0.0004, which is very close to the best estimate of -0.6696. This state, however, assumes zero staggered magnetization, which contradicts the nonzero value of about 0.3 found by the accurate calculations presented next. The more recent work of Zivkovic *et al.* (1990) summarizes the results obtained with the various resonating-valence-bond-type wave functions.

2. Staggered magnetization

In a finite Heisenberg spin system there is no symmetry breaking and the ground state is spherically symmetric. Since the Hamiltonian does not commute with any component of the staggered magnetization, the latter cannot be a conserved quantity. Furthermore, the ground state must be a singlet (Marshall, 1955; Lieb and Mattis, 1962), and therefore the antiferromagnetic ordering of this quantum-mechanical system is more interesting and quite different from that occurring in a classical or a ferromagnetic model. The first question we wish to address is whether the ground state of the model possesses antiferromagnetic long-range order. Following the definition given by Eqs. (1.9) and (1.10), we need to introduce an external staggered field, perform the calculation for various size lattices, extrapolate to the infinite-lattice limit, repeat this calculation for various values of the external field, and finally extrapolate to the zero-field limit. This is a rather involved task and assumes knowledge of two extrapolation formulas. Instead, in most numerical calculations, the staggered magnetization is defined as the square root of the expectation value

$$m^{\dagger 2}\equiv\left\langle\Psi_0\left|\left[\frac{1}{N}\sum_{\mathbf{r}}(-1)^{\|\mathbf{r}\|}\mathbf{S}_{\mathbf{r}}\right]^2\right|\Psi_0\right\rangle , \tag{3.19a}$$

calculated in the absence of external fields. We expect that, in the thermodynamic limit, this definition coincides with the definition (1.9), (1.10). This has recently been questioned by Kaplan, Horsch, and Linden (1989). We believe, however, that in the thermodynamic limit $m^{\dagger}$ is a macroscopic quantity and therefore free of fluctuations. Miyashita (1990), with his Monte Carlo simulation, gives support to these expectations. Another, closely related, definition uses the asymptotic behavior of the staggered spin-spin correlation function

$$C(\mathbf{r})=\left[\frac{-1}{N}\right]^{\|\mathbf{r}\|}\sum_{\mathbf{R}}\langle\Psi_0|\mathbf{S}_{\mathbf{R}}\cdot\mathbf{S}_{\mathbf{R}+\mathbf{r}}|\Psi_0\rangle , \tag{3.19b}$$

$$m^{\dagger 2}=C(L/2,L/2) , \tag{3.19c}$$

where $\mathbf{r}=(L/2,L/2)$ is the longest possible distance in the L^2 size square lattice with periodic boundary conditions. Assuming that there is long-range order, it is straightforward to verify that the definitions (3.19c) and (3.19a) differ only by corrections of order $1/N(N=L^2)$ and can be ignored because the leading finite-size correction with either definition is of order $1/L$. Assuming that $m^{\dagger}$ is finite in the thermodynamic limit, based on the spin-wave analysis and on arguments given by Huse (1988), Reger and Young (1988), Gross *et al.* (1989), and Neuberger and Ziman (1989), we expect the leading finite-size dependence of $m^{\dagger}(L)$ to be of order $1/L$,

$$m^{\dagger}(L)=m^{\dagger}(\infty)+\mu L^{-1}+\cdots . \tag{3.20}$$

The results for the staggered magnetization are compared in Fig. 6 and are summarized in Table II. We give the result of the exact diagonalization (cross) of a 4^2-size system (Dagotto and Moreo, 1988; Tang and Lin, 1988; Tang and Hirsch, 1988). In the Green's function Monte Carlo calculation, $m^{\dagger}(L)$ is calculated from the correlation function, that is, using Eq. (3.19c). We notice that the size dependence of the Green's function Monte Carlo results of Trivedi and Ceperley and the variational results of Liu and Manousakis (1989), who used the definition

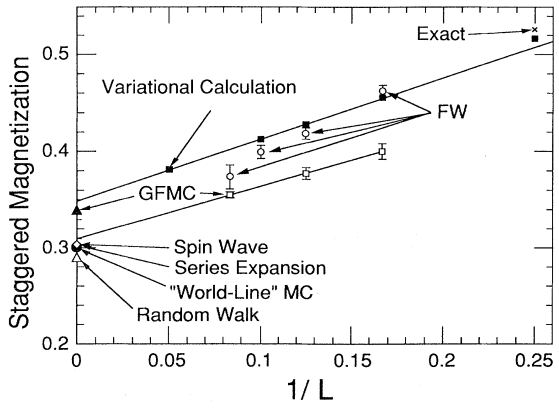

FIG. 6. Comparison of the results for the ground-state staggered magnetization obtained with various calculations. See text for details.

TABLE II. Comparison of the infinite-lattice extrapolation of ground-state staggered magnetization calculated with various methods.

Method	Staggered Magnetization
Linear Spin-Wave Theory	0.303
Spin-Wave Theory	0.303
Series expansions (Davis, 1960)	0.382
Series expansions (Parrinello-Arai, 1974)	0.362
Series expansions (Huse, 1988)	0.313
Series expansions (Singh, 1989)	0.308±0.008
Green's function Monte Carlo (Trivedi-Ceperley, 1989)	0.31±0.02
Green's function Monte Carlo (Carlson, 1989)	0.34±0.01
Variational Monte Carlo (Yokoyama-Shiba, 1987)	~0.43
Variational Monte Carlo (Huse-Elser, 1988)	~0.4
Variational Monte Carlo (Liu-Manousakis, 1989)	0.349±0.002
Variational Monte Carlo (Shankar-Murphy, 1989)	0.29
World-line Monte Carlo (Reger-Young, 1988)	0.31
Projector Monte Carlo (Gross *et al.*, 1989)	0.29
Forward Walking (Runge-Runge, 1990)	~0.3
Exact diagonalization (Tang-Hirsch, 1988)	0.25
Exact diagonalization (Tang-Lin, 1989)	0.245

(3.19a), agree with the scaling law (3.20). The value obtained by Liu and Manousakis for an infinite lattice is $m^{\dagger}(\infty)=0.349\pm0.001$. The extrapolated estimate obtained from the Green's function Monte Carlo calculation of Trivedi and Ceperley is $m^{\dagger}(\infty)=0.31\pm0.01$, while that obtained by Carlson is 0.34 ± 0.01. In this case the discrepancy is due to the fact that the mixed estimate of the expectation value of an operator that does not share eigenstates with the Hamiltonian is not exact, and the corrections depend on the accuracy of the variational wave function used as guiding function in the calculation. Calculations (Runge and Runge, 1990) using forward walking can avoid the problem of the mixed estimate. The open circles with error bars are the results of Runge and Runge,[2] who used the definition (3.19a) for the staggered magnetization. It may be noted that these results are also consistent with an extrapolated value of similar magnitude to that of the Green's function Monte Carlo value of Trivedi and Ceperley. The results of the spin-wave approximation (Anderson, 1952; Kubo, 1952; Oguchi, 1960), the series expansion (Huse, 1988; Singh, 1989), the "world-line" Monte Carlo simulation (Reger and Young, 1988), and the random walk (Gross *et al.*, 1989) are close. Series expansions have been obtained earlier (Davis, 1960; Parrinello and Arai, 1974) which are low-order and slowly convergent. Huse (1988) and Singh (1989) and Singh and Huse (1989) have calculated terms up to tenth order and used extrapolation techniques to calculate the staggered magnetization at the isotropic limit; they found the value 0.308 ± 0.04. Oitmaa and Betts (1978) used $1/L^2$ to extrapolate to the infinite-size lattice, which contradicts Eq. (3.20); furthermore, they calculated the mean-squared staggered magnetization along the z direction, $m_z^{\dagger 2}$, instead of Eq. (3.19). Their ground state is a rotationally invariant singlet; thus one needs to multiply their value for the root-mean-square z component of the staggered magnetization, i.e., $m_z^{\dagger}$, by $\sqrt{3}$ and perform the extrapolation given by Eq. (3.20) (Huse, 1988). It seems, however, that the lattice sizes accessible to the exact diagonalization calculations are not large enough for an accurate extrapolation to the $L\rightarrow\infty$ limit. Notice that the value of the staggered magnetization for the 4×4 lattice, given by the cross in Fig. 6, is too far from the value at $L^{-1}=0$ when plotted as a function of $1/L$; thus we believe that other numerical calculations, such as the Green's function, forward walk, or random walk Monte Carlo can give better estimates for $m^{\dagger}(\infty)$. Moreover, we believe a value around 0.31 ± 0.02 to be a good estimate, because the estimates obtained by the Green's function Monte Carlo work of Trivedi and Ceperley, world-line Monte Carlo, series expansions, random walk Monte Carlo, spin-wave theory, and an extrapolation obtained from the forward walk Monte Carlo method (Runge, 1990) all are within this range. Shankar and Murthy (1989) found that $m^{\dagger}$ for spin-$\frac{1}{2}$ is somewhat smaller than calculated using spin-wave theory; they did so by using Padé approximants to approximate the series for $m^{\dagger}$ in powers of $1/S$, the facts that the leading $1/S$ correction is known from spin-wave theory, and the fact that $m^{\dagger}\sim(S-S_c)^{\beta}$ at the critical point $S=S_c$.

The wave function of Liang, Doucot, and Anderson (1988) gives zero staggered magnetization, in contradiction with the results of all the above methods. The authors initially argued that the 2D spin-$\frac{1}{2}$ antiferromagnetic Heisenberg model is close to criticality, because their energy is close to the "true" ground-state energy. Anderson (1990), however, in a reply to a recent comment by Kaplan (1990), suggests that such resonating

[2]The points corresponding to lattices 10×10 and 12 were obtained from private communication.

valence bond states should be and are currently modified to possess the necessary antiferromagnetic moment required in a spin-$\frac{1}{2}$ Heisenberg antiferromagnet on a square lattice.

If the square-lattice spin-$\frac{1}{2}$ quantum antiferromagnet lacks antiferromagnetic long-range order, then the spin-spin correlation function must satisfy a rigorous upper-bound requirement shown by Kennedy, Lieb, and Shastry (1988). Liang (1990) used the projector Monte Carlo method to calculate the spin-spin correlation function and found that this model must exhibit antiferromagnetic long-range order because this upper-bound requirement was violated.

3. Excitation spectrum

Assuming that the picture suggested by spin-wave theory is correct, we expect a gapless excitation spectrum in the limit $L \to \infty$. Furthermore, the gap should be proportional to L^{-2} according to the arguments given by Gross *et al.* (1989) and Neuberger and Ziman (1989), so that we expect the scaling

$$\Delta E = E_1 - E_0 = \frac{\kappa}{L^2} , \tag{3.21}$$

where $E_1(E_0)$ is the total energy of the system in the lowest-energy state with total $S_z=1$ ($S_z=0$). In Fig. 7, we plot ΔE versus $1/L$ as obtained by the Green's function Monte Carlo calculation of Carlson (1989). The calculation agrees with the scaling (3.21). The cross that overlaps with the Green's function Monte Carlo result for the 4×4 lattice is obtained from exact diagonalization (Dagotto and Moreo, 1988).

The parameter f [Eq. (2.51b)] can be calculated to the same accuracy as the ground-state energy. The variational Monte Carlo calculation of Liu and Manousakis (1989) and the Green's function Monte Carlo calculation of Triverdi and Ceperley (1989) give $f \simeq 0.125J$, a value very close to what one might expect from the analogy with Bose fluids using the continuum version of the sum rules. The second derivative of the energy with respect to the magnetization, ϵ'', can also be calculated accurately because the ground-state energy and its derivatives have small error in both calculations. There are no Green's function Monte Carlo calculations of ϵ''. The variational calculation (Liu and Manousakis, 1989) gives $\epsilon''=12.00\pm0.08J$; therefore the spin-wave velocity obtained from the variational Monte Carlo calculation is $Z_c=c/c_0=1.22\pm0.02 (c_0=\sqrt{2}Ja)$, which is in reasonable agreement with the result of spin-wave theory, $Z_c=1.156$. The result of spin-wave theory is in good agreement with those of the Green's function Monte Carlo calculation by Trivedi and Ceperley (1989), who found $Z_c=1.14\pm0.05$ and the result $Z_c=1.18\pm0.02$ obtained by series expansions (Singh, 1989; Singh and Huse, 1989).

In Fig. 8 the structure function $S(\mathbf{q})$ along the [10] direction is shown. The dashed line gives the result obtained with the linear spin-wave theory [Eq. (2.23c)]; the crosses with the error bars are the results of the Green's function Monte Carlo calculation of Trivedi and Ceperley, while the open circles with error bars the results of the variational Monte Carlo calculation of Liu and Manousakis. The solid line has slope f/c [Eq. (2.54b)] (using for f and c the results of the variational Monte Carlo calculation). In the inset the $\omega(\mathbf{q})$ obtained from Eq. (2.54a) is shown. The straight line is $\omega=cq$ with $c=1.22c_0$. Table III compares the spin-wave velocity obtained in spin-wave theory with the values reported by Green's function Monte Carlo, series expansions, random walk, and variational Monte Carlo calculations. In this Table we also give the results for $Z_\chi \equiv \chi_\perp/\chi_{\perp,0}$, where $\chi_{\perp,0}\equiv 1/8J$ (the perpendicular susceptibility obtained in linearized spin-wave theory). For easy reference, in

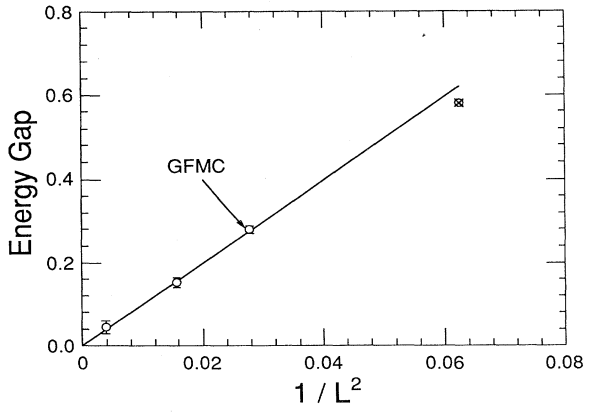

FIG. 7. The results for the energy gap obtained with the Green's function Monte Carlo calculation.

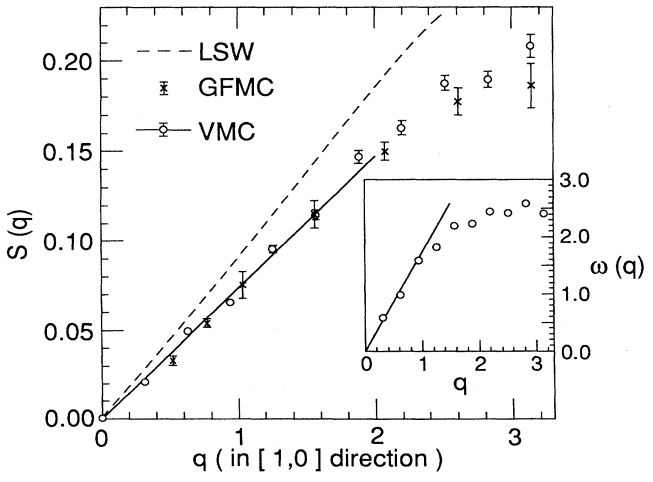

FIG. 8. The results for $S(q)$ obtained from the variational calculations with Marshall-Jastrow-type wave function and Green's function Monte Carlo calculations compared with that obtained in linear spin-wave theory. In the inset we give $\omega(q)$ along the [10] direction obtained from Eq. (2.54a).

TABLE III. Comparison of the ratios Z_c and Z_χ. Here, c is the spin-wave velocity, $c_0 \equiv 2^{1/2}Ja$, χ is the perpendicular susceptibility, and $\chi_{\perp,0} \equiv 1/8J$. We also give the spin-stiffness constant $\rho_s = \frac{1}{4} Z_\chi Z_c^2 J$ calculated by various methods for comparison.

Method	$Z_c = c/c_0$	$Z_\chi = \chi_\perp/\chi_{\perp,0}$	Spin stiffness (ρ_s/J)
Linear Spin-Wave Theory	1	1	0.25
Spin-Wave Theory	1.158	0.448	0.1505J
Series expansions (Singh, 1989)	1.18±0.02	0.53±0.04	0.183±0.01
Green's function Monte Carlo (Trivedi-Ceperley, 1989)	1.14±0.05		
Variational Monte Carlo (Liu-Manousakis, 1989)	1.22±0.02	0.667±0.004	0.25±0.01
Projector Monte Carlo (Gross *et al.*, 1989)	1.18±0.10	0.71±0.04	0.25±0.05

Table III we give the spin-stiffness constant ρ_s, which is not an independent parameter and is given in terms of c and $\chi_\perp$ by Eq. (2.56).

IV. CALCULATIONS AT FINITE TEMPERATURES. ANALYTICAL APPROACHES

In this section we study the low-temperature properties of the spin-$\frac{1}{2}$ Heisenberg antiferromagnet on a square lattice with analytical techniques. In 2D, antiferromagnetic long-range order is destroyed at any finite temperature (Mermin and Wagner, 1966) by thermal fluctuations. Hence conventional spin-wave theory or series expansions around the Ising limit cannot be applied without appropriate modification. First, we discuss the mean-field approximations in a path-integral formulation of the theory using the Schwinger-boson representation used by Arovas and Auerbach (1988), the fermion representation used by Affleck (1988), and Marston and Affleck (1989), and a modified spin-wave theory introduced by Takahashi (1989a). Second, we derive the quantum nonlinear σ model from the large-S quantum Heisenberg antiferromagnet in the long-wavelength limit and we discuss the role of the Hopf term in one and two space dimensions. Third, the renormalization-group calculations of Chakravarty, Halperin, and Nelson (1988, 1989) with the β function calculated in one-loop and two-loop order will be discussed. Finally, we study the quantum nonlinear σ model using the saddle-point approximation.

A. Path-integral formulation. Schwinger boson representation

Arovas and Auerbach (1988) used a path-integral formulation in the Schwinger representation (Schwinger, 1952). Let us introduce two operators u_i and v_i at the site i, obeying standard boson commutation relations and

$$S_i^+ = u_i^\dagger v_i \ , \tag{4.1a}$$

$$S_i^- = u_i v_i^\dagger \ , \tag{4.1b}$$

$$S_i^z = \tfrac{1}{2}(u_i^\dagger u_i - v_i^\dagger v_i) = u_i^\dagger u_i - S \ , \tag{4.1c}$$

where the last equality follows from the constraint

$$\hat{S} \equiv \tfrac{1}{2}(u_i^\dagger u_i + v_i^\dagger v_i) = S \ . \tag{4.1d}$$

In the case of a square lattice we can perform the unitary transformation $u \to -v$ and $v \to u$ in the A sublattice, and so $S_i^+ = -u_i v_i^\dagger$, etc. With the above transformation the Hamiltonian (1.2) takes the form

$$H = -\frac{J}{2} \sum_{\langle ij \rangle} \hat{L}_{ij}^\dagger \hat{L}_{ij} + NdJS^2 \ , \tag{4.2a}$$

$$\hat{L}_{ij} = u_i u_j + v_i v_j \ , \tag{4.2b}$$

while the constraint (4.1d) remains the same. Considering the two kinds of bosons (u and v) as the two flavors of an SU(2) symmetry, Arovas and Auerbach generalize the symmetry to one of SU(n) by considering bosons $\hat{\phi}_i^\alpha$, $\alpha = 1, \ldots, n$ of n different flavors. In this generalization the link operator is given by

$$\hat{L}_{ij} = \sum_{\alpha=1}^{n} \hat{\phi}_i^\alpha \hat{\phi}_j^\alpha \ , \tag{4.3a}$$

and the constraint (4.1d) is written as

$$\hat{S} \equiv \frac{1}{n} \sum_{\alpha=1}^{n} \hat{\phi}_i^{\dagger\alpha} \hat{\phi}_i^\alpha = S \ . \tag{4.3b}$$

The Hamiltonian

$$\hat{H}(\{\hat{\phi}_i^{\dagger\alpha}\}, \{\hat{\phi}_i^\alpha\}) = -\frac{J}{n} \sum_{\langle ij \rangle} :\hat{L}_{ij}^\dagger \hat{L}_{ij}: \tag{4.3c}$$

for $n = 2$ reduces to Eq. (1.2) within a constant equal to $NdJS^2$. Note that this generalization to an SU(n)-invariant Heisenberg model, by allowing the spin index to run from 1 to n, is different from letting the electrons have higher spin. In the latter case the coupling between the spins does not have the simple form given by Eq. (4.3c). The partition function $Z = \mathrm{Tr} e^{-\beta \hat{H}}$ can be expressed in a path integral using the coherent basis

$$|\phi_i^\alpha\rangle \equiv \exp(\phi_i^\alpha \hat{\phi}_i^{\dagger\alpha}) |0\rangle \ , \tag{4.4}$$

for every lattice site i ($|0\rangle$ here denotes the vacuum state). Here ϕ_i^α is a complex number and we consider only those states that respect the constraint (4.3b). First, we write the partition function as $Z = \lim_{\epsilon \to 0} \mathrm{Tr} \prod_{\nu=1}^{M} (1 - \epsilon \hat{H})$, with $M\epsilon = \beta$. Next, we introduce the resolution of the identity operator in the

coherent basis (4.4) for every site, between the operators $1-\epsilon\hat{H}$, and we evaluate the matrix elements using $\langle\phi|\hat{H}(\hat{\phi}^{\dagger},\hat{\phi})|\phi'\rangle=H(\phi^*,\phi)\langle\phi|\phi'\rangle$ and $\langle\phi|\phi'\rangle=e^{\phi^*\phi'}$. Finally, we take into account the constraint (4.3b) and the limit $\epsilon\to 0$ to obtain

$$Z=\int D[\phi,\phi^*,\lambda]\exp(-S[\phi,\phi^*,\lambda]) \tag{4.5}$$

and

$$S[\phi,\phi^*,\lambda]=\int_0^{\beta}d\tau\left[\tfrac{1}{2}\sum_{i,\alpha}(\phi_i^{*\alpha}\dot{\phi}_i^{\alpha}-\dot{\phi}_i^{*\alpha}\phi_i^{\alpha})-\frac{J}{n}\sum_{\langle ij\rangle}L_{ij}^*L_{ij}+\sum_{i,\alpha}\lambda_i(\phi_i^{*\alpha}\phi_i^{\alpha}-S)\right], \tag{4.6}$$

where $L_{ij}=\sum_{\alpha=1}^{n}\phi_i^{\alpha}\phi_j^{\alpha}$. The notation $\int D[\phi,\phi^*,\lambda]$ denotes a path integral over all independent fields $\phi_i(\tau)$ and $\phi_i^*(\tau)$ and a field $\lambda_i(\tau)$. The auxiliary field $\lambda_i(\tau)$ is introduced at every site in order to take care of the constraint (4.3b); it can easily be seen that by integrating out λ, using $\delta(x)=\int_{-i\infty}^{i\infty}(d\lambda/2\pi i)e^{\lambda x}$, the constraint is recovered in the form of a δ function.

Introducing a Hubbard-Stratonovich field Q_{ij} on each bond of the lattice to decouple the quartic interaction term, we obtain

$$Z=\int D[\phi,\phi^*,Q,Q^*,\lambda]\exp(-S'[\phi,\phi^*,Q,Q^*,\lambda]), \tag{4.7a}$$

where

$$S'=\int_0^{\beta}d\tau\left[\tfrac{1}{2}\sum_{i,\alpha}(\phi_i^{*\alpha}\dot{\phi}_i^{\alpha}-\dot{\phi}_i^{*\alpha}\phi_i^{\alpha})+\frac{n}{J}\sum_{\langle ij\rangle}Q_{ij}^*Q_{ij}+\sum_{\langle ij\rangle}(Q_{ij}^*L_{ij}+Q_{ij}L_{ij}^*)+\sum_{i,\alpha}\lambda_i(\phi_i^{*\alpha}\phi_i^{\alpha}-S)\right]. \tag{4.7b}$$

This action is quadratic in the ϕ fields, which implies that they can be integrated out to obtain

$$Z=\int D[Q,Q^*,\lambda]\exp(-nS_{\rm eff}[Q,Q^*,\lambda]). \tag{4.8}$$

In the saddle-point approximation the extrema of $S_{\rm eff}$ are determined from

$$\frac{\delta S_{\rm eff}}{\delta Q_{ij}(\tau)}=\frac{\delta S_{\rm eff}}{\delta Q_{ij}^*(\tau)}=\frac{\delta S_{\rm eff}}{\delta\lambda_i(\tau)}=0. \tag{4.9}$$

In general, the solutions of (4.9) can be (Euclidean) time dependent and nonuniform, with perhaps a nontrivial phase factor. Because it is difficult to find all possible solutions and calculate their contribution to the generating functional, it is common to seek the uniform and time-independent solutions: $Q_{ij}(\tau)=Q_{ij}^*(\tau)=Q$ and $\lambda_i(\tau)=\lambda$. Affleck and Marston (1988) used the fermion representation and allowed for a simple spatial variation of the phase of the Hubbard-Stratonovich field, and their results will be discussed in Sec. IV.D. Let us allow for a simple spatial variation of the phase of Q by writing $Q_{ij}=Qt_{\delta}$ where $|t_{\delta}|=1$. The partition function (4.7), when Q is a constant, can be obtained from the following mean-field Hamiltonian:

$$\hat{H}^{\rm MF}=\frac{n}{J}NdQ^2-nNS\lambda+\tfrac{1}{2}\sum_{\mathbf{k},\alpha}[\lambda(\hat{\phi}_{\mathbf{k}}^{\dagger\alpha}\hat{\phi}_{\mathbf{k}}^{\alpha}+\hat{\phi}_{-\mathbf{k}}^{\dagger\alpha}\hat{\phi}_{-\mathbf{k}}^{\alpha})+2dQ(t_{\mathbf{k}}^*\hat{\phi}_{\mathbf{k}}^{\alpha}\hat{\phi}_{-\mathbf{k}}^{\alpha}+t_{\mathbf{k}}\hat{\phi}_{\mathbf{k}}^{\dagger\alpha}\hat{\phi}_{-\mathbf{k}}^{\dagger\alpha})], \tag{4.10a}$$

where

$$t_{\mathbf{k}}=\frac{1}{z}\sum_{\delta}t_{\delta}e^{-i\mathbf{k}\cdot\delta}. \tag{4.10b}$$

Performing the Bogoliubov transformation

$$\hat{w}_{\mathbf{k}}^{\alpha}=\cosh\theta_{\mathbf{k}}\hat{\phi}_{\mathbf{k}}^{\alpha}+\sinh\theta_{\mathbf{k}}\hat{\phi}_{-\mathbf{k}}^{\dagger\alpha} \tag{4.11a}$$

$$\hat{w}_{\mathbf{k}}^{\dagger\alpha}=\cosh\theta_{\mathbf{k}}\hat{\phi}_{\mathbf{k}}^{\dagger\alpha}+\sinh\theta_{\mathbf{k}}\hat{\phi}_{-\mathbf{k}}^{\alpha}, \tag{4.11b}$$

we find that $\hat{H}^{\rm MF}$ takes a diagonal form,

$$\hat{H}^{\rm MF}=\frac{n}{J}NdQ^2-nNS\lambda+\sum_{\mathbf{k},\alpha}\omega_{\mathbf{k}}(\hat{w}_{\mathbf{k}}^{\dagger\alpha}\hat{w}_{\mathbf{k}}^{\alpha}+\tfrac{1}{2}), \tag{4.11c}$$

where

$$\omega_{\mathbf{k}}=\lambda\sqrt{1-\eta^2|t_{\mathbf{k}}|^2}, \tag{4.12a}$$

$$\eta=2dQ/\lambda, \tag{4.12b}$$

and the angle $\theta_{\mathbf{k}}$ is chosen such that

$$\tanh 2\theta_{\mathbf{k}}=\eta t_{\mathbf{k}}. \tag{4.12c}$$

Let us change integration variables in the path integral from the fields $\phi_{\mathbf{k}},\phi_{\mathbf{k}}^*$ to new fields corresponding to the operators $\hat{w}_{\mathbf{k}}^{\alpha}$ and $\hat{w}_{\mathbf{k}}^{\dagger\alpha}$. These new fields can be integrated out to obtain

$$F^{\rm MF}=\frac{-1}{N\beta}\ln Z=dQ^2-\tfrac{1}{2}(2S+1)\lambda+\frac{1}{\beta}\frac{1}{N}\sum_{\mathbf{k}}\ln[2\sinh(\tfrac{1}{2}\beta\omega_{\mathbf{k}})]. \tag{4.13a}$$

The saddle-point equations $\delta F^{\rm MF}/\delta Q=\delta F^{\rm MF}/\delta\lambda=0$ give

$$2S+1=\frac{1}{N}\sum_{\mathbf{k}}\frac{\coth\left[\frac{1}{2}\frac{\sqrt{1-\eta^2|t_{\mathbf{k}}|^2}}{k_BT_{\lambda}}\right]}{\sqrt{1-\eta^2|t_{\mathbf{k}}|^2}}, \tag{4.13b}$$

$$\lambda=d\frac{1}{N}\sum_{\mathbf{k}}\frac{|t_{\mathbf{k}}|^2\coth\left[\frac{1}{2}\frac{\sqrt{1-\eta^2|t_{\mathbf{k}}|^2}}{k_BT_{\lambda}}\right]}{\sqrt{1-\eta^2|t_{\mathbf{k}}|^2}}, \tag{4.13c}$$

where $T_{\lambda}\equiv T/\lambda$. Assuming that $t_{\delta}=1$, we have $t_{\mathbf{k}}=\gamma_{\mathbf{k}}$. For given values of S and T_{λ} we can solve Eq. (4.13b) to obtain $\eta=\eta(T_{\lambda},S)$. We substitute $\eta(T/\lambda,S)$ in Eq.

(4.13c) and solve to obtain $\lambda(T,S)$, which can then be substituted back in $\eta(T/\lambda,S)$ to find η as a function of T and S. These equations will be solved in Sec. IV.C. In the next section we derive Eq. (4.13) again, using a modified spin-wave theory proposed by Takahashi (1989).

B. Modified spin-wave theory

Low-dimensional quantum ferromagnets at finite temperatures have been studied using conventional techniques by several authors (see, for example, Dalton and Wood, 1967; Yamaji and Kondo, 1973; Takahashi, 1987, 1990). The standard spin-wave theory is not applicable without modification. In this section we discuss a variational density-matrix approach proposed by Takahashi (1989a) for antiferromagnets.

The consequence of the Mermin-Wagner theorem in Takahashi's approach is enforced by hand, as explained below. Takahashi uses the Dyson-Maleev (Dyson, 1956; Maleev, 1957) transformation for antiferromagents instead of the Holstein-Primakoff transformation [Eqs. (2.7) and (2.8)]. In this transformation the boson operators are defined as

$$S_i^+=(2S-a_i^\dagger a_i)a_i,\quad S_i^-=a_i^\dagger\ , \tag{4.14a}$$

$$S_i^z=S-a_i^\dagger a_i\ , \tag{4.14b}$$

for i on the A sublattice and

$$S_j^+=-b_j^\dagger(2S-b_j^\dagger b_j),\quad S_j^-=-b_j\ , \tag{4.15a}$$

$$S_j^z=-S+b_j^\dagger b_j\ , \tag{4.15b}$$

for j on the B sublattice. In terms of these operators the Hamiltonian is given by

$$H=-NdJS^2+\sum_{\langle ij\rangle}[\,S(a_i^\dagger a_i+b_j^\dagger b_j-a_i^\dagger b_j^\dagger-a_i b_j) +\tfrac{1}{2}a_i^\dagger(b_j^\dagger-a_i)^2 b_j\,]\ , \tag{4.16}$$

Next, Takahashi introduces the following ansatz for the density matrix:

$$\rho=\exp\left[-(k_B T)^{-1}\sum_{\mathbf{k}}\omega_{\mathbf{k}}(\alpha_{\mathbf{k}}^\dagger\alpha_{\mathbf{k}}+\beta_{-\mathbf{k}}^\dagger\beta_{-\mathbf{k}})\right]\ , \tag{4.17}$$

where $\alpha_{\mathbf{k}}$ and $\beta_{\mathbf{k}}$ are operators that are related to the original boson operators $a_{\mathbf{k}}$ and $b_{\mathbf{k}}$ via the canonical transformation

$$\alpha_{\mathbf{k}}=\cosh\theta_{\mathbf{k}}a_{\mathbf{k}}-\sinh\theta_{\mathbf{k}}b_{\mathbf{k}}^\dagger\ , \tag{4.18a}$$

$$\beta_{\mathbf{k}}=-\sinh\theta_{\mathbf{k}}a_{\mathbf{k}}^\dagger+\cosh\theta_{\mathbf{k}}b_{\mathbf{k}}\ . \tag{4.18b}$$

Here, $\omega_{\mathbf{k}}$ and the angle $\theta_{\mathbf{k}}$ are variational parameters to be determined by minimizing the free energy,

$$F=E-T\Sigma\ , \tag{4.19a}$$

$$E\equiv\langle\hat{H}\rangle=-\frac{JN}{2}\sum_{\delta}[S+\tfrac{1}{2}-f(0)+g(\delta)]^2\ , \tag{4.19b}$$

where Σ denotes the entropy and

$$f(\mathbf{r}_{ij})\equiv\langle a_i^\dagger a_j\rangle+\tfrac{1}{2}\delta_{ij}=\langle b_i^\dagger b_j\rangle+\tfrac{1}{2}\delta_{ij}=\frac{1}{N}\sum_{\mathbf{k}}\cosh(2\theta_{\mathbf{k}})e^{-i\mathbf{k}\cdot\mathbf{r}_{ij}}(\bar{n}_{\mathbf{k}}+\tfrac{1}{2})\ , \tag{4.19c}$$

$$g(\mathbf{r}_{ij})\equiv\langle a_i^\dagger b_j^\dagger\rangle=\langle a_i b_j\rangle=\frac{1}{N}\sum_{\mathbf{k}}\sinh(2\theta_{\mathbf{k}})e^{-i\mathbf{k}\cdot\mathbf{r}_{ij}}(\bar{n}_{\mathbf{k}}+\tfrac{1}{2})\ . \tag{4.19d}$$

The summation is over the entire Brillouin zone and

$$\bar{n}_{\mathbf{k}}\equiv\langle\alpha_{\mathbf{k}}^\dagger\alpha_{\mathbf{k}}\rangle=\langle\beta_{\mathbf{k}}^\dagger\beta_{\mathbf{k}}\rangle=\frac{1}{e^{\omega_{\mathbf{k}}/k_B T}-1}\ . \tag{4.19e}$$

Takahashi approximated the entropy Σ by the expression for an ideal gas of noninteracting quasiparticles created by $\alpha_{\mathbf{k}}^\dagger$ or $\beta_{\mathbf{k}}^\dagger$ operators,

$$\Sigma=2\sum_{\mathbf{k}}[(\bar{n}_{\mathbf{k}}+1)\ln(\bar{n}_{\mathbf{k}}+1)-\bar{n}_{\mathbf{k}}\ln(\bar{n}_{\mathbf{k}})]\ . \tag{4.20}$$

The minimization of the free energy $F(\theta_{\mathbf{k}},\omega_{\mathbf{k}},T)$ is performed subject to the constraint

$$\langle S_i^z\rangle=S+\tfrac{1}{2}-f(0)=0\ . \tag{4.21}$$

The minimum of F is found via $\partial(F-\mu\langle S_i^z\rangle)/\partial\theta_{\mathbf{k}}=0$ and $\partial(F-\mu\langle S_i^z\rangle)/\partial\omega_{\mathbf{k}}=0$, where μ is the Lagrange multiplier that enforces the constraint (4.21). The minimization and the constraint (4.21) give equations identical to (4.12) and (4.13) obtained in the previous section with the Schwinger boson mean-field theory, with Q and λ in this case defined as

$$Q\equiv\langle a_i^\dagger b_{i+\delta}^\dagger\rangle=g(\delta)\ , \tag{4.22a}$$

$$\lambda=2dJQ-\mu\ . \tag{4.22b}$$

The correlation function is obtained as

$$\langle\mathbf{S}_i\cdot\mathbf{S}_j\rangle=f^2(\mathbf{r}_{ij})-\tfrac{1}{4}\delta_{ij}-g^2(\mathbf{r}_{ij})\ . \tag{4.23}$$

Using the combination of (4.19) and (4.12c), we find that $f(\mathbf{r})=0$ for $(-1)^{\|\mathbf{r}\|}=-1$ and $g(\mathbf{r})=0$ when $(-1)^{\|\mathbf{r}\|}=1$ (here, $\|\mathbf{r}\|=x+y$ where x and y are the coordinates of $\mathbf{r}$ in lattice spacing units). Therefore the correlation length can be found by looking at the asymptotic behavior of $f^2(\mathbf{r})$ or $g^2(\mathbf{r})$ in the A or B sublattice.

The same equations have been obtained by Hirsch and Tang (1989b, 1989c; see also Tang *et al.*, 1989) with the aid of the Holstein-Primakoff transformation. In the next section we solve Eqs. (4.13b) and (4.13c) at $T=0$ and low T and discuss the correlation functions.

C. Low-T solution and correlation functions

Equations (4.13) can be written as

$$2S+1=\frac{2}{\pi^2}\int_0^1 dt\, K[\sqrt{1-t^2}]\frac{\coth\left[\frac{1}{2}\frac{\sqrt{1-\eta^2t^2}}{k_BT_\lambda}\right]}{\sqrt{1-\eta^2t^2}}\,, \tag{4.24a}$$

$$2S+1-\frac{\eta^2\lambda}{2}=\frac{2}{\pi^2}\int_0^1 dt\, K[\sqrt{1-t^2}]\coth\left[\frac{1}{2}\frac{\sqrt{1-\eta^2t^2}}{k_BT_\lambda}\right]\sqrt{1-\eta^2t^2}\,, \tag{4.24b}$$

where $K(x)$ is the complete first-order elliptic integral, i.e., $(1/N)\sum_{\mathbf{k}}\delta(t-t_{\mathbf{k}})=(2/\pi^2)K[\sqrt{1-t^2}]$, with $0<t<1$. At $T=0$, the right-hand side of Eq. (4.24a) is bounded from above by its maximum value attained at $\eta=1$. This maximum value is $2\epsilon+1$, where ϵ is given by Eq. (2.20) and $\epsilon\simeq 0.197$ for a square lattice. Hence, in order to satisfy (4.24), S must be less than ϵ. Since this condition is not satisfied for $S\geq\frac{1}{2}$, at $T=0$ and $S=\frac{1}{2}$ the disordered solution does not exist. This is consistent with the existence of a ground state having broken symmetry such as antiferromagnetic long-range order. In order to satisfy Eq. (4.24a), we need to go back to the step where we replaced the summation over the $\mathbf{k}$ by the integral. If we allow for $1/N^2$ corrections to $1-\eta^2$, we find that Eq. (4.24a) is satisfied with $1-\eta^2=1/4(S-\epsilon)^2N^2$. These corrections vanish in the thermodynamic limit; thus the $T=0$ value of η is $\eta_0=1$. From Eq. (4.24b) we obtain the $T=0$ value of λ as

$$\lambda_0=4SJ\left[1+\frac{\zeta}{2S}\right]\,, \tag{4.25}$$

where ζ is given by Eq. (2.16d). Substituting in Eqs. (4.12) and (4.13) the values of η and λ for $T=0$, we find that the ground state and spin excitation energy $\omega_{\mathbf{k}}$ are the same as those given by Eqs. (2.18a) and (2.18b), respectively.

In the limit $T_\lambda\to 0$, Takahashi worked out the asymptotic forms of Eqs. (4.24a) and (4.24b) in the interval $1-\eta\ll T_\lambda^2\ll 1$; he found

$$2S+1=\frac{4}{\pi^2}K[0]T_\lambda\left[\frac{1}{\eta}\ln\left[\frac{1+\eta}{1-\eta}\right]-2\ln\left[\frac{2}{T_\lambda}\right]\right]+\frac{2}{\pi^2}\int_0^1 dt\, K[\sqrt{1-t^2}](1-\eta^2t^2)^{-1/2}+O(T_\lambda^3)\,, \tag{4.26a}$$

$$2S+1-\frac{\eta^2\lambda}{2}=\frac{2}{\pi^2}\int_0^1 dt\, K[\sqrt{1-t^2}](1-\eta^2t^2)^{-1/2}+\frac{4}{\pi^2}K[0]\zeta(3)T_\lambda^3+O(T_\lambda^5)\,. \tag{4.26b}$$

The first part of Eq. (4.26a) is the most singular part of the integral (4.24a) arising from the $1/x$ singular term of $\coth x$ when $x\to 0$, and the second part corresponds to the $T_\lambda=0$ value of the integral. The low-T solutions to the above two equations are

$$\eta=1-\frac{1}{2}\left[\frac{T}{\lambda_0}\right]^2\exp\left[-\frac{\pi\lambda_0(S-\epsilon)}{k_BT}\right][1+O((T/J)^2)]\,, \tag{4.27a}$$

$$\lambda=\lambda_0-\frac{16J}{\pi}\left[\frac{T}{\lambda_0}\right]^3+O(T^5)\,. \tag{4.27b}$$

Using Eq. (4.19c) for $f(\mathbf{r})$ and Eq. (4.12c) to calculate $\sinh 2\theta_{\mathbf{k}}$ with the above approximation for η, we can find

$$f(r)=\frac{T}{\pi^2\eta^2\lambda}\int\int d^2k\frac{\exp(i\mathbf{k}\cdot\mathbf{r})}{k^2+(2\xi)^{-2}}\simeq 2T_\lambda\left[\frac{\xi}{\pi r}\right]^{1/2}e^{-r/2\xi} \tag{4.28a}$$

for $\mathbf{r}$ such that $(-1)^{\|\mathbf{r}\|}=1$ and

$$\xi\equiv\frac{1}{\sqrt{8(\eta^2-1)}}=\frac{S\hbar c}{k_BT}\exp\left[\frac{2\pi\rho_s}{k_BT}\right][1+O(T^2)]\,, \tag{4.28b}$$

$$\rho_s\equiv S\left[1+\frac{\zeta}{2S}\right](S-\epsilon)J\,. \tag{4.28c}$$

For the spin-$\frac{1}{2}$ square-lattice antiferromagnet, $\rho_s=0.175\,66J$. The spin-spin correlation function is given by

$$\langle\mathbf{S}_0\cdot\mathbf{S}_{\mathbf{r}}\rangle\simeq(-1)^{\|\mathbf{r}\|}\left[\frac{2T}{\lambda_0}\right]^2\frac{\xi}{\pi r}e^{-r/\xi}\,. \tag{4.28d}$$

The uniform susceptibility is defined as $\chi=T^{-1}\sum_i\langle S_0^zS_i^z\rangle$ and at low T is given by (Takahashi, 1989a)

$$\chi(T\to 0)=\frac{1}{12J\left[1+\frac{\zeta}{2S}\right]}(S-\epsilon)+\frac{k_B T}{2\pi J\left[1+\frac{\zeta}{2S}\right]}+O(T^3)\ . \tag{4.29}$$

The zero-temperature classical value of χ is $\frac{2}{3}$ times the classical perpendicular susceptibility.

Auerbach and Arovas (1988) have calculated the dynamical structure function at finite temperature T as the Fourier transform of the imaginary part of the spin-density correlation function

$$S(\mathbf{q},\omega,T)=\frac{1}{\pi}\mathrm{Im}\langle S^z(\mathbf{q},\omega)S^z(-\mathbf{q},\omega)\rangle\ , \tag{4.30a}$$

using the Schwinger boson mean-field Hamiltonian (4.10). They obtained

$$\begin{aligned}S(\mathbf{q},\omega,T)=&\tfrac{1}{4}\sum_{\mathbf{k}}\{\cosh[2(\theta_{\mathbf{k}}+\theta_{\mathbf{k}+\tilde{\mathbf{q}}})]+1\}n_{\mathbf{k}}(n_{\mathbf{k}+\tilde{\mathbf{q}}}+1)\delta(\omega_{\mathbf{k}+\tilde{\mathbf{q}}}-\omega_{\mathbf{k}}-\omega)\\&+\tfrac{1}{8}\sum_{\mathbf{k}}\{\cosh[2(\theta_{\mathbf{k}}+\theta_{\mathbf{k}+\tilde{\mathbf{q}}})]+1\}[n_k+\Theta(\omega)][n_{\mathbf{k}+\tilde{\mathbf{q}}}+\Theta(\omega)]\delta(\omega_{\mathbf{k}+\tilde{\mathbf{q}}}+\omega_{\mathbf{k}}-|\omega|)\ ,\end{aligned} \tag{4.30b}$$

where $\Theta(\omega)$ is the step function and $\tilde{\mathbf{q}}\equiv\mathbf{q}-(\pi,\pi)$. This expression includes processes where the incident particle creates quasiparticle excitations as well as scattering from thermally excited quasiparticles. Auerbach and Arovas calculated $S(\mathbf{q},\omega,T)$ by expanding ω_k up to order quadratic in $\mathbf{k}$ and $\tilde{\mathbf{k}}$. They defined a dimensionless frequency ν and a dimensionless momentum κ as

$$\nu\equiv\frac{\xi\omega}{c}\ , \tag{4.31a}$$

$$\kappa\equiv\xi q\ . \tag{4.31b}$$

There are two distinct regimes. The first is $(\nu,\kappa)\lesssim(1,1)$, where $S(q,\omega,T)$ has a quasielastic peak that increases in strength and narrows with increasing $\xi(T)$. This peak turns into a magnetic Bragg peak at $T=0$, where there is antiferromagnetic long-range order. The second regime is $(\nu,\kappa)\gg(1,1)$. In this case the wavelength of the incident neutron is shorter than the correlation length and the energy is higher than the spin-wave energy. Two quasiparticle peaks at positive and negative energy appear, corresponding to standard spin waves. In this case the integrations in Eq. (4.30) are dominated by the regions of the Brillouin zone around $k\simeq 0$ and $\tilde{k}\simeq 0$. Auerbach and Arovas find that

$$S(q,\omega,T\to 0)=\left[\frac{4\pi\xi}{\lambda_{\mathrm{th}}}\right]^2 f(\kappa)\frac{\xi}{c}\Phi(\kappa,\nu)\ , \tag{4.33a}$$

$$f(\kappa)=\frac{\ln(\kappa+\sqrt{1+\kappa^2})}{\kappa\sqrt{1+\kappa^2}}\ , \tag{4.33b}$$

$$\Phi(\kappa,\nu)=\frac{1}{2f(\kappa)|\nu|\sqrt{\kappa^2+(\kappa^2-\nu^2)^2}}\left\{\Theta(\nu^2-\kappa^2-1)+\Theta(\kappa^2-\nu^2)\left[\frac{2}{\pi}\right]\tan^{-1}\left[|\nu|\left[\frac{\kappa^2-\nu^2}{\kappa^2+(\kappa^2-\nu^2)^2}\right]^{1/2}\right]\right\}\ . \tag{4.33c}$$

There are two contributions $[(\kappa^2>\nu^2)$ and $(\nu^2>\kappa^2+1)]$ to the scaling function Φ, which are separated by a gap. These two regions contribute equally to the normalization of $\Phi(\kappa,\nu)[\int\Phi(\kappa,\nu)d\nu=1]$. The static structure factor $S(q)=(4\pi\xi/\lambda_{\mathrm{th}})^2 f(\xi q)$ is in reasonable agreement with the semiphenomenological scaling form proposed by Tyc, Halperin, and Chakravarty (1989), as explained in Sec. VI. For $\kappa<1$ $(q^{-1}>\xi)$, the two contributions are

$$S(q,\omega>0,T)\simeq\frac{\sqrt{2}S\left[1-\frac{\epsilon}{2S}\right]}{3\tilde{q}}(n_{\tilde{q}}+1)\delta(\omega-c\tilde{q})\ , \tag{4.32}$$

where terms of order $c\tilde{q}/T$ or higher have been neglected. The quantity ϵ is the same as that defined by Eq. (2.19), and its numerical value for a square lattice is $\epsilon\simeq 0.197$. This expression is similar to the $T=0$ result obtained with the linear spin-wave theory [Eq. (2.23)] for scattering near (π,π). There is a numerical difference in the prefactor, presumably due to $1/S$ corrections and to the fact that the rotational symmetry, which is spontaneously broken in the ground state, is restored at any $T\neq 0$.

Chen and Schüttler (1989) have studied $S(\mathbf{q},\omega,T=0)$ using exact numerical diagonalization on a 4^2 periodic square lattice. They compared their results to those obtained from Eq. (4.30) for the same finite lattice and found good agreement.

Kopietz (1990b) was able to perform the integral in (4.30b) analytically in the case of low T and for wavelengths larger than the thermal de Broglie wavelength $\lambda_{\mathrm{th}}=\hbar c/T$. Since the correlation length is exponentially large for $T\to 0$, it is larger than λ_{th}. Kopietz finds that the dynamic structure function takes the scaling form

separated by a rather large gap. In this range, however, long-wavelength low-energy spin waves, having wavelengths longer than $\xi(T)$, are not well defined excitations (see Sec. VI); Kopietz notes, however, that the gap might be an artifact of the mean-field approximation. For $\kappa \gg 1$, Φ has peaks at $\kappa^2 \simeq \nu^2$, i.e., at the spin-wave energy $\omega_q = cq$ and the gap $G(\kappa)$ relative to the peak energy, i.e., $G(\kappa)/\kappa \ll 1$; the width of the peaks is $\Gamma_q/\omega_q \sim 1/q\xi$, which, as we discuss in Sec. VI, disagrees with experiment and with other more accurate calculations.

Further microscopic calculations of the dynamic structure factor would be most welcome in order to make more definite predictions about this theory at finite temperatures.

D. Path-integral formulation. Fermion representation

Affleck and Marston (1988) have used the fermion representation to perform a $1/n$ expansion. The spin-$\frac{1}{2}$ antiferromagnetic Heisenberg model in terms of the fermion operators is given by the H_2 part of the t-J model (1.1). We can write

$$H = -\frac{J}{2}\sum_{\langle ij\rangle} \hat{F}_{ij}^{\dagger}\hat{F}_{ij} + \frac{NdJ}{4} , \tag{4.34a}$$

$$\hat{F}_{ij} = c_{i\uparrow}^{\dagger}c_{j\uparrow} + c_{i\downarrow}^{\dagger}c_{j\downarrow} . \tag{4.34b}$$

Affleck and Marston generalized Eq. (4.34) to the SU(n) case by allowing for n fermion flavors. In this case

$$\hat{F}_{ij} = \sum_{\alpha=1}^{n} \hat{c}_{\alpha i}^{\dagger}\hat{c}_{\alpha j} , \tag{4.35a}$$

and the constraint is now written as

$$\frac{1}{n}\sum_{\alpha=1}^{n} \hat{c}_{\alpha i}^{\dagger}\hat{c}_{\alpha i} = S . \tag{4.35b}$$

Apart from a constant, the Hamiltonian is obtained as

$$H = -\frac{J}{n}\sum_{\langle ij\rangle} :\hat{F}_{ij}^{\dagger}\hat{F}_{ij}: . \tag{4.35c}$$

Using the coherent basis

$$|\psi_i^{\alpha}\rangle \equiv e^{\psi_i^{\alpha}\hat{c}_{\alpha i}^{\dagger}}|0\rangle , \tag{4.36}$$

where ψ_i^{α} is a Grassmann number, we obtain formally the same path-integral representation as that in Eqs. (4.5) and (4.6), with ϕ replaced by Grassmann variables ψ. Introducing a Hubbard-Stratonovich field Q_{ij} as in the boson case, we find

$$Z_{1/2} = \int D[\psi,\psi^*,Q,Q^*,\lambda] \times \exp(-S_{1/2}[\psi,\psi^*,Q,Q^*,\lambda]) , \tag{4.37a}$$

where

$$S_{1/2} = \int_0^{\beta} d\tau \left[\frac{1}{2}\sum_{i,\alpha} (\psi_i^{*\alpha}\dot{\psi}_i^{\alpha} - \dot{\psi}_i^{*\alpha}\psi_i^{\alpha}) + \frac{n}{J}\sum_{\langle ij\rangle} Q_{ij}^*Q_{ij} + \sum_{\langle ij\rangle} (Q_{ij}^*F_{ij} + Q_{ij}F_{ij}^*) + \sum_{i,\alpha} \lambda_i(\psi_i^{*\alpha}\psi_i^{\alpha} - \tfrac{1}{2}) \right] . \tag{4.37b}$$

Here $F_{ij} = \sum_{\alpha=1}^{n} \psi_i^{*\alpha}\psi_j^{\alpha}$, and antiperiodic boundary conditions at (Euclidean) times $\tau = 0$ and $\tau = \beta$ are imposed. The mean-field Hamiltonian is now given by

$$\hat{H}^{\mathrm{MF}} = \frac{n}{J}NdQ^2 - \tfrac{1}{2}nN\lambda + \lambda\sum_{i,\alpha} c_{i\alpha}^{\dagger}c_{i\alpha} + |Q|\sum_{\langle ij\rangle,\alpha} (t_{ij}c_{i\alpha}^{\dagger}c_{j\alpha} + \mathrm{H.c.}) , \tag{4.38}$$

where $Q_{ij} = Qt_{ij}$.

In one dimension, the phase factor $t_{ij} = e^{i\phi_{ij}}$ can be absorbed into the fermion operator via a local gauge transformation $c_{i\alpha} \to c_{i\alpha}e^{-i\phi_i}$, where $\phi_{ij} = \phi_j - \phi_i$. In a square lattice, however, there are two link variables t_{ij} per site and only one fermion; hence the phase transformations cannot be absorbed. The Hubbard-Stratonovich fields Q_{ij} act as gauge fields due to particle conservation at each site: a local and time-dependent gauge transformation of the fermion operators must be accompanied by a transformation of Q_{ij} in order to leave the Hamiltonian invariant. This means that the phases ϕ_{ij} act as components of a gauge field, and the sum of ϕ_{ij} around a plaquette (which corresponds to magnetic flux through the plaquette) is gauge invariant. Such compact gauge symmetries cannot be spontaneously broken on a lattice, which means that only gauge-invariant quantities have nonzero expectation values. In the simplest saddle-point solution Q_{ij} has a uniform real value on all links. However, Affleck and Marston have shown that there is another solution with lower free energy called "flux" phase. In this case the phases of all $\hat{y}$-directed links $\phi_{i,i+\hat{y}} = 0$, while those of $\hat{x}$-directed links $\phi_{i,i+\hat{x}} = \phi$ if the electron hopping in the H^{MF} is from the sublattice A to B, and $\phi_{i,i+\hat{x}} = -\phi$ if the hopping is from sublattice B to A. In this case the Hamiltonian (4.38) can be diagonalized to obtain

$$\hat{H}^{\mathrm{MF}} = \frac{n}{J}2NQ^2 - \tfrac{1}{2}nN\lambda + \sum_{\mathbf{k},\alpha}{}' (E_{\mathbf{k}}^{+}d_{\mathbf{k}\alpha,+}^{\dagger}d_{\mathbf{k}\alpha,+} + E_{\mathbf{k}}^{-}d_{\mathbf{k}\alpha,-}^{\dagger}d_{\mathbf{k}\alpha,-}) , \tag{4.39a}$$

$$E_{\mathbf{k}}^{\pm} = \lambda \pm |h_{\mathbf{k}}| , \tag{4.39b}$$

$$h_{\mathbf{k}} = 2(\cos k_y + e^{i\phi}\cos k_x) , \tag{4.39c}$$

$$d_{\mathbf{k}\alpha,\pm} = \frac{1}{\sqrt{2}}\left[\frac{h_{\mathbf{k}}}{|h_{\mathbf{k}}|}c_{\mathbf{k},\alpha}^{A} \pm c_{\mathbf{k},\alpha}^{B} \right] , \tag{4.39d}$$

where the prime to the summation symbol means that

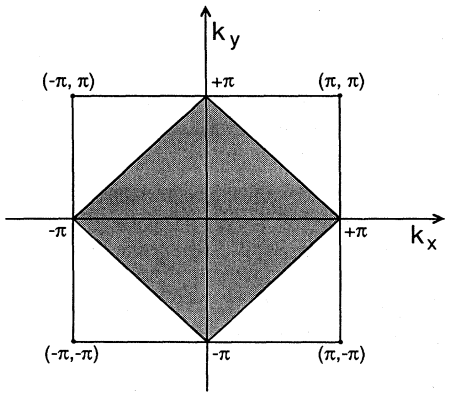

FIG. 9. The Brillouin zone of the original square lattice and the Brillouin zone (shaded area) that corresponds to the magnetic unit cell in the real space.

the sum is over the "half-Brillouin" zone, which is the square defined by the vertices at the four points $\mathbf{k}=(0,\pm\pi),(\pm\pi,0)$ (see Fig. 9), and where $c^{A}_{\mathbf{k},\alpha}(c^{B}_{\mathbf{k},\alpha})$ is the Fourier transform of the fermion operator $c_{i,\alpha}$ with i being only on the $A(B)$ sublattice and $\mathbf{k}$ taking values from the "half-Brillouin" zone.

The free energy per degree of freedom of a system of noninteracting fermions such as those described by the Hamiltonian (4.39) can be easily calculated to obtain

$$F^{\mathrm{MF}}=2Q^2-\tfrac{1}{2}\lambda-\frac{T}{2N}\sum_{\mathbf{k}}[\ln(1+e^{-E^{+}_{\mathbf{k}}/T}) +\ln(1+e^{-E^{-}_{\mathbf{k}}/T})] . \tag{4.40a}$$

The summation here is over the entire Brillouin zone. The minimum of the above free energy is obtained at

$$\phi=\frac{\pi}{2} , \tag{4.40b}$$

$$\lambda=0 , \tag{4.40c}$$

$$Q=\frac{2\sqrt{2}}{\pi^2}\int_0^1 dy\, y^2 K[2y\sqrt{1-y^2}]\tanh\left[\frac{\sqrt{2}Qy}{T}\right] . \tag{4.40d}$$

In the Baskaran, Zou, and Anderson (1987) mean-field theory, a Bogoliubov-Hartree-Fock factorization of the four-fermion J interaction in the t-J model is used, assuming that the expectation value

$$\Delta_{ij}\equiv\langle c_{i\uparrow}c_{j\downarrow}-c_{i\downarrow}c_{j\uparrow}\rangle \tag{4.41}$$

is nonzero for nearest neighbors. Later, Kotliar carried out a mean-field calculation in which allowance was made for Δ_{ij} to be different for links $\mathbf{r}_{ij}=\hat{\mathbf{x}},\hat{\mathbf{y}}$ (running in the $\hat{\mathbf{x}}$ or $\hat{\mathbf{y}}$ directions). At half-filling, he found that the s wave, i.e., $\Delta_{\hat{\mathbf{x}}}=\Delta_{\hat{\mathbf{y}}}$, and the d wave, i.e., $\Delta_{\hat{\mathbf{x}}}=-\Delta_{\hat{\mathbf{y}}}$, were equivalent. He found, however, that a mixed state having $\Delta_{\hat{\mathbf{x}}}=i\Delta_{\hat{\mathbf{y}}}$ has lower energy.

Affleck, Zou, Hsu, and Anderson (1988) have shown that the Baskaran *et al.* mean-field theory is equivalent to that of Affleck and Marston when the phase $\phi=0$. They have also shown that Kotliar's mixed phase $s+id$ is equivalent to the "flux" phase, i.e., with $\phi=0$. This was shown as a straightforward consequence of the SU(2) gauge symmetry of the Heisenberg model; these local gauge transformations, defined as

$$c^{\dagger}_{i\uparrow}\rightarrow\alpha_i c^{\dagger}_{i\uparrow}+\beta_i c_{i\downarrow} , \tag{4.42a}$$

$$c_{i\downarrow}\rightarrow-\beta^{*}_i c^{\dagger}_{i\uparrow}+\alpha^{*}_i c_{i\downarrow} , \tag{4.42b}$$

with the constraint $|\alpha_i|^2+|\beta_i|^2=1$, mix particles of spin σ and holes of spin $-\sigma$. Under such local gauge transformations the spin-$\frac{1}{2}$ antiferromagnetic Heisenberg model remains invariant. The three independent parameters in these transformations give rise to the three generators of SU(2) local gauge symmetry. Note that the U(1) gauge symmetry, sometimes discussed for this model, is a subgroup of the SU(2) transformation obtained by setting $\beta_i=0$. Using the transformation $c_{i\uparrow}\rightarrow c^{\dagger}_{i\downarrow}$ and $c_{i\downarrow}\rightarrow-c^{\dagger}_{i\uparrow}$, the order parameter Δ_{ij} transforms to the Affleck and Marston Hubbard-Stratonovich field as

$$\Delta_{12}\rightarrow Q^{*}_{12},\quad \Delta_{23}\rightarrow Q_{23} ,\quad \Delta_{43}\rightarrow Q_{43},\quad \Delta_{14}\rightarrow Q^{*}_{14} . \tag{4.43}$$

It is interesting that the Baskaran, Zou, and Anderson mean-field theory, which assumes $\phi=0$, is unstable against the "flux" phase. However, the free energy for the "flux" phase at $T=0$ is $E^{\mathrm{MF}}\simeq-0.458n$, which is higher than that obtained in Schwinger boson mean-field theory or spin-wave theory, i.e., $E^{\mathrm{SWT}}=-0.671n$. However, the "flux" phase could be a better starting point when a fraction of holes is present and the antiferromagnetic long-range order is absent, as discussed by Marston and Affleck (1989) and by Nori, Abrahams, and Zimanyi (1990).

The quasiparticle spectrum in the "flux" phase is given by

$$E^{\pm}_{\mathbf{k}}=\pm 2Q\sqrt{\cos k_x^2+\cos k_y^2} , \tag{4.44}$$

with zero gap at the four points $\mathbf{k}=(\pm\pi/2,\pm\pi/2)$. Only the dispersion relation for particle-hole excitations is meaningful. At these four points of the Brillouin zone the density of states vanishes linearly, the specific heat at low T is $C\sim T^2$, and the susceptibility $\chi\sim T$. The structure factor $S(\mathbf{q})$ is nondivergent at $T=0$. The spin correlation function decays algebraically with distance. In Fig. 10(a), we give the instantaneous spin-spin correlation function

$$\langle\mathbf{S}_{\mathbf{q}}\cdot\mathbf{S}_{-\mathbf{q}}\rangle=\int d\omega\,\langle\mathbf{S}_{\mathbf{q}}(\omega)\cdot\mathbf{S}_{-\mathbf{q}}(0)\rangle , \tag{4.45a}$$

and in Fig. 10(b) a low-energy correlation function defined as

$$\langle\mathbf{S}_{\mathbf{q}}\cdot\mathbf{S}_{-\mathbf{q}}\rangle_{\Delta}=\int d\omega\, e^{-\omega^2/2\Delta^2}\langle\mathbf{S}_{\mathbf{q}}(\omega)\cdot\mathbf{S}_{-\mathbf{q}}(0)\rangle , \tag{4.45b}$$

as computed by Marston and Affleck (1989). The low-

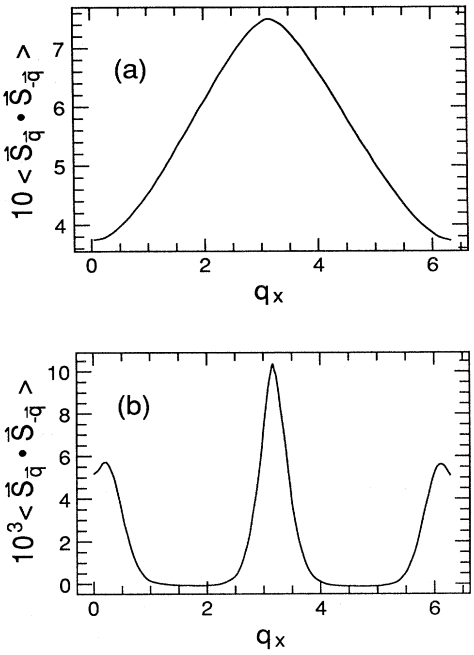

FIG. 10. (a) The instantaneous spin-spin correlation function (structure factor) in the "flux" phase, as calculated by Marston and Affleck (1989). (b) The low-energy correlation function, as defined by Eq. (4.45b) using $\Delta=0.14J$.

energy correlation is used for illustration purposes and because, in the neutron scattering experiments, one has to use a cutoff (in these plots the value of $\Delta=0.14J$ is used). There is a peak at (π,π) in both the Baskaran-Zou-Anderson uniform phase and in the "flux" phase. In the low-energy correlation function there are peaks at $(0,\pi)$ and $(\pi,0)$. In the neutron scattering experiments from the undoped La_2CuO_4, the instantaneous correlation function has a sharp peak at (π,π), whose width, however, is only 5% of the zone width. Furthermore, it is not sensitive to the energy cutoff and there are no peaks at other points.

Arovas and Auerbach (1988) find that if they allow t_{ij} to acquire a phase in their Schwinger boson mean-field calculation, the energy of the uniform link field $Q=|Q|$ is lower. This makes the conventional antiferromagnetic ordered ground state the lowest free-energy state.

E. Path-integral formulation. Nonlinear σ model

In this part we derive the path-integral representation of the partition function of the antiferromagnetic Heisenberg model using coherent states for spins. From this representation we can pass to the continuum limit, where the quantum-mechanical nonlinear σ model in two space and one time dimension is obtained as a field-theoretical model that describes smooth spin fluctuations. In this formulation the state of a spin at a given site is expressed in the following coherent basis:

$$|\Omega\rangle \equiv |\theta,\phi\rangle \equiv e^{-i\phi(\hat{S}_z - S)} e^{-i\theta \hat{S}_y} |S\rangle \ , \tag{4.46}$$

where Ω is a vector on the unit sphere with spherical coordinates $(1,\theta,\phi)$, $0\le\theta<\pi$ and $0\le\phi<2\pi$, and the state $|S\rangle$ is the eigenstate of $\hat{S}_z$ with the largest possible eigenvalue S. Note that with the definition (4.46) we have established a one-to-one correspondence between coherent states and points on the unit sphere except for the case of the south pole. This is a singular point of the mapping, since all the states $|\theta=\pi,\phi\rangle = e^{2S\phi}|-S\rangle$ differ from one another by only a phase factor and correspond to the south pole. We need to calculate the matrix elements of the unit operator and the Hamiltonian (1.2) in order to write down the partition function in the basis (4.46). We shall follow an elementary procedure to do this; the state (4.46) can be written as

$$|\Omega\rangle = \sum_{m=-S}^{S} C_m(\theta,\phi)|m\rangle \ , \tag{4.47a}$$

where $|m\rangle$ is the eigenstate of $\hat{S}_z$ with eigenvalue m and

$$\begin{aligned} C_m(\theta,\phi) &= e^{i(S-m)\phi}\langle m|e^{-i\theta\hat{S}_y}|S\rangle \\ &= e^{-im\phi}\left[\frac{(2S)!}{(S+m)!(S-m)!}\right]^{1/2} \\ &\quad\times\left[\sin\frac{\theta}{2}\right]^{S-m}\left[\cos\frac{\theta}{2}\right]^{S+m} . \end{aligned} \tag{4.47b}$$

A proof of the above equation can be found in Baym's *Lectures in Quantum Mechanics* (1969, p. 386). Therefore it follows that

$$\begin{aligned} \langle\Omega'|\Omega\rangle &= \sum_{m=-S}^{S} \frac{(2S)!}{(S+m)!(S-m)!}\left[e^{-i(\phi'-\phi)}\sin\frac{\theta}{2}\sin\frac{\theta'}{2}\right]^{S-m}\left[\cos\frac{\theta}{2}\cos\frac{\theta'}{2}\right]^{S+m} \\ &= \left[\cos\frac{\theta}{2}\cos\frac{\theta'}{2}+e^{-i(\phi'-\phi)}\sin\frac{\theta}{2}\sin\frac{\theta'}{2}\right]^{2S} . \end{aligned} \tag{4.47c}$$

Let us write

$$\langle\Omega'|\Omega\rangle = |\langle\Omega'|\Omega\rangle| e^{-i\Phi} \ , \tag{4.48a}$$

and it can be easily verified that

$$|\langle\Omega'|\Omega\rangle| = [\tfrac{1}{2}(1+\Omega'\cdot\Omega)]^S . \tag{4.48b}$$

Assuming smooth paths in imaginary time, i.e., that the vectors Ω and Ω' are close, we obtain

$$\Phi=(1-\cos\theta)\Delta\phi+\cdots \tag{4.48c}$$

where the ellipsis stands for higher-order terms in $\Delta\phi$ and $\Delta\theta$. Notice that Φ coincides with the area of the spherical triangle formed by the north pole and the tips of the unit vectors Ω and Ω'. Inserting the resolution of the identity operator

$$I=\int\frac{d\Omega}{4\pi}|\Omega\rangle\langle\Omega| \tag{4.49a}$$

at each site and writing $e^{-\beta\hat{H}}=\prod_{i=1}^{M}(1-\epsilon\hat{H})$, with $\beta=M\epsilon$, the partition function Z takes the form

$$Z=\int[D\Omega]\prod_{i=1}^{M}\langle\Omega_1(\tau_i+\epsilon)\cdots\Omega_N(\tau_i+\epsilon)|1-\epsilon\hat{H}|\Omega_1(\tau_i)\cdots\Omega_N(\tau_i)\rangle\ . \tag{4.49b}$$

The real part of the overlap between neighboring (in time) coherent states is

$$|\langle\Omega'|\Omega\rangle|=\exp[S\ln(1-\tfrac{1}{4}|\Omega'-\Omega|^2)]$$
$$\simeq\exp\left[-\frac{S}{4}\left[\frac{\partial\Omega}{\partial\tau}\right]^2\epsilon^2\right]\ . \tag{4.50}$$

Furthermore, it is straightforward to show that

$$\langle\Omega|\hat{\mathbf{S}}|\Omega\rangle=S\Omega\ , \tag{4.51a}$$

from which it follows that

$$H\equiv\langle\{\Omega_i\}|\hat{H}|\{\Omega_i\}\rangle=S^2J\sum_{\langle ij\rangle}\Omega_i\cdot\Omega_j\ . \tag{4.51b}$$

Hence the partition function is given by

$$Z=\int[D\Omega]\exp\left[-iS\int_0^\beta(1-\cos\theta)d\phi\right.$$
$$\left.-S^2J\int_0^\beta\sum_{\langle ij\rangle}\Omega_i\cdot\Omega_j d\tau\right]\ . \tag{4.52}$$

The first term is the total solid angle α_i, which is the area of the closed trajectory of the vector $\Omega_i(\tau)$ characterizing the state of the ith spin to start from the north pole and end up at the same point at $\tau=\beta$, as shown in Fig. 11. Using Stokes' theorem, we can write the area on the sphere as $\int\int\Omega\cdot\Omega d\sigma=\oint\mathbf{A}\cdot d\Omega$, where $d\sigma$ is the surface element of the sphere and the vector potential $\mathbf{A}$ is given as a solution to the equation

$$\nabla_\Omega\times\mathbf{A}(\Omega)=\Omega\ . \tag{4.53}$$

The vector potential $\mathbf{A}(\Omega)$ is known up to a gauge transformation $\mathbf{A}\rightarrow\mathbf{A}+\nabla_\Omega\lambda$. The phase factor $iS\alpha_i$ is also known as the Berry phase (Berry, 1984) for the adiabatic motion of a quantum spin.

Haldane (1988) has derived a continuum field theory of the 2D Heisenberg antiferromagnet using the coherent spin-basis representation (4.52) as follows. The Fourier expansion of the field Ω_i can be written as

$$\Omega_i(\tau)=\sum_{HBZ}\mathbf{a}_\mathbf{k}(\tau)e^{i\mathbf{k}\cdot\mathbf{r}_i}+(-1)^{\|\mathbf{r}_i\|}\sum_{HBZ}\mathbf{b}_\mathbf{k}(\tau)e^{i\mathbf{k}\cdot\mathbf{r}_i}\ , \tag{4.54}$$

where the entire Brillouin zone has been divided into two parts as shown in Fig. 9. The first is the square with vertices $(\pm\pi,\pm\pi)$ and the second part consists of the other four pieces. The summation is over the first half-Brillouin zone. The other four pieces can be shifted by one of the four vectors $(\pm\pi,\pm\pi)$ to the origin. The factor $(-1)^{\|\mathbf{r}_i\|}$ with $\|\mathbf{r}_i\|=x_i+y_i$ comes from the phase factor $e^{i(\pm\pi,\pm\pi)\cdot\mathbf{r}_i}$ as a result of the shift. All the coefficients $\mathbf{a}_\mathbf{k}$ and $\mathbf{b}_\mathbf{k}$ are of order $1/N$, except $\mathbf{b}_\mathbf{k}$ for $\mathbf{k}=0$ which, if there is Néel order, is of order 1. In an antiferromagnet, smooth paths can be written as combination of two fields,

$$\Omega_i(\tau)\simeq(-1)^{\|\mathbf{r}_i\|}\left[1-\left[\frac{a^d\mathbf{L}_i(\tau)}{S}\right]^2\right]^{1/2}\mathbf{n}_i(\tau)$$
$$+\frac{a^d}{S}\mathbf{L}_i(\tau)\ , \tag{4.55}$$

where $\mathbf{n}_i(\tau)$ is a slowly varying field that describes fluctuations around the corners of the original Brillouin zone, and the second slowly varying field $\mathbf{L}_i(\tau)$ describes fluctuations around $\mathbf{k}=0$, both being low-energy fluctuations; $\mathbf{L}_i(\tau)$ takes into account fluctuations of the local ferromagnetic spin density. The square-root normalization factor puts $\mathbf{n}_i(\tau)$ on the unit sphere. In the original Hamiltonian formulation of the model, the field $\mathbf{n}$ corresponds to the local expectation value of the staggered magnetization operator and $\mathbf{L}$ to the total spin in a small

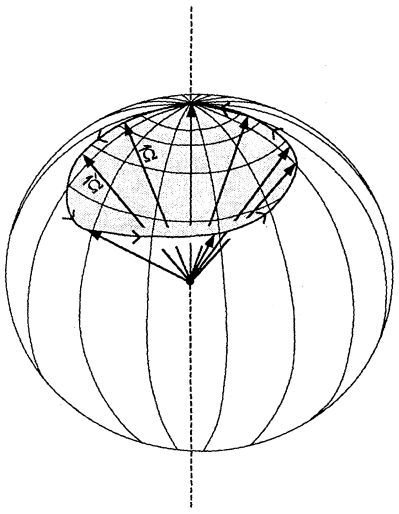

FIG. 11. The trajectory of the unit vector $\Omega(\tau)$ on the unit sphere during the Euclidean "time" evolution in the nonlinear σ model.

region of space containing a large number of microscopic degrees of freedom. Therefore $\mathbf{L}$ is the generator of rotations in spin space and satisfies the constraint $\mathbf{L}\cdot\mathbf{n}=0$. Substituting Eq. (4.55) in the expression for the Berry phase, expanding about the Néel state, and keeping terms quadratic in $\mathbf{L}$ and $\nabla\mathbf{n}$, we obtain

$$S\sum_i(-1)^{\|i\|}\Sigma(\mathbf{n}_i)+\int d^dx\int_0^\beta d\tau(\mathbf{n}\cdot\partial_\tau\mathbf{n}\times\mathbf{L})\ , \tag{4.56}$$

where $\Sigma(\mathbf{n})$ is the area covered by the unit vector $\mathbf{n}$ on the unit sphere during the entire Euclidean time evolution. Furthermore, substituting Eq. (4.55) in (4.51b) and keeping terms up to order $|\nabla n|^2$ and L^2, we obtain

$$H=\tfrac{1}{2}\int d^dr\left[\frac{|\mathbf{L}|^2}{\chi_\perp^0}+\rho_s^0|\nabla\mathbf{n}|^2\right], \tag{4.57}$$

where $\chi_\perp^0$ and ρ_s^0 are the bare perpendicular susceptibility and spin-stiffness constant. These constants at the cutoff level are given by $\rho_s^0=JS^2a^{2-d}$ and $\chi_\perp^0=1/4dJa^d$, and they are correct in the classical limit $S\to\infty$. The resulting action is quadratic in the field $\mathbf{L}$, which can be integrated out to yield the nonlinear σ model,

$$Z=\int[D\mathbf{n}]\exp\left[-\frac{\rho_s^0}{2}\int_0^\beta d\tau\,d^dr(|\nabla\mathbf{n}|^2+c_\sigma^{-2}|\partial_\tau\mathbf{n}|^2)+i\Theta\right], \tag{4.58}$$

where $c_\sigma=\sqrt{\rho_s^0/\chi_\perp^0}=2\sqrt{d}\,SJa$ is the bare spin-wave velocity. Here Θ is the purely topological part of the Berry phase $\Theta=S\sum_i(-1)^{\|i\|}\Sigma(\mathbf{n}_i)$.

The nonlinear σ model can be derived directly from the spin-operator representation of the Heisenberg model (Affleck, 1985, 1986, 1988) by changing variables and taking the large-S continuum limit. In one dimension and in the continuum, the Berry phase can be interpreted as $\Theta=S/2\int dx\,(\partial_x\Sigma)$, which is equal to $S/2$ times the area of the unit sphere. Therefore this phase distinguishes integer- from half-integer-spin chains and, in the case of half-integer-spin chains, we have fermion (topological) excitations due to the Berry phase factor of $e^{i\pi}$. The dynamics of such configurations can lead to destructive quantum interference between the paths because of the antisymmetry with respect to the interchange of these neutral fermions. Hence the continuum limit of the antiferromagnetic Heisenberg spin chain is a different field theory for integer and half-integer spins.

In $2+1$ or higher dimensions this phase vanishes for smooth configurations. In $2+1$ dimensions, assuming smooth configurations, the phase Θ can be interpreted as $\Theta=S\sum_y(-1)^y\Theta_y$, where $\Theta_y=\int dx\,(\partial_x\Sigma(n(x,y,\tau))$. For a continuous field $\mathbf{n}(x,y,\tau)$, Θ_y is a continuous function of y and, since it can only take integer multiples of 4π, it must be a constant. Therefore Θ vanishes in $2+1$ dimensions. This result, obtained by Haldane (1988), shows that the conjecture of Dzyaloshinskii, Polyakov, and Wiegmann (Dzyaloshinskii *et al.*, 1988; Polyakov, 1988; Wiegmann, 1988) of the existence of a Hopf term that distinguishes half-integer from integer spins in $2+1$ dimensions cannot be justified on the basis of the quantum antiferromagnetic Heisenberg model. Several other authors (Dombre and Read, 1988; Fradkin and Stone, 1988; Ioffe and Larkin, 1988; Wen and Zee, 1988) have given arguments leading to similar conclusions.

The quantum nonlinear sigma model can be introduced using arguments based on more general grounds. As long as the continuous $O(3)$ symmetry is spontaneously broken, the symmetry of the problem requires that the interaction of the Goldstone modes of the system in the long-wavelength limit be described by this model regardless of the details of the microscopic Hamiltonian and the value of the spin (Shankar, 1989a; Rosenstein *et al.*, 1989). Thus the quantum nonlinear σ model on its own deserves further study, with or without the addition of holes in the model (Shankar, 1989a, 1989b; Bitar and Manousakis, 1991).

F. Renormalization-group calculations

In this section we discuss the renormalization-group approach of Chakravarty, Halperin, and Nelson (1988, 1989). We shall outline the approach and certain main results; for more details the reader is referred to the long paper of Chakravarty *et al.* (1989). In addition, for a discussion of certain aspects of the critical behavior of quantum spin systems the reader is referred to a review article by Hertz (1976). First we discuss their one-loop calculation. Chakravarty *et al.* regularize the integrals by introducing a momentum cutoff Λ. The partition function (4.58) of the σ model with $\Theta=0$ can be written as

$$Z=\int\prod_{\mathbf{x},x_0}d\mathbf{n}(\mathbf{x},x_0)\delta[|\mathbf{n}(\mathbf{x},x_0)|^2-1]\exp\left[-\frac{1}{2g_0}\int_0^u dx_0\int d^dx(|\nabla\mathbf{n}|^2+|\partial_{x_0}\mathbf{n}|^2)+h\int_0^u\int dx_0\,d^dx\,\sigma(\mathbf{x},x_0)\right], \tag{4.59}$$

where the space and "time" coordinates have been rescaled, respectively, as $\mathbf{x}=\Lambda\mathbf{r}$ and $x_0=\tau c_\sigma\Lambda$, and

$$g_0\equiv\frac{\hbar c_\sigma\Lambda^{d-1}}{\rho_s^0}\ , \tag{4.60a}$$

$$u\equiv\beta c_\sigma\Lambda\ , \tag{4.60b}$$

so that in Eq. (4.59) all the parameters are dimensionless. The field $\sigma(\mathbf{x},x_0)$ is one of the components of the vector field $\mathbf{n}(\mathbf{x},x_0)\equiv(\boldsymbol{\pi}(\mathbf{x},x_0),\sigma(\mathbf{x},x_0))$ coupled to the external field h; $\boldsymbol{\pi}(\mathbf{x},x_0)$ is an $M-1$ component field (for the case of our interest $M=3$). Integrating out the σ field, we obtain higher-order terms in the $\boldsymbol{\pi}$ field due to the δ function, which expresses the constraint

$$Z=\int\prod_{\mathbf{x},x_0}\frac{d\boldsymbol{\pi}(\mathbf{x},x_0)}{\sqrt{1-\boldsymbol{\pi}^2(\mathbf{x},x_0)}}\exp\left[-\frac{1}{2g_0}\int_0^u dx_0\int d^dx\left[(\partial_\mu\boldsymbol{\pi})^2+\frac{(\boldsymbol{\pi}\cdot\partial_\mu\boldsymbol{\pi})^2}{1-\boldsymbol{\pi}^2}\right]+h\int_0^u dx_0\,d^dx\sqrt{1-\boldsymbol{\pi}^2}\right]. \tag{4.61}$$

The field $\boldsymbol{\pi}$ can be Fourier expanded as follows:

$$\boldsymbol{\pi}(\mathbf{x},x_0)=\sum_{n=-\infty}^{n=\infty}\int\frac{d^dk}{(2\pi)^d}\boldsymbol{\pi}(\mathbf{k},\omega_n)\exp(i\mathbf{k}\cdot\mathbf{x}+i\omega_n x_0) \tag{4.62}$$

where $k<1$ (because we have rescaled the space coordinates by Λ) and the Matsubara frequencies are $\omega_n=2\pi n/u$ with $n=0,\pm1,\pm2,\ldots$. The factors $(1-\boldsymbol{\pi}^2)^{-1}$ and $\sqrt{1-\boldsymbol{\pi}^2}$ can be expanded to obtain vertices such as $\boldsymbol{\pi}^2,(\boldsymbol{\pi}\cdot\partial_\mu\boldsymbol{\pi})^2,((\boldsymbol{\pi})^2)^2,\boldsymbol{\pi}^2(\boldsymbol{\pi}\cdot\partial_\mu\boldsymbol{\pi})^2,\ldots$. Following Wilson and Kogut (1975) and Nelson and Pelcovits (1977), Chakravarty *et al.* (1988) break up the $\boldsymbol{\pi}$ degrees of freedom as

$$\boldsymbol{\pi}(\mathbf{k},\omega_n)=\begin{cases}\boldsymbol{\pi}_<(\mathbf{k},\omega_n), & 0<k<e^{-l},\\ \boldsymbol{\pi}_>(\mathbf{k},\omega_n), & e^{-l}<k<1,\end{cases} \tag{4.63}$$

and integrate out the fast degrees of freedom $\boldsymbol{\pi}_>$, keeping terms up to one-loop order in perturbation theory. How one carries out such a procedure is described in the pedagogical review paper by Wilson and Kogut (1975) for the one-component case and for the classical $O(3)$ 2D model by Nelson and Pelcovits (1977) and Polyakov (1975). After completion of such integration the effective action involves only $\boldsymbol{\pi}_<$. Let us rescale the k's so that their range is $0<k\le1$ and the field $\boldsymbol{\pi}$ by a renormalization factor ζ, i.e.,

$$\mathbf{k}'=\mathbf{k}e^{l}, \tag{4.64a}$$

$$\boldsymbol{\pi}'=\boldsymbol{\pi}_</\zeta, \tag{4.64b}$$

so that the effective action takes the same form as the expanded form of Eq. (4.61). The new parameters must be defined as

$$u'=ue^{-l}, \tag{4.65a}$$

$$\frac{u'}{g_0'}=\zeta^2e^{-(d+2)l}\left[\frac{u}{g_0}+I\right], \tag{4.65b}$$

$$h'u'=\zeta^2e^{-dl}[hu+\tfrac{1}{2}hg_0(M-1)I], \tag{4.65c}$$

where

$$I=\sum_{n=-\infty}^{\infty}\int_>\frac{d^dk}{(2\pi)^d}\frac{1}{k^2+\omega_n^2+hg_0}=\frac{K_du}{2}\int_{e^{-l}}^1 dk\frac{k^{d-1}}{\sqrt{k^2+hg_0}}\coth\left[\frac{u}{2}\sqrt{k^2+hg_0}\right]. \tag{4.65d}$$

Here I is the one-loop integral and $K_d^{-1}=2^{d-1}\pi^{d/2}\Gamma(d/2)$. Hence the dimensionless slab thickness u in the imaginary direction scales trivially. The spin rescaling factor ζ is determined such that the external field term also transforms trivially under momentum-space renormalization-group transformations, i.e., $h'u'=\zeta hu$, so we obtain

$$\zeta=e^{dl}\left[1-\frac{g_0}{2u}(M-1)I\right]. \tag{4.66}$$

Setting the external field to zero, one finds the following equations:

$$\frac{dg}{dl}=(1-d)g+\frac{K_d}{2}(M-2)g^2\coth(g/2t), \tag{4.67a}$$

$$\frac{dt}{dl}=(2-d)t+\frac{K_d}{2}(M-2)gt\coth(g/2t), \tag{4.67b}$$

where $t\equiv g/u=k_BT\Lambda^{d-2}/\rho_s$. The dimensionless slab thickness is obtained as $du/dl=-u$. These differential equations can be solved subject to the initial conditions $t=t_0\equiv k_BT\Lambda^{d-2}/\rho_s^0$ and $g=g_0$ [Eq. (4.60a)].

It is straightforward to see, using Eq. (4.67a), that at $T=0$ there is a fixed point at $g=g_c$ for $d>1$ and $M=3$ given by

$$g_c(d>1)=\frac{2(d-1)}{K_d}. \tag{4.68a}$$

Furthermore, from Eq. (4.67b) we see that for $d\le2$ there is no finite-temperature fixed point, while for $d>2$ there is a fixed point at

$$t_c(d>2)=\frac{d-2}{K_d}. \tag{4.68b}$$

In Fig. 12(a) we show the renormalization-group flows for $d\ge3$. The shaded region is characterized by long-range order. For $d\to2^+$, $t_c\to0$ and the shaded area collapses to a line as shown in Fig. 12(b). From now on we focus on the $d=2$ case. The renormalization-group flows are also shown in Fig. 12. At $T>0$, there is no long-range order, as expected. At $T=t=0$, there is a nontrivial critical point at g_c given by Eq. (4.68a) that separates the ordered from the disordered phase.

It is straightforward to solve Eqs. (4.67a) and (4.67b) with initial conditions $t(l=0)=t_0$ and $g(l=0)=g_0$; for $d=2$ and $M=3$ we find

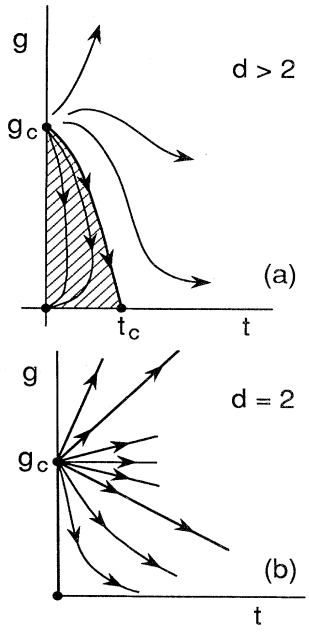

FIG. 12. (a) The phase diagram and the renormalization-group flow in the nonlinear σ model in more than two space dimensions. (b) The same as part (a) in two space dimensions.

$$\frac{\bar{g}}{\bar{g}_0}=\frac{\bar{t}}{\bar{t}_0}e^{-l}, \tag{4.69a}$$

$$e^{-l}=\frac{\bar{t}_0}{\bar{g}_0}\sinh^{-1}\left[\sinh\left[\frac{\bar{g}_0}{\bar{t}_0}\right]\exp\left[\frac{1}{\bar{t}}-\frac{1}{\bar{t}_0}\right]\right], \tag{4.69b}$$

where we have defined $\bar{g}=g/g_c=g/4\pi$, $\bar{g}_0=g_0/4\pi$, $\bar{t}=t/2\pi$, and $\bar{t}_0=t_0/2\pi$. The renormalized correlation length is given by $\xi(l)=\xi e^{-l}$, where ξ is the correlation length when $l=0$.

For $\bar{g}<1+\bar{t}$ (i.e., at $T=0$, $\bar{g}>1$), $d\bar{g}/dl<d\bar{t}/dl$ and hence $\bar{t}$ grows faster than $\bar{g}$. In this regime we let l^* be such that $\bar{t}(l^*)=1$ and we define $\xi^*=\xi(l^*)$. At the temperature $\bar{t}=1$ the thermal de Broglie wavelength $\hbar c/k_BT$ is small, and the correlation length is of the order of the lattice spacing. However, the precise value of ξ^* cannot be determined with the renormalization-group method. In this case $\xi=\xi^* e^{l^*}$, and we find

$$\xi^{-1}=\frac{2}{C^*}\left[\frac{k_BT}{\hbar c}\right]\sinh^{-1}\left[\sinh\left[\frac{\bar{g}_0}{\bar{t}_0}\right]\exp\left[1-\frac{1}{\bar{t}_0}\right]\right], \tag{4.70}$$

where $C^*\equiv\xi^*\Lambda$ is a dimensionless number that cannot be determined within the renormalization-group approach. Therefore the value of the prefactor depends on the value of the correlation length at the matching point; the result depends weakly on the matching condition, as Chakravarty, Halperin, and Nelson have pointed out. The actual value of C^* must be supplied and cannot be determined within the renormalization-group method alone, since it is a function of the constant of integration of the renormalization-group differential equations. At the critical point $\bar{g}_0=1$, and for low T we find

$$\xi(\bar{g}_0=1)\simeq C_{\rm cr}\frac{\hbar c}{k_BT}, \tag{4.71}$$

where $C_{\rm cr}=\ln[e/2+\sqrt{1+(e/2)^2}]C^*/2$. When $\bar{g}_0<1$ and $\bar{t}_0\to 0$, from Eq. (4.70) we obtain

$$\xi(\bar{g}_0<1)\simeq D\frac{\hbar c}{k_BT}\exp\left[\frac{2\pi\rho_s}{k_BT}\right], \tag{4.72}$$

where $D=C^*/e$, and where we have defined

$$\rho_s=\rho_s^0(1-\bar{g}_0). \tag{4.73}$$

Chakravarty, Halperin, and Nelson show that the $T=0$ renormalized spin stiffness in one-loop perturbation theory is given by Eq. (4.73), and the renormalized perpendicular susceptibility also is given by $\chi_\perp=\chi_\perp^0(1-\bar{g}_0)$. They also note that the form (4.71) approximates the behavior of the correlation length in the regime $1-\bar{t}<\bar{g}<1+\bar{t}$ called the *quantum critical* regime (see Hertz, 1976). Note that in the quantum critical regime the correlation length is controlled by the fixed point at $\bar{g}=1$. The regime $\bar{g}<1-\bar{t}$, where $\xi(T)$ is given by Eq. (4.72), is called the *renormalized classical* region, and the exponential behavior of the correlation length is the same as in the classical model with a renormalized value of the ρ_s.

In the regime $\bar{g}>1+\bar{t}$ (i.e., at $T=0$, $\bar{g}>1$), $d\bar{g}/dl>d\bar{t}/dl$ and hence $\bar{g}$ grows faster than $\bar{t}$. In this case we define l^* such that $\bar{g}(l^*)=2$ and let the value of ξ at this value of l^* be ξ^*, that is, $\xi^*\equiv\xi(l^*)$. The value of $g(l^*)$ needs to be any value significantly larger than 1, so that ξ^* is of the order of the lattice spacing. The value of $\bar{g}=2$ is chosen for convenience. In this case, as $t\to 0$ we find

$$\xi(\bar{g}_0>1)\simeq\frac{\xi^*}{2}\frac{\bar{g}_0}{(\bar{g}_0-1)+\bar{t}_0\exp\left[-4\left[\frac{\bar{g}_0-1}{\bar{t}_0}\right]\right]}. \tag{4.74}$$

Notice that in this case the correlation length tends to a constant as $T\to 0$, and the leading correction to the constant value at low T is exponentially small ($\sim Te^{-{\rm const}/T}$). This regime is characterized by a finite correlation length even at $T=0$ because the quantum fluctuations are so strong that they destroy the long-range order. This is a regime controlled by the *quantum disordered* phase, and there are crossover lines separating the three regimes.

The reader may notice that the correlation length ξ given by Eq. (4.72) in the regime controlled by the $T=0$ ordered phase coincides with that given in Sec. IV.C by Eq. (4.28b) obtained with either the Schwinger boson mean-field theory or Takahashi's variational approach, which are variants of spin-wave approximation. Howev-

er, as Chakravarty *et al.* suggest, the prefactor of the exponential will be canceled by higher-order corrections. Such corrections are of two-loop order in the renormalization-group approach. Hence Takahashi's attempt to fit the neutron scattering data with a $1/T$ prefactor gives a somewhat underestimated value for the antiferromagnetic coupling J. We discuss such corrections next.

In the *renormalized classical* regime, the physical meaning of Eq. (4.72) is that at $T\rightarrow 0$ the system behaves as a classical 2D spin system with a spin-stiffness constant reduced by zero-temperature quantum fluctuations to a value given by Eq. (4.73). It is plausible to assume that higher-order perturbative corrections would not destroy this picture. Let us split off the zero-frequency mode from the rest,

$$\pi(\mathbf{k},\omega_n)=\begin{cases}\pi_<(\mathbf{k}), & \omega_n=0\ ,\\ \pi_>(\mathbf{k},\omega_n), & \omega_n\neq 0\ .\end{cases} \tag{4.75}$$

The non-zero-frequency components can be integrated out in the one-loop approximation, in the same way as in the momentum-shell integration, to obtain the classical effective action

$$S_{\rm cl}=\frac{1}{2g'}\int d^2x\,(\nabla\bar{n})^2\ , \tag{4.76}$$

where $\bar{n}(\mathbf{x})$ is a Euclidean time average (zero-frequency component) of the field $\mathbf{n}(\mathbf{x},x_0)$, which is still normalized on the surface of the unit sphere. The effective coupling constant g' is given by

$$\frac{1}{g'}=\frac{1}{k_BT}\left[\rho_s+\frac{k_BT(M-2)}{2\pi}\ln\left[\frac{\Lambda\hbar c}{k_BT}\right]+O(T^2)\right]\ , \tag{4.77}$$

where ρ_s is the zero-temperature spin-stiffness constant renormalized by quantum fluctuations and given by Eq. (4.73).

The model (4.76) in 2D is the classical nonlinear σ model, which has been extensively studied by elementary-particle theorists (for a review, see Kogut, 1983) because it is believed to share intimately aspects of asymptotic freedom, dynamical mass generation via dimensional transmutation, and topological instanton excitations with quantum chromodynamics. For example, the renormalization-group β function has been calculated to high order in weak-coupling perturbation theory, and up to two loops is given by (Creutz, 1983)

$$\frac{dg'}{dl}=\beta_2 g'^2+\beta_3 g'^3+\cdots\ , \tag{4.78}$$

where $\beta_2=(M-2)/2\pi$ and $\beta_3=(M-2)/(2\pi)^2$. Integrating these equations, in a way similar to the one-loop case, we can find the correlation length up to an integration constant

$$\xi=\frac{C_m}{\Lambda}g'^{\beta_3/\beta_2^2}e^{1/\beta_2 g'}\ . \tag{4.79}$$

Again the constant C_m/Λ cannot be determined within the renormalization-group approach, and direct calculation of the correlation function at a given value of the coupling constant is required.

Chakravarty, Halperin, and Nelson used the classical Monte Carlo calculation of Shenker and Tobochnik (1980) to determine the constant C_m. However, Shenker and Tobochnik used a lattice regularization of the model (4.76), while Chakravarty *et al.* used a momentum-space regularization. Parisi (1980) has given a prescription that relates two constants C_1 and C_2 obtained in two different regularization schemes by holding ξ fixed and relating the two different values of the coupling constant at the one-loop level. More specifically, he calculated C_1/C_2 for lattice and Pauli-Villars regularizations. Chakravarty *et al.* used this approach to calculate the ratio of the constants C_L for lattice and C_m for momentum-space regularization schemes. With the aid of this formula and the value of the constant C_L obtained by the lattice calculation of Shenker and Tobochnik, Chakravarty *et al.* determined the approximate value of the C_m. The details of this calculation are given by Chakravarty *et al.* (1989), and we shall omit them here.

Substituting the values of β_2,β_3, and g' for $n=3$ in Eq. (4.79), one obtains the expression

$$\xi=C_\xi\exp\left[\frac{2\pi\rho_s}{k_BT}\right]\ , \tag{4.80}$$

with $C_\xi=C_m\hbar c/\rho_s$.

The constant C_ξ is determined in Sec. V directly, using the results of the direct Monte Carlo simulation of the quantum nonlinear σ model. There, it will be demonstrated that the temperature dependence of the correlation length obtained from both the spin-$\frac{1}{2}$ antiferromagnetic Heisenberg model and the quantum nonlinear σ model agrees with Eq. (4.80) and disagrees with the results of the one-loop calculation of Chakravarty *et al.* and the other low-order calculations.

G. Saddle-point approximation for the quantum nonlinear σ model

In this section we calculate the correlation length using a saddle-point approximation. In order to compare the results of the saddle-point approximation with the results of Monte Carlo simulation, we regularize the quantum nonlinear σ model by putting the theory on the $2+1$ dimensional lattice

$$S_\sigma=-\frac{1}{2g}\sum_{\mathbf{x}}\sum_{\mu=1}^{3}\mathbf{n}_l(\mathbf{x})\cdot[\mathbf{n}_l(\mathbf{x}+\hat{\mathbf{e}}_\mu)+\mathbf{n}_l(\mathbf{x}-\hat{\mathbf{e}}_\mu)]\ , \tag{4.81}$$

where $\mathbf{x}$ covers the $2+1$ dimensional space-time lattice of size L^2L_β and lattice spacing a, that is, $x_1,x_2=1,2,\ldots,L$ and $x_3=1,2,\ldots,L_\beta$,

$$\beta\hbar c_\sigma = L_\beta a \ , \tag{4.82a}$$

and

$$g = \hbar c_\sigma / \rho_0 a \ , \tag{4.82b}$$

where c_σ is the "bare" spin-wave velocity, a free parameter of the σ model. This parameter is different from the real spin-wave velocity, which is an observable characterizing the spectrum of the elementary excitations of the theory. We need to impose periodic boundary conditions in the Euclidean time direction, $\mathbf{n}_l(\mathbf{x}+L_\beta\hat{\mathbf{e}}_3)=\mathbf{n}_l(\mathbf{x})$.

The action (4.81) with the field $\mathbf{n}_l$ constrained on the unit sphere can be obtained from

$$S_{\sigma,\lambda}=\sum_{\mathbf{x}}\left[-\frac{1}{2g}\sum_{\mu=1}^{3}\mathbf{n}_l(\mathbf{x})\cdot[\mathbf{n}_l(\mathbf{x}+\hat{\mathbf{e}}_\mu)+\mathbf{n}_l(\mathbf{x}-\hat{\mathbf{e}}_\mu)] +\lambda(|\mathbf{n}_l(\mathbf{x})|^2-1)^2\right] , \tag{4.83}$$

in the limit $\lambda\to\infty$. The additional term in that limit gives $\delta(|\mathbf{n}_l|^2-1)$. Hence we can study the theory (4.83) and choose to take the limit $\lambda\to\infty$ at the end of the calculation. We have considered the more general case in which the field $\mathbf{n}$ has M components.

We define the generating functional in the standard way,

$$Z[J]=\int[d\mathbf{n}]\exp\left[-S_{\sigma,\lambda}+\sum_{\mathbf{x}}\mathbf{J}(\mathbf{x})\cdot\mathbf{n}(\mathbf{x})\right] , \tag{4.84a}$$

and using the identity

$$\sqrt{\alpha/\pi}\int d\rho(\mathbf{x})\exp-\alpha[\rho(\mathbf{x})-i|\mathbf{n}_l(\mathbf{x})|^2]^2=1 \ , \tag{4.84b}$$

we can introduce the auxiliary scalar field $\rho(\mathbf{x})$ in the generating functional on every site of the lattice. The term $\lambda(|\mathbf{n}_l|^2)^2$ can be canceled by choosing $\alpha=\lambda$. Finally, shifting the field $\mathbf{n}_l(\mathbf{x})$ by a nonfluctuating vector field $\mathbf{C}(\mathbf{x})$,

$$\mathbf{n}_l(\mathbf{x})=\boldsymbol{\phi}(\mathbf{x})+\mathbf{C}(\mathbf{x}) \ , \tag{4.85a}$$

and choosing $\mathbf{C}(\mathbf{x})$ such that the coefficient of the term linear in $\boldsymbol{\phi}(\mathbf{x})$ vanishes, we find

$$\mathbf{C}(\mathbf{x})=g\sum_{\mathbf{y}}K^{-1}(\mathbf{x},\mathbf{y})\mathbf{J}(\mathbf{y}) \ , \tag{4.85b}$$

where K^{-1} is the inverse of the matrix K with matrix elements given by

$$K(\mathbf{x},\mathbf{y})=-\sum_{\mu=1}^{3}(\delta_{\mathbf{x},\mathbf{y}+\hat{\mathbf{e}}_\mu}+\delta_{\mathbf{x},\mathbf{y}-\hat{\mathbf{e}}_\mu}-2\delta_{\mathbf{x},\mathbf{y}}) -\delta_{\mathbf{x},\mathbf{y}}[6+4\lambda g(1+i\rho(\mathbf{x}))] \ . \tag{4.85c}$$

K is diagonal in the internal space of the components of the field. After some straightforward algebra we obtain

$$Z[J]=C'\int\prod_{\mathbf{x}}d\rho(\mathbf{x})\prod_{\mathbf{x},\alpha}d\phi_\alpha(\mathbf{x})\exp\left[-\lambda\sum_{\mathbf{x}}\rho^2(\mathbf{x})+\sum_{\mathbf{x},\mathbf{y},\alpha}\left[\frac{1}{2g}\phi_\alpha(\mathbf{x})K(\mathbf{x},\mathbf{y})\phi_\alpha(\mathbf{y})+\frac{g}{2}J_\alpha(\mathbf{x})K^{-1}(\mathbf{x},\mathbf{y})J_\alpha(\mathbf{y})\right]\right] . \tag{4.86}$$

The exponent of Eq. (4.86) is quadratic in the $\boldsymbol{\phi}$ field, and hence $\boldsymbol{\phi}$ can be integrated out to obtain

$$Z[J]=C'\int\prod_{\mathbf{x}}d\rho(\mathbf{x})\exp\left[-S'+\frac{g}{2}\sum_{\mathbf{x},\mathbf{y},\alpha}J_\alpha(\mathbf{x})K^{-1}(\mathbf{x},\mathbf{y})J_\alpha(\mathbf{y})\right] , \tag{4.87}$$

$$S'\equiv\lambda\sum_{\mathbf{x}}\rho^2(\mathbf{x})+\frac{M}{2}\mathrm{Tr}(\ln(K)) \ . \tag{4.88}$$

The vector field $\mathbf{n}_l$ has been eliminated at the expense of the scalar field $\rho(\mathbf{x})$. From the saddle-point equation $\delta S'/\delta\rho(\mathbf{x})=0$, and for a constant solution we obtain

$$\rho-Mgi\ \mathrm{Tr}(K^{-1})=0 \ , \tag{4.89a}$$

where

$$\mathrm{Tr}(K^{-1})=\frac{1}{V}\sum_{\mathbf{p}}\frac{1}{2\sum_{\mu}(1-\cos p_\mu)-[6+4\lambda g(1+i\rho(\mathbf{x}))]} \ , \tag{4.89b}$$

and $p_\mu=2\pi n_\mu/L_\mu,\mu=1,2,3$ and $L_1=L_2=L,L_3=L_\beta$ and $n_\mu=0,1,2,\ldots,L_\mu-1$ and $V=L^2L_\beta$. We define

$$m_0^2\equiv-[6+4\lambda g(1+i\rho)] \ . \tag{4.90}$$

Here m_0^2 is the solution of

$$\frac{1}{4M\lambda g^2}(m_0^2+4\lambda g+6)=\frac{1}{V}\sum_{\mathbf{p}}\frac{1}{2\sum_{\mu}(1-\cos p_\mu)+m_0^2} \ . \tag{4.91}$$

The two-point correlation function (second derivative of $Z[J]$ with respect to J) in the saddle-point approximation is

given by $gK^{-1}(\mathbf{x},\mathbf{y})$, and in momentum space

$$G(p)=\frac{g}{2\sum_{\mu}(1-\cos p_{\mu})+m_0^2} . \tag{4.92}$$

To find the correlation length, we transform the correlation function in Minkowski space and look for poles of the form $p_1=p_2=0, p_3=\xi_l^{-1}$. The correlation length is given as a solution of $2(1-\cosh\xi_l^{-1})+m_0^2=0$. We obtain

$$\xi_l=\frac{1}{2\sinh^{-1}(m_0/2)} , \tag{4.93a}$$

and if $m_0 \ll 1$ then

$$\xi_l \simeq m_0^{-1} . \tag{4.93b}$$

Taking the limit $\lambda\to\infty$, we find the equation

$$\frac{1}{Mg}=\frac{1}{V}\sum_{\mathrm{p}}\frac{1}{2\sum_{\mu}(1-\cos p_{\mu})+m_0^2} . \tag{4.94}$$

The above equation can be solved for m_0 numerically for any value of g and L_μ to find ξ_l using Eq. (4.93). A direct comparison of the numerical solution for finite lattices with the results of Monte Carlo simulation for the same lattice sizes has been made by Manousakis and Salvador (1989c). Here we shall discuss how to obtain an approximate solution at low T. First we take the limit $L\to\infty$, and we keep L_β finite. When we change $p_3=2\pi n_3/L_\beta$ to the variable $\epsilon=i2\pi n_3/L_\beta$, Eq. (4.94) takes the form

$$\frac{1}{Mg}=\frac{1}{L_\beta}\sum_{\epsilon_n=i2\pi n/L_\beta}\int_{-\pi}^{\pi}\frac{d^2p}{(2\pi)^2}\frac{1}{2(1-\cosh\epsilon)+2\sum_{\mu}(1-\cos p_{\mu})+m_0^2} . \tag{4.95}$$

Notice that in Eqs. (4.94) and (4.95) the lattice-spacing constant a is assumed as a unit. The sum over ϵ_n can be transformed to an integral over ϵ along the contour, shown in Fig. 13, which encloses all the poles on the imaginary axis (see Dashen *et al.*, 1975). Using

$$\frac{1}{L_\beta}\sum_{\epsilon_n=i2\pi n/L_\beta}=-\int\frac{d\epsilon}{2\pi i}\frac{1}{e^{L_\beta\epsilon}-1} \tag{4.96a}$$

and Eq. (4.95), we obtain

$$\frac{1}{Mg}=-\int_{-\pi}^{\pi}\frac{d^2p}{(2\pi)^2}\int\frac{d\epsilon}{2\pi i}\frac{1}{e^{L_\beta\epsilon}-1}\frac{1}{2(1-\cosh\epsilon)+2\sum_{\mu}(1-\cos p_{\mu})+m_0^2} . \tag{4.96b}$$

The contour can be deformed into two closed contours, one enclosing the pole at $\epsilon=\epsilon_{\mathrm{p}}$ and another the pole at $\epsilon=-\epsilon_{\mathrm{p}}$ (see Fig. 13), where

$$\epsilon_{\mathrm{p}}=\cosh^{-1}\left[1+\frac{m_0^2}{2}+\sum_{\mu=1,2}(1-\cos p_{\mu})\right] . \tag{4.97}$$

Calculating the residue of these poles, we find

$$\frac{1}{Mg}=A(m_0)+B(m_0,L_\beta) , \tag{4.98a}$$

$$A(m_0)=\frac{1}{2}\int_{-\pi}^{\pi}\frac{d^2p}{(2\pi)^2}\frac{1}{\left[\left[1+\frac{m_0^2}{2}+\sum_{\mu=1,2}(1-\cos p_{\mu})\right]^2-1\right]^{1/2}} , \tag{4.98b}$$

$$B(m_0,L_\beta)=\int_{-\pi}^{\pi}\frac{d^2p}{(2\pi)^2}\frac{1}{\left[\left[1+\frac{m_0^2}{2}+\sum_{\mu=1,2}(1-\cos p_{\mu})\right]^2-1\right]^{1/2}}\frac{1}{e^{L_\beta\epsilon}-1} . \tag{4.98c}$$

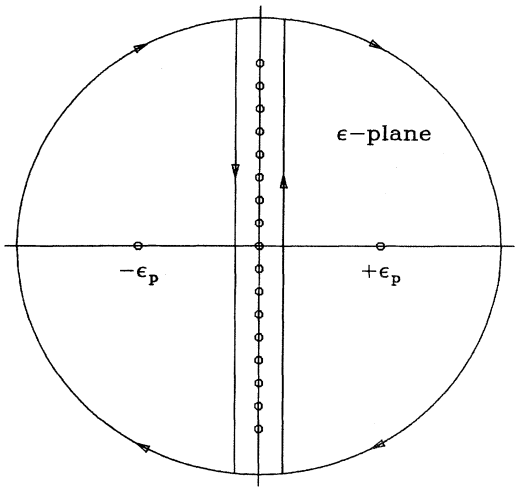

FIG. 13. The summation over the poles at even multiples of $2\pi i$ [Eq. (4.96)] is converted to an integral over the closed contour (vertical segments) which includes these poles. Since the contribution at infinity vanishes, this contour can be deformed to include the two poles on the real axis.

At $T=0$, which corresponds to the $L_\beta\to\infty$, we find that $B(m_0\neq 0, L_\beta=\infty)$ vanishes. In this case the equation

$$\frac{1}{Mg}=A(m_0) \tag{4.99}$$

defines the function $m_0(g)$, from which we find the $T=0$ correlation length in lattice-spacing units, i.e., $\xi_l(g)$. Holding ξ fixed at a given known physical value $\xi=m^{-1}$, we can determine $g(a)$. The critical point g_c is defined as $m_0(g=g_c)=0$, that is, $g_c=1/A(0)M$. Near the critical point $m_0(g\to g_c)\to 0$, we can keep terms up to linear in m_0 to obtain

$$\frac{1}{Mg}=A(0)-\frac{1}{4\pi}m_0+\cdots\ , \tag{4.100a}$$

and we find

$$m_0(g\to g_c, T=0)=\frac{4\pi}{Mg_c^2}(g-g_c)\ . \tag{4.100b}$$

Notice that $A(m_0)<A(0)$ for real nonzero values of m_0, and therefore we use Eq. (4.99) (when $L_\beta=\infty$) to find that $g\geq g_c$. For $g<g_c$, Eq. (4.98) can be satisfied only if $m_0(L_\beta\to\infty)\to 0$ as shown below. In other words, in the phase with a broken symmetry ($g<g_c$) there are massless modes as expected.

Let us now consider $T\to 0$, i.e., the case where L_β is finite but large. We need to distinguish three different cases:

(a) $g>g_c$. In this case there is a solution to Eq. (4.98) in which $m_0(g,L_\beta)$ remains finite as $L_\beta\to\infty$. If $m_0(L_\beta\to\infty)$ is finite, then $B(m_0)$ will be exponentially small, namely, $B(m_0, L_\beta\to\infty)\sim e^{-L_\beta m_0}$. The temperature-independent part of m_0 is given as a solution of Eq. (4.99), and, close to the critical point, $g=g_c$ where m_0 is small by Eq. (4.100b). Taking the continuum limit close to g_c, we find that ξ is a constant given by m^{-1}, the constant used to remove the cutoff and to define the function $g(a)$. There are corrections to ξ due to the B term that are exponentially small.

(b) $g<g_c$. In this case $m_0L_\beta\to 0$ as $L_\beta\to\infty$. Thus only momenta with ϵ_p small give significant contributions to the integral (4.98c) because of the exponential factor. Hence $\sum_{\mu=1,2}(1-\cos p_\mu)\to p^2/2$, and p^2 is small, and

$$\epsilon_p=\sqrt{m_0^2+p^2}\ , \tag{4.101a}$$

and

$$B(m_0\to 0, L_\beta\to\infty)=\int_{-\pi}^{\pi}\frac{d^2p}{(2\pi)^2}\frac{1}{\sqrt{m_0^2+p^2}}\frac{1}{e^{L_\beta(m_0^2+p^2)^{1/2}}-1}\ . \tag{4.101b}$$

Since in this limit only the $p\to 0$ part of the Brillouin zone contributes to the integral, we obtain

$$B(m_0\to 0, L_\beta\to\infty)=-\frac{1}{2\pi L_\beta}\ln(1-e^{-L_\beta m_0})\ . \tag{4.101c}$$

Furthermore, for $m_0L_\beta\to 0$, we find that

$$\frac{1}{Mg}=\frac{1}{Mg_c}-\frac{1}{4\pi}m_0-\frac{1}{2\pi L_\beta}\ln(L_\beta m_0)\ , \tag{4.102}$$

and in this limit the linear term vanishes faster than the last term of Eq. (4.102). Using Eq. (4.82a), we find

$$\xi(T)=\frac{\hbar c_\sigma}{k_BT}\exp\left[\frac{m}{2}\frac{\hbar c_\sigma}{k_BT}\right]\ , \tag{4.103a}$$

where

$$m\equiv 4\pi\left[\frac{1}{Mg}-\frac{1}{Mg_c}\right]a\ . \tag{4.103b}$$

Notice that the solution satisfies the required property that for $g<g_c$, $m_0L_\beta\to 0$. At constant T and in the continuum limit ($g\to g_c$), ξ should be independent of g and a. This can be achieved by defining a function $a=a(g)$ such that, as $g\to g_c$, m is independent of g and a. Notice that, at $g\to g_c$, $a(g)$ defined via Eq. (4.103b) is of the same form as Eq. (4.100b).

(c) $g=g_c$. In this case it is clear from Eq. (4.101c) that

$$m_0=\frac{\lambda}{L_\beta}\ , \tag{4.104a}$$

where λ is a constant given by $\lambda=2\ln(2/\sqrt{5}-1)$. Therefore the correlation length in physical units is given as

$$\xi(T)=m_0^{-1}a=\frac{L_\beta a}{\lambda}=\frac{1}{\lambda}\frac{\hbar c_\sigma}{k_BT}\ . \tag{4.104b}$$

Similar results have been also obtained by Rosenstein *et al.* (1990), and by Rodriguez (1990) using a $1/M$ expansion and a momentum-space regularization. The same forms were obtained in Sec. IV.F with the one-loop renormalization-group approach of Chakravarty *et al.* It is worth noticing that the same behavior as that given by Eq. (4.103) was found by Arovas and Auerbach and by Takahashi, as explained in Secs. IV.A and IV.B for the spin-$\frac{1}{2}$ antiferromagnetic Heisenberg model, using very similar approaches. The reader might have expected this in view of the believed equivalence between the two models. However, as we discussed in Sec. IV, higher-order corrections (two-loop) modify the prefactor and, as Chakravarty *et al.* noticed, the prefactor is a constant [Eq. (4.80)].

V. CALCULATIONS AT FINITE TEMPERATURES. NUMERICAL RESULTS

In this section we first review results obtained for the low-temperature properties of the spin-$\frac{1}{2}$ antiferromagnetic Heisenberg model on a square-lattice with quantum Monte Carlo methods. Second, we review Monte Carlo results obtained on the quantum nonlinear σ model at low temperatures and in $2+1$ dimensions. Finally, the continuum limit of the latter model is studied and the equivalence between the two models is investigated.

A. Quantum Monte Carlo calculations on the Heisenberg model

The spin-spin correlation length has been measured by neutron scattering on La_2CuO_4 and has a clear 2D nature. Other thermodynamic quantities of the material, for instance specific heat, magnetic susceptibility, and the staggered magnetization at finite temperature, have significant contributions from other effects; hence the calculation of the correlation length has unique importance for comparing theory with experiment. Therefore we shall place particular emphasis on the calculations of the temperature dependence of the correlation length.

Manousakis and Salvador (1988, 1989a, 1989b, 1989c) and Gomez-Santos, Joannopoulos, and Negele (1989) studied the spin-$\frac{1}{2}$ antiferromagnetic Heisenberg model using Handscomb's quantum Monte Carlo method (Handscomb, 1962, 1964) and suggested that the observed correlation lengths can be understood using a value of J of the same magnitude as the value reported by neutron and Raman scattering experiments. Next we briefly explain this method as it has been extended to study antiferromagnets (see Lyklema, 1982; Lee *et al.*, 1984).

The Hamiltonian (1.2), apart from a constant, can be expressed as

$$-\beta H=\beta J/2\sum_{\langle ij\rangle}(h_{ij}^2-h_{ij}) , \tag{5.1a}$$

$$h_{ij}\equiv S_i^+S_j^-+S_i^-S_j^+ , \tag{5.1b}$$

where h_{ij} flips antiparallel spins and gives zero in the case of parallel spins located at sites $\langle ij\rangle$. The matrix elements of h_{ij}^2 are zero except those diagonal elements obtained with states in which the spin of i and j are antiparallel, which matrix elements are equal to 1.

An observable $\hat{O}$ can be calculated using the distribution $\Pi(C_r)$ defined as

$$\langle\hat{O}\rangle\equiv\frac{\mathrm{Tr}(\hat{O}e^{-\beta\hat{H}})}{\mathrm{Tr}(e^{-\beta\hat{H}})}=\frac{\sum_{r=0}^{\infty}\sum_{C_r}\Pi(C_r)\Omega(C_r)}{\sum_{r=0}^{\infty}\sum_{C_r}\Pi(C_r)} , \tag{5.2a}$$

$$\Pi(C_r)=(-1)^{r_1}\frac{(\beta J/2)^r}{r!}\mathrm{Tr}(Q_{i_1}Q_{i_2}\cdots Q_{i_r}) , \tag{5.2b}$$

$$\Omega(C_r)=\frac{\mathrm{Tr}(\hat{O}Q_{i_1}Q_{i_2}\cdots Q_{i_r})}{\mathrm{Tr}(Q_{i_1}Q_{i_2}\cdots Q_{i_r})} , \tag{5.2c}$$

where $Q_{i_n}=h_{ij}^2$ or h_{ij}. Here r_1 and r_2 are the number of h's and h^2's in the sequence $C_r=\{Q_{i_r}\cdots Q_{i_2}Q_{i_1}\}$ of $r=r_1+r_2$ operators. Note that $\Pi(C_r)$ can be nonzero only if the h operators in the sequence form closed loops. Therefore $\Pi(C_r)$ for a bipartite lattice is non-negative, because such closed loops involve an even number of h operators. Imagine that we define a Markov process in an abstract sample space consisting of sequences C_r. If we succeed in prescribing such a process, which provides an ensemble of C_r's distributed according to $\Pi(C_r)$, then the thermodynamic average of the operator $\hat{O}$ can be calculated as an average over the sequences that have been drawn from the distribution $\Pi(C_r)$. The first step is to give an algorithm to calculate the trace (5.2b) and the second to define the Markov process. Both steps are explained in the Appendix.

For illustration, Fig. 14 gives an equilibrium configuration of clusters inside a 20×20 lattice, for temperature $T=0.5J$ (top figure), where the correlation length is about 3.5. The black (white) circles denote up- (down-) spins. A cluster is a set of points connected by operators in the sequence. The clusters are drawn by solid lines. There is a large cluster involving most of the lattice sites and some other smaller ones. The lower part of Fig. 14 shows the clusters for a 10×10-size lattice and temperatures $0.4J$ (left) and $1.5J$ (right).

The correlation length can be extracted by calculating the z component of the staggered correlation function, i.e., using Eq. (5.2) and

$$G(\mathbf{r})=(-1)^{\|\mathbf{r}\|}\frac{1}{N}\sum_{\mathbf{R}}\langle\hat{\sigma}_z(\mathbf{R})\sigma_z(\mathbf{R}+\mathbf{r})\rangle , \tag{5.3}$$

where $\|\mathbf{r}\|=x+y$, i.e., the sum of the two components of $\mathbf{r}$ in lattice spacing units. Depending on the boundary conditions (BC), the large-distance behavior of the correlation function is given by

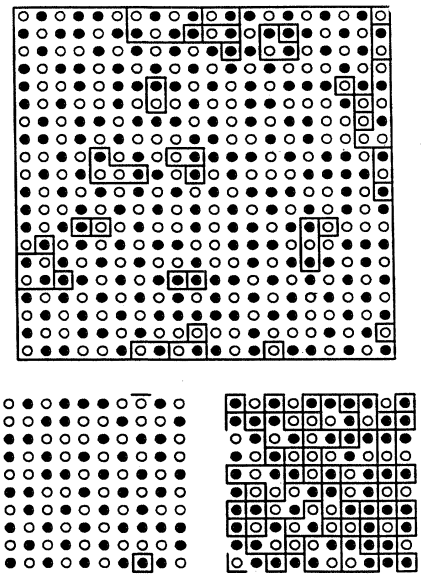

FIG. 14. The clusters in an equilibrium configuration inside a 20×20 lattice, for temperature $T=0.5J$ (top figure), where the correlation length is about 3.5. The black (white) circles denote up(down) spin. The clusters are drawn by solid lines. There is a large cluster involving most of the lattice sites and some other smaller ones. The lower part of the figure shows the clusters for a 10×10-size lattice and temperatures $0.4J$ (left) and $1.5J$ (right).

$$\lim_{r\to\infty} G(r)=\begin{cases} Ae^{-r/\xi(T)} & \text{open BC} \\ A\cosh\left[\dfrac{r-L/2}{\xi(T)}\right] & \text{periodic BC}\ , \end{cases} \tag{5.4}$$

where L is the size of the lattice. In general there is a power of r in front of the exponential. At sufficiently large distances, i.e., in the interval $n\xi<r<(n+m)\xi$ with $n\gg1$ and $m\ll n$, the variation of the power can be ignored and the correlation function behaves as an exponential. Several authors (Fox *et al.*, 1982; Parisi, 1982) have used the projected correlation function $G_p(x)$, defined by

$$G_p(x)=\langle\bar{S}_z(0)\bar{S}_z(x)\rangle=\frac{1}{L}\sum_y G(x,y)\ , \tag{5.5a}$$

which is the correlation function of the operator

$$\bar{S}_z(x)=\frac{1}{L}\sum_y S_z(x,y)\ . \tag{5.5b}$$

The zero-momentum projection is used to avoid fluctuations around the lowest mode. These fluctuations are responsible for the power law in front of the exponential, and $G_p(x)$ behaves according to Eqs. (5.4). Extraction of correlation lengths from this correlation function, however, involves larger statistical errors. Manousakis and Salvador (1989a) have used Eqs. (5.3) and (5.5) to extract the correlation length, and the results are reasonably close.

The correlation function (5.3) can be easily calculated with Handscomb's method by noticing that in a given state C_r of the system, the sites $\mathbf{R}$ and $\mathbf{R}+\mathbf{r}$ must belong to the same cluster, otherwise they are uncorrelated.

When this paper was ready for submission we received an interesting paper by Ding and Makivic (1990, 1991), who studied the spin-$\frac{1}{2}$ antiferromagnetic Heisenberg model on a square-lattice using the world-line Monte Carlo method explained in Sec. III.B. Ding and Makivic created an effective algorithm by implementing the following ideas. First, instead of using the standard (Hirsch *et al.*, 1981, 1982) checkerboard breakup explained in Sec. III.B, they used a "bond-type" breakup: they wrote $H=H_1+H_2+H_3+H_4$, where $H_1(H_2)$ is the sum of all the bonds $(\mathbf{r},\mathbf{r}+\hat{\mathbf{x}})$ oriented in the x direction and $\mathbf{r}$ is in the $A(B)$ sublattice; H_3 or H_4 is the sum of bonds $(\mathbf{r},\mathbf{r}+\hat{\mathbf{y}})$ oriented in the y direction, and $\mathbf{r}$ is in the A or B sublattice, respectively. This breakup couples only four spins (each pair on different "time" slice) instead of the eight spins involved in the checkerboard breakup of Fig. 3. To cover the entire sample space, they supplied the algorithm with local and global moves of the kinds explained in Sec. III.B. Their vectorized code, which uses 32-bit words to represent the state of the spin in the "time" direction, runs on a parallel computer very efficiently because of the local interaction, which allows fast communication between processors. Parallelism is also achieved by running several independent lattices simultaneously. This algorithm allowed them to calculate correlation functions and extract correlation lengths on large lattices (up to 128^2); their results are compared to the other calculations next.

B. Comparison of the results on the Heisenberg model

In this section, we compare the results for the correlation length obtained for the spin-$\frac{1}{2}$ antiferromagnetic Heisenberg model using the various analytical and numerical methods discussed in this and the last section. The form (4.28b) derived with both Schwinger boson mean-field theory by Arovas and Auerbach (1988) and the modified spin-wave theory (Takahashi, 1989a) coincides with Eq. (4.72) obtained by the one-loop calculation explained in Sec. IV. These are low-order calculations, and they give

$$\xi(T\to0)=C\frac{\hbar c}{k_BT}\exp\left[\frac{2\pi\rho_s}{k_BT}\right]\ . \tag{5.6}$$

The improved two-loop calculation of Chakravarty *et al.* (1988, 1989), however, shows that there are important two-loop corrections; these corrections convert the $1/T$ prefactor of the exponential into a constant,

$$\xi(T\to0)=C_\xi\exp\left[\frac{2\pi\rho_s}{k_BT}\right]\ . \tag{5.7}$$

It is interesting to look at the historical evolution of the ideas concerning the behavior of the correlation length as a function of T. Manousakis and Salvador (1988), who simulated the model (1.2) using Handscomb's quantum Monte Carlo method, explained in Sec. V.A, found that the form (5.6), $\xi(T)=a/T\exp(2\pi\rho_i/k_BT)$, does not fit their results for the correlation length. Due to the disagreement of the form (5.6) with the numerical results, Manousakis and Salvador (1988) attempted to fit their results to the Kosterlitz-Thouless form $\xi(T)=A\exp(B/\sqrt{T-T_c})$ (Kosterlitz and Thouless, 1973; Kosterlitz, 1974) to examine whether a phase with topological excitations (Belavin and Polyakov, 1975) is favored. The latter form fitted their data, and they concluded that either (a) the form (5.6) is *incorrect* (possibly valid at lower T inaccessible to their simulation) or (b) a transition to a phase with zero staggered magnetization and infinite correlation length due to topological defects might be possible. The Schwinger boson mean-field theory of Arovas and Auerbach (1988), the modified spin-wave theory of Takahashi (1989a), and the one-loop calculation by Chakravarty, Halperin, and Nelson suggested the asymptotic form (5.6) also. It was subsequently, demonstrated by Manousakis and Salvador (1989b, 1989c) and by Gomez-Santos, Joannopoulos, and Negele (1989) that Eq. (5.7), obtained by the two-loop calculation of Chakravarty *et al.*, fits well their quantum Monte Carlo; furthermore, there is no need to invoke the role of topological excitations in the model.

Gomez-Santos *et al.* have performed similar simulations of the spin-$\frac{1}{2}$ antiferromagnetic Heisenberg model. In Fig. 15, we show their results for each reference. They find overall agreement with the results of Manousakis and Salvador at higher temperatures, but somewhat smaller correlation lengths at lower temperatures. Gomez-Santos *et al.* argue that the origin of the discrepancy may be that their new algorithm searches the phase space more efficiently. Manousakis and Salvador (1989b, 1989c) have argued that the discrepancy may also be due to finite-size effects: the values of the correlation length given by Gomez-Santos *et al.* at a given low temperature increases when one increases the lattice size (see Fig. 15), whereas in the Manousakis and Salvador calculation finite-size effects appear at larger correlation lengths (somewhat lower temperatures). This difference may be due to the different methods of calculating the correlation function in the two approaches. In Gomez-Santos *et al.*'s calculation, averages are not taken over the entire lattice, i.e., using Eq. (5.3), but by making some selections of points. Hence it is possible that the results of Manousakis and Salvador (1988), represented by the dashed line in Fig. 15, approximate the infinite lattice better. These arguments are supported by the results of more recent quantum Monte Carlo calculation by Ding and Makivic (1990, 1991), which we discuss next.

The results of the calculation by Manousakis and Salvador (1988, 1989a), obtained with the projected correlation function (5.5), are shown in Fig. 16. For illustration the function $T/J\ln\xi(T)$ is plotted. The function can be clearly approximated by a straight line, strongly suggesting that $\xi(T)$ can be approximated by Eq. (5.7). By fitting the low-T data points (the data points that correspond to $k_BT/J<1$) we obtain $\rho_s=0.22\pm0.02J$ and $C_\xi=0.26\pm0.02$; by fitting a much broader temperature range, we obtain only slightly different parameter values, namely, $\rho_s=0.22J$ and $C_\xi=0.25$ (see Manousakis and Salvador, 1989a, 1989b, 1989c) for which the line is shown in Fig. 16. The results obtained by fitting the regular correlation function Eq. (5.3), as calculated by Manousakis and Salvador, are $\rho_s=0.20\pm0.02J$ and $C_\xi=0.27\pm0.02$. To obtain the latter values, we excluded the value of the correlation Manousakis and Salvador reported (1988) at the lowest temperature, as it is subject to significant finite-size effects. It is notable that this value

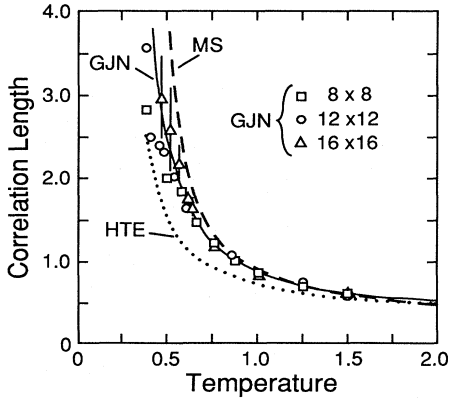

FIG. 15. We show the results of Gomez-Santos, Joannopoulos, and Negele (1989) for easy reference. Their results are the data points and the solid line labeled GJN. The results of Manousakis and Salvador (1988) are represented by the dashed line labeled MS. The dotted line is the leading term $1/\ln(4T/J)$ of high-temperature expansion obtained by Manousakis and Salvador.

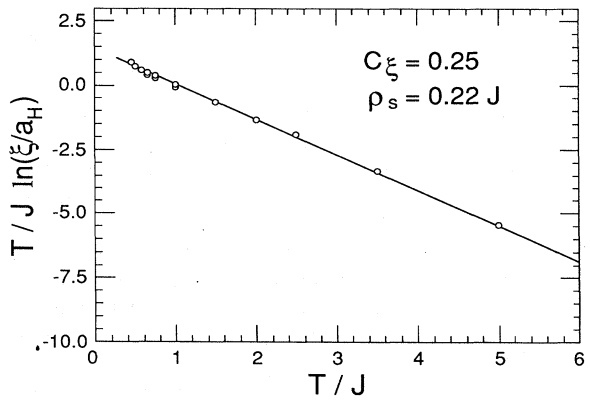

FIG. 16. The function $T/J\ln\xi(T)$, plotted to illustrate the validity of Eq. (5.7) obtained by the two-loop renormalization-group calculation of Chakravarty *et al.* (1988, 1989). The results of the quantum Monte Carlo calculation by Manousakis and Salvador (1988, 1989a) for ξ have been used in this plot.

TABLE IV. Comparison of the results for the values of the parameters C_ξ and ρ_s that enter in Eq. (5.7), which fits the results for the correlation length obtained from the various quantum Monte Carlo simulations. The second column indicates whether the correlation length was extracted from the regular (Eq. 5.3) or from the projected (Eq. 5.5) correlation function.

Author	Correlation function	C_ξ	ρ_s/J
Manousakis and Salvador (1988)	Regular	0.27±0.02	0.20±0.02
Manousakis and Salvador (1989b)	Projected	0.26±0.02	0.22±0.02
Ding and Makivic (1990)	Regular	0.276±0.006	0.199±0.002
Gomez-Santos *et al.* (1989)	Regular	0.32	0.159

of ρ_s is very close to that found by two other independent calculations of the ground-state properties (Gross *et al.*, 1989b; Liu and Manousakis, 1989), namely $\rho_s \simeq 0.25J$.

Ding and Makivic (1990, 1991) studied the spin-$\frac{1}{2}$ antiferromagnetic Heisenberg on a square lattice using the method outlined in Sec. V.A. Their efficient algorithm allowed them to perform the calculation on large lattices (up to 128^2). The calculated correlation length $\xi(T)$ was also consistent with the form (5.7), giving $C_\xi = 0.276 \pm 0.006$ and $\rho_s = 0.199 \pm 0.002J$. The results for the correlation length obtained with the quantum Monte Carlo calculations are compared in Table IV and in Fig. 17. The results of Manousakis and Salvador (1988), obtained from the regular correlation function [Eq. (5.3)], are very close to those of Ding and Makivic. The values obtained from the projected correlation function [Eq. (5.5)] are within 10% in agreement with those reported by Ding and Makivic. The results of Ding and Makivic, however, differ from those suggested by Gomez-Santos *et al.* ($C_\xi = 0.32$ and $\rho = 0.159J$) by about 20%, which suggests that the results of Gomez-Santos *et al.* have strong finite-size effects.

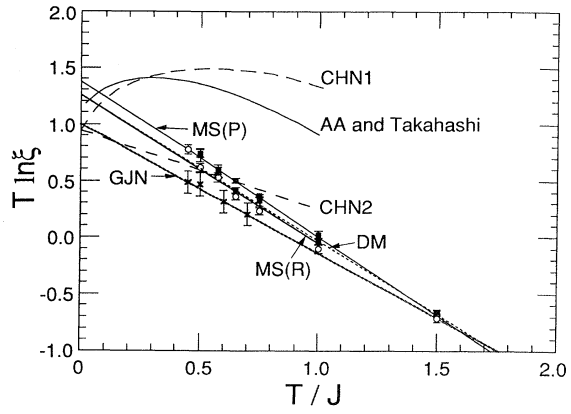

FIG. 17. Comparison of results for the correlation length obtained with various calculations. The dashed line labeled CHN1 represent the renormalization-group calculation of Chakravarty, Halperin, and Nelson (1988) with the β function calculated up to one-loop order. The dashed line labeled CHN2 shows the results of Chakravarty *et al.* (1988, 1989) with the β function calculated up to two-loop order. The results of Arovas and Auerbach (AA) and Takahashi (1989a, 1989b) are shown by a solid line. The open circles and the solid line fit are the results of Manousakis and Salvador (MS) (1988), extracted from the regular spin-spin correlation function [Eq. (5.3)], while the solid squares are those obtained from the projected correlation function [Eq. (5.5) (Manousakis and Salvador, 1989). The dotted line labeled DM represents the results of Ding and Makivic (1990). The crosses joined by the wide "chain" line labeled GJN are the results of a calculation by Gomez-Santos, Joannopoulos, and Negele (1989).

Notice that the one-loop calculation of Chakravarty, Halperin, and Nelson (denoted by CHN1 in the figure) and the Schwinger boson mean-field theory (and the modified spin-wave theory) are close. The differences between CHN1 and the Schwinger-boson mean-field theory are due to differences in the value of the constant prefactor C in Eq. (5.6). The solid squares and open circles with error bars are the results of Manousakis and Salvador extracted from the projected [Eq. (5.5)] and regular [Eq. (5.3)] correlation functions. The solid lines are the straight-line fits to the regular and projected correlation function. The crosses with the error bars are the results of Gomez-Santos *et al.*, The dashed line labeled DM represents the recent results of Ding and Makivic. The dashed line labeled CHN2 shows the results of the two-loop calculation of Chakravarty *et al.* (1989), obtained as described in Sec. IV.F. As can be seen, there are large differences between the one-loop and two-loop calculations. It is very important to know the correct temperature dependence of the correlation length before we attempt to fit the experimental data. Notice that the results obtained by Ding and Makivic agree with those obtained by Manousakis and Salvador from the regular correlation function within error bars. For purposes of comparison with the experimental results, we shall consider these as the most accurate results, since they were obtained on larger lattices. The results obtained from the projected correlation function are less accurate, as mentioned earlier. Nevertheless, they are within 10% agreement with the results reported by Ding and Makivic. In order to clarify the situation further, Manousakis and Salvador simulated the quantum nonlinear sigma model, which makes these conclusions even stronger. This calculation is explained in Sec. V.D.

Using the world-line Monte Carlo method, Okabe and Kikuchi (1988, 1990) have calculated the energy, specific heat, and uniform susceptibility of the spin-$\frac{1}{2}$ antiferromagnetic Heisenberg model for up to 16^2 square lattices. Their results for the susceptibility compare well (Okabe *et al.*, 1988) with the results of the Schwinger boson mean-field theory of Arovas and Auerbach at low temperatures. At higher temperatures they are in good

agreement with the high-temperature series-expansion results (Rushbrooke and Wood, 1958; Lines, 1970; de Jongh and Miedema, 1974). The coefficient of the T^2 leading term in the low-temperature specific heat, defined as $\delta \equiv \lim_{T\to 0} C_v/[T/S(S+1)J]^2$, is found to be $\delta = 1.1 \pm 0.2$ (Okabe *et al.*, 1988), in agreement with the Schwinger boson mean-field theory.

C. High-temperature series expansion for the correlation length

The structure function has been calculated with standard techniques of high-temperature series expansion only up to fourth order (Collins, 1970). To extract the correlation length, however, one needs to know the correlation function $G(r)$ at least up to an order $n > \xi_{\text{latt}}$, where ξ_{latt} is the correlation length in lattice units. The reason for this is explained below and originates simply from the fact that, if $G(r)$ is calculated only up to nth order, then $G(r>n)=0$. Here, we calculate the leading order (see Manousakis and Salvador, 1989a) to the correlation function $G(r)$ directly.

The leading contribution to the expectation value of $\hat{S}_z(0)\hat{S}_z(r)$ is of rth order. If the order n is less than r, the sites 0 and r cannot be joined with a line of operators, because the available operators are only n, and therefore the trace of such an unlinked term vanishes. In rth order we obtain

$$\lim_{T\to\infty} G(r) = \left[\frac{\beta J}{2}\right]^r \frac{1}{r!} \sum_{(l_1,\ldots,l_{r-1},l_r)} \frac{\mathrm{Tr}(\sigma_z(0)\sigma_z(r)h_{l_1}^2 h_{l_2}^2 \cdots h_{l_r}^2)}{\mathrm{Tr}(1)} , \tag{5.8a}$$

where the sum is over all possible orderings $(l_1,\ldots,l_r)$ of the r links $(0,1),(1,2),\ldots,(r-1,r)$ joining the sites $0,1,\ldots,r$. The application of the above r operators in any order on the r links of the string with $r+1$ sites gives the same result. Hence the factor $1/r!$ is canceled by the $r!$ possible rearrangements of r operators corresponding to links between the sites 0 and r:

$$\lim_{T\to\infty} G(r) = \left[\frac{\beta J}{2}\right]^r \frac{\mathrm{Tr}(\sigma_z(0)\sigma_z(r)h_{01}^2 h_{12}^2 \cdots h_{r-1r}^2)}{\mathrm{Tr}(1)} . \tag{5.8b}$$

The trace of the denominator is 2^N because there are N monomers. The trace of the numerator is 2^{N-r} because there are $N-r-1$ monomers and one cluster with $r+1$ sites. Therefore

$$\lim_{T\to\infty} G(r) = \left[\frac{\beta|J|}{4}\right]^r = e^{-r/\xi(T)} , \tag{5.9a}$$

where the correlation length ξ is given by

$$\lim_{T\to\infty} \xi(T) = \frac{1}{\ln\left[\frac{4T}{J}\right]} . \tag{5.9b}$$

Higher-order corrections will be of order $1/T$,

$$\lim_{T\to\infty} \xi(T) = \frac{1}{\ln\left[\frac{4T}{J}\right] + O(1/T)} . \tag{5.9c}$$

Such corrections become important for $T/J \sim 1$. Hence we have shown that it is possible to calculate the correlation function $G(r)$ directly using high-temperature series expansion, and the leading term is of rth order; it seems to us possible to extend this approach to calculate n additional terms, i.e., $G(r)$ up to order $r+n$, by developing a linked-cluster expansion for the correlation function in the above spirit. Here, however, we restrict ourselves only to the leading contribution, which compares remarkably well with the Manousakis and Salvador results for $T/J > 1$ (see the dotted line in Fig. 15).

D. Simulation of the quantum nonlinear σ model

In this section we discuss certain results obtained by the direct simulation of the quantum nonlinear σ model (Manousakis and Salvador, 1989b, 1989c). Manousakis and Salvador used the heat-bath algorithm to generate configurations $\{\mathbf{n}_l(x_\mu)\}$ distributed according to the distribution $e^{-S_\sigma(\{\mathbf{n}_l(x_\mu)\})}$, where S_σ is the action of the quantum nonlinear σ model on lattice regularization given by Eq. (4.81).

Let us study the $T=0$ case first. In this case we consider $L_\beta = L \to \infty$, and the theory has only one parameter, the dimensionless parameter g. Manousakis and Salvador have calculated the staggered magnetization expectation value, defined as

$$\bar{n}_l = \left\langle \left[\frac{1}{L^3}\sum_{x_\mu} \mathbf{n}_l(x_\mu)\right]^2 \right\rangle , \tag{5.10}$$

where the expectation value is taken with respect to the distribution $e^{-S_\sigma(\{\mathbf{n}_l(x_\mu)\})}$. We expect the ground-state staggered magnetization to obey the finite-size scaling given by Eq. (3.20). In Fig. 18(a), $\bar{n}_l$ is plotted versus $1/L$ for 16 values of g: $g=0.1,0.2,\ldots,1.6$. There is a critical value of $g_c \simeq 1.45$ such that $\bar{n}_l(g>g_c, L\to\infty)=0$. From this figure, it is clear that $\bar{n}_l(g<g_c, L\to\infty)$ scale with $1/L$ as expected. The extrapolated values

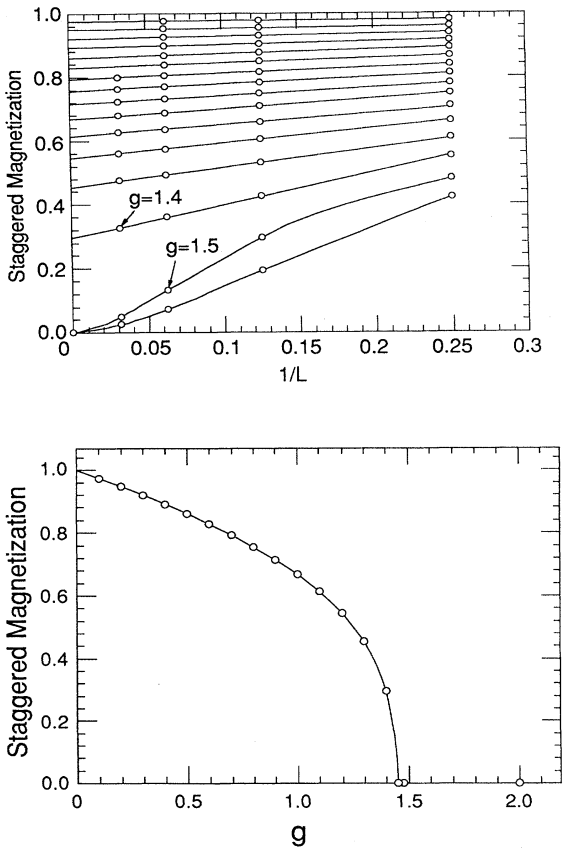

FIG. 18. (a) The order parameter $\bar{n}$ (g,L) of the σ model defined by Eq. (5.10) is plotted versus $1/L$ for 16 values of g: $g=0.1,0.2,\ldots,1.6$. There is a critical value of $g_c \simeq 1.45$ such that $\bar{n}_l(g>g_c, L\to\infty)=0$. From this figure, it is clear that $\bar{n}_l(g<g_c, L\to\infty)$ scale with $1/L$, as expected. The scaling is violated above the critical point in the disordered phase, as expected. (b) The extrapolated values $n_0(g)=\bar{n}_l(g<g_c, L\to\infty)$ as a function of g.

TABLE V. The staggered magnetization for the σ model for several values of g, obtained from simulation after extrapolation to an infinite lattice as shown in Fig. 18.

g	$\bar{n}(g)$
0.1	0.974
0.2	0.948
0.3	0.912
0.4	0.891
0.5	0.860
0.6	0.828
0.7	0.793
0.8	0.756
0.9	0.715
1.0	0.668
1.1	0.613
1.2	0.545
1.3	0.454
1.4	0.295
1.5	0.000

$n_0(g)\equiv\bar{n}_l(g,L\to\infty)$ are shown in Fig. 18(b) and are tabulated in Table V. Assuming that the spin-S quantum Heisenberg antiferromagnet is equivalent to the quantum nonlinear σ model, the parameter g corresponds to the different possible spin values. There is a value of g that gives the same staggered magnetization as that extracted from the quantum spin-$\frac{1}{2}$ antiferromagnetic Heisenberg model. In Sec. III we determined the expectation value of the staggered magnetization to be about $60\pm1\%$ of its classical value. From Table V and taking the wave-function renormalization constant as unity, we find that at $g=1.125$ the two models give the same staggered magnetization.

At $T=0$ and $g<g_c$, the system is in the ordered phase, where there is a finite correlation length at any $g<g_c$ that is associated with small fluctuations in the magnitude of the order parameter. At low T and for $g<g_c$, there are two different correlation lengths in the theory—a large correlation length associated with angular fluctuations of the vector order parameter and a short correlation length associated with fluctuations of the length of the vector order parameter. The former becomes infinite at $T=0$, while the latter remains finite at $T=0$ (3D theory) and diverges only at the critical point g_c. Above g_c, in the quantum disordered phase, and at $T=0$ the correlation length is finite and diverges at the critical point with a critical exponent ν,

$$\xi_l(g\to g_c)=\frac{C}{|g-g_c|^{\nu}}\ , \tag{5.11}$$

where ξ_l is the correlation length in lattice-spacing units a. Close to the critical point g_c, it is possible to define a continuum theory. In such a theory, we are interested in observables expressed in physical units. As $g\to g_c$, $\xi_l\to\infty$, and we shall hold the physical value of

$$\xi\equiv\xi_l(g)a \tag{5.12}$$

fixed. This can be done by defining a function $g=g(a)$ or $a=a(g)$ such that ξ takes a constant physical value m^{-1} for any $g\to g_c$. In order to hold ξ constant and equal to m^{-1}, we need

$$a(g)=a_0|g-g_c|^{\nu}\ , \tag{5.13}$$

where $a_0=(Cm)^{-1}$. The critical exponents ν and η of the 3D O(3) model have been calculated using various methods, including perturbation theory up to three loops (Hikami and Brézin, 1978), $1/M$ expansion (M is the number of components of the vector order-parameter) up to $(1/M)^3$ (Ma, 1973, Okabe and Oku, 1978), and ϵ expansion (Brézin *et al.*, 1973). However, these series have to be evaluated at a large value of the corresponding expansion parameter and they are at best asymptotic, thus, one uses Padè-Borel summation techniques to perhaps obtain more plausible values (Le Guillou and Zinn-Justin, 1980). Similarly, the high-temperature series expansion method (see Domb and Green; 1974, Ferer and Hamid-Aidinejad, 1986) has been used to calculate the critical

exponents of the equivalent 3D classical Heisenberg model. These techniques give a value for $\nu \simeq 0.7$ which is the textbook value (see, for instance, Amit, 1984) and a very small value for $\eta \sim 0.04$.

Manousakis and Salvador (1989c) calculated the β function with a finite-size scaling technique by holding one lattice dimension (say, the Euclidean time dimension) finite. We shall take the limit $L \to \infty$ and keep the time dimension finite, so that Eq. (4.82a) is satisfied. If L is large enough that $\xi_l \ll L$, the correlation length is only a function of L_β and g, and in physical units is given by

$$\xi = \xi_l(g, L_\beta) a \ . \tag{5.14}$$

For continuum limit behavior and for eliminating finite-size effects, ξ_l must satisfy $1 \ll \xi_l \ll L$. Substituting a from (4.82a) in (5.14), we obtain

$$\frac{\xi}{\beta \hbar c_\sigma} = \frac{\xi_l(g, L_\beta)}{L_\beta} \ . \tag{5.15}$$

At this point we wish to hold the correlation length ξ fixed in units of the length scale $\hbar c_\sigma \beta$, while $L_\beta \to \infty$. Clearly this can be done provided that a value of $g = g_c$ exists at which $\xi_l(g_c, L_\beta \to \infty) \to \infty$ in such a way that the ratio

$$b = \frac{\xi_l(g, L_\beta)}{L_\beta} \tag{5.16}$$

remains constant. A similar discussion in the framework of finite-size scaling at the phase transition can be found in a paper by Brézin (1982; see also Brézin and Zinn-Justin, 1976a, 1976b). The critical point $g = g_c$ is a fixed point of the scale transformation $L_\beta \to L'_\beta$ and $g \to g'$ defined as

$$\frac{\xi_l(g, L_\beta)}{L_\beta} = \frac{\xi_l(g', L'_\beta)}{L'_\beta} \ . \tag{5.17}$$

For large L_β this equation defines $g(L_\beta)$, which, via (4.82a), gives the function $g(a)$. In Fig. 19, b is given as a function of g calculated at $L_\beta = 2,4,8$ (for large enough spatial extent L that finite-size effects on ξ_l due to finite L are negligible). We clearly see the presence of a critical point at $g_c \simeq 1.45$. The β function [and $a(g)$] determined via (5.17) close to the critical point is given by

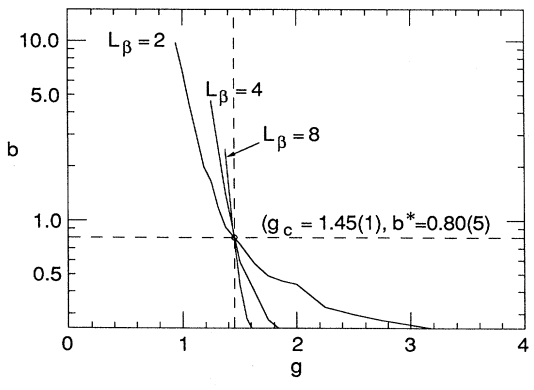

FIG. 19. The b defined by Eq. (5.16), given as a function of g calculated at $L_\beta = 2,4,8$ and for large enough space extent L so that finite-size effects on ξ_l due to finite L are negligible. We clearly see the presence of a critical point at $g_c \simeq 1.45$.

$$\beta(g) = -\beta_1 (g - g_c) + \cdots \tag{5.18}$$

At low T, where the correlation length is large, the function $g(a)$ is determined by holding the correlation length fixed in physical units. Manousakis and Salvador find that $\beta_1 \simeq 1.3$. By integrating Eq. (5.18) to obtain $a(g)$ or differentiating Eq. (5.13) to obtain $\beta(g)$, we can easily show that $\beta_1 = 1/\nu \simeq 1.4$ by taking $\nu \simeq 0.7$. Using $\beta(g)$ as given by Eq. (5.18), and the definition $\beta(g) \equiv -a(dg(a)/da)$, one finds that $a(g)$ is given by Eq. (5.13) where a_0 is a constant of integration.

Ignoring for the moment the anomalous dimension η (which for this model is very small), we can determine the function $a(g)$ approximately from the scaling behavior of the staggered magnetization. Holding g dimensionless, we see that the action (4.81) in the continuum limit and at $T = 0$ takes the form

$$S_\sigma = \frac{1}{g} \int d^3x \sum_\mu [\partial_\mu \mathbf{n}(\mathbf{x})]^2 \ , \tag{5.19}$$

where the field $\mathbf{n}(\mathbf{x})$ has been defined as

$$\mathbf{n}(\mathbf{x}) \equiv \frac{\mathbf{n}_l(\mathbf{x})}{\sqrt{a}} \ , \tag{5.20}$$

and the lattice spacing $a \to 0$. Let us assume that the expectation value of $\mathbf{n}(\mathbf{x})$ for an infinite-size system below g_c is finite and its absolute value is given in physical units by $\bar{n}$. We wish to find a function $g = g(a)$ such that $\bar{n}$ remains constant at all values of small lattice spacing a (large correlation lengths), independently of the value of g. This means that $g(a)$ is defined so that

$$\bar{n} \equiv \frac{n_0(g(a))}{\sqrt{a}} \ , \tag{5.21}$$

for all $a \to 0$. The function $n_0(g)$ is the infinite lattice value of the staggered magnetization, which is only a function of g, and its calculation has been explained earlier (Fig. 18 and Table V). The above equation defines the function $g(a)$ from which we can calculate the β function shown in Fig. 20. With this method we find that the critical point $g_c = 1.45$ and $\beta_1 = 1/(2\beta) = 1.40 \pm 0.05$ (where β is the magnetization critical exponent). We see that the results within error bars agree with those obtained from the correlation length, and they are consistent with the assumption that η is small.

Having approximately determined the function $a = a(g)$, by the three different ways discussed above, we can proceed to study the behavior of the correlation length at low T. As $T \to 0$, we may take for $a = a(g)$ the

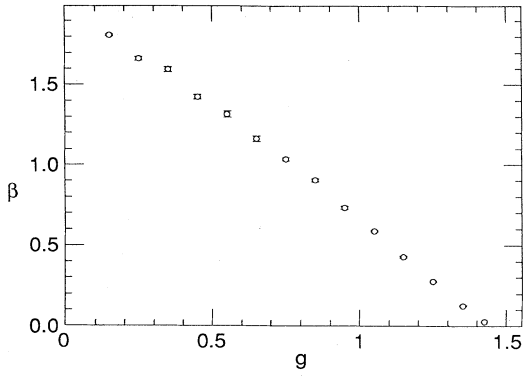

FIG. 20. The approximate β function calculated from $n_0(g)$.

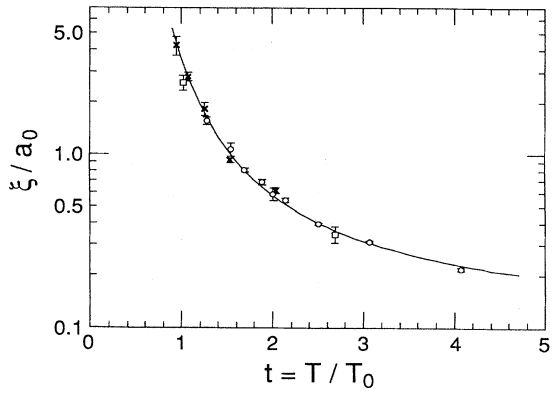

FIG. 21. The collapse of the calculated correlation lengths for various values of g and L_β to a universal curve $\xi_0(t)$, using the calculated $a=a(g)$. The solid line represents the best fit to Eq. (5.23).

function (5.13) with $\nu=0.7$; a_0 is an unknown physical length scale, whose value is dictated by the specific physical problem. Notice that the results do not depend strongly on the errors in the determination of the function $a(g)$, i.e., the precise value of ν. In this paper we shall use the textbook value of ν, and we shall find essentially the same results as those obtained by Manousakis and Salvador (1989c), who computed $a(g)$ using the finite-size scaling technique discussed previously.

Next we shall determine the temperature-dependent correlation length. Using Eq. (4.82a) and $a(g)$ we find that

$$t\equiv\frac{T}{T_0}=\frac{1}{L_\beta|g-g_c|^\nu}\ , \tag{5.22a}$$

where the constant temperature scale T_0 is defined as

$$k_B T_0\equiv\frac{\hbar c_\sigma}{a_0}\ . \tag{5.22b}$$

Furthermore, substituting Eq. (5.13) in Eq. (5.14), we obtain

$$\xi_0\equiv\frac{\xi}{a_0}=\xi_l(g,L_\beta)|g-g_c|^\nu\ . \tag{5.22c}$$

Given the value of the correlation length $\xi_l(g,L_\beta)$ for given values of g and L_β using Eqs. (5.22), we can calculate the physical correlation length in units of the constant length scale a_0 and the physical temperature in units of the constant temperature scale T_0 defined by (5.22b). Using the calculated correlation lengths for various values of $g<g_c$ and L_β, we can calculate ξ_0 and the corresponding t and plot them to obtain a single curve $\xi_0(t)$, shown in Fig. 21.

The fact that $\xi(T)$ obeys the expression obtained by the two-loop calculation of Chakravarty *et al.*, i.e., Eq. (5.7), is demonstrated in Fig. 22, where the function $t\ln(\xi_0(t))$ can be approximated by a straight line. A straight-line fit gives

$$\xi/a_0=A\exp\left[B\frac{T_0}{T}\right]\ , \tag{5.23}$$

with $A=0.093\pm0.002$ and $B=3.64\pm0.02$. The constants a_0 and T_0 cannot be determined within the nonlinear σ model. They correspond to the two free parameters of the model, namely, g and c_σ. Assuming that the σ model describes the continuum limit of the spin-$\frac{1}{2}$ antiferromagnetic Heisenberg model, we can determine a_0 and T_0 in terms of J and the lattice spacing a_H of the lattice, in which the spin-$\frac{1}{2}$ antiferromagnetic Heisenberg model is defined. Comparing these results with those obtained from the Heisenberg model in Sec. V.B, i.e., $\xi(T)=0.276a_H\exp(2\pi\rho_s/T)$, with $\rho_s=0.20J$, we find $a_0=3.0a_H$ and $T_0=0.345J$. Using Eq. (5.22b), we find $\hbar c_\sigma=1.02Ja_H$. Again we emphasize that c_σ is not the physical spin-wave velocity, but a free parameter of the σ model. The generation of such finite length and energy scales (here, the scales a_0 and T_0) from a continuum model where the lattice spacing vanishes is known in

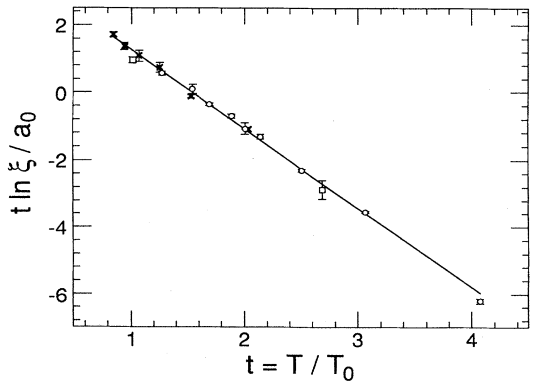

FIG. 22. The fact that Eq. (5.23) fits the data of Manousakis and Salvador (1989c) for the σ model is illustrated. The function $t\ln(\xi_0(t))$ can be approximated by a straight line.

quantum field theory as dimensional transmutation (Coleman and Weinberg, 1973).

VI. DAMPING OF SPIN WAVES

In this section we briefly discuss finite-lifetime effects for spin-wave excitations in 2D quantum antiferromagnets. At $T=0$ and in the long-wavelength limit the spin-wave excitations are well defined excitations because their dispersion curve has negative curvature. A single-magnon excitation created above the ground state cannot decay into a three-magnon excitation or multimagnon excitation unless the single-magnon dispersion curve is anomalous (Pitaevskii, 1959, 1961). If the single-magnon spectrum as a function of the magnon momentum $\mathbf{k}$ is a convex function, it does not allow the spontaneous decay of a single-magnon excitation into multimagnon excitations. Studies of the linewidths of spin-wave peaks in response functions at nonzero temperature, for the case of the spin-$\frac{1}{2}$ square-lattice antiferromagnetic Heisenberg model, have recently begun. Furthermore, from the experimental point of view, it is beyond our present capabilities to measure these linewidths (Aeppli *et al.*, 1989). Our feeling is that it will be more appropriate to review this subject in detail at a later time, and here we discuss only the results of the few calculations that are available now.

Tyč and Halperin (1990) have calculated the spin-wave damping $\Gamma_k(T)$, that is, the imaginary part of the magnon self-energy $\Sigma(\mathbf{k},\omega)$ at the center frequency of the magnon peak $\omega=\omega(\mathbf{k})$, using spin-wave theory. Their main conclusion is that at low T, where ξ is exponentially large, spin-wave excitations with wavelengths short compared to the correlation length, are well-defined excitations; $\Gamma_k/\omega(\mathbf{k})\to 0$ when $k\to 0$ and $T\to 0$ in such a way that $k\xi(T)\gg 1$. A single-magnon excitation has a finite lifetime at nonzero T, due to scattering of the magnon by other thermally excited magnon excitations. Again the contribution of spontaneous decay into multimagnon excitation is zero, due to energy-momentum conservation. The rate $\Gamma_k(T)$ assumes different forms in four regimes defined by the relative size of the reduced temperature $\tau\equiv 2T/JzS$ (where z is the number of nearest neighbors) and the wave vector ka in lattice-spacing units, namely,

Regime A: $k_m(\tau)\ll k\ll\tau^3/2\pi S^2\ll 1$

$$\hbar\Gamma_k/J=\frac{ze(\mathbf{k})\tau^2}{2\pi S}\left[\ln\left[\frac{2\pi S^2}{\tau^2}\right]+C_A\right], \tag{6.1a}$$

where C_A is a constant of order unity and $e(\mathbf{k})=\sqrt{1-\gamma_k^2}$. Here $k_m(\tau)$ is a lower bound, because at $T\neq 0$ the order is destroyed and the spin-wave excitations can only be defined for wavelengths smaller than a temperature-dependent cutoff of the order of the correlation length.

Regime B: $\tau^3/2\pi S^2\ll k\ll\tau\ll 1$

$$\hbar\Gamma_k/J=\frac{ze(\mathbf{k})\tau^2}{2\pi S}\left[\ln\left[\frac{\tau}{k}\right]+C_B\right], \tag{6.1b}$$

where C_B is also a constant of order unity.

Regime C: $\tau\ll k\ll\tau^{1/3}\ll 1$

$$\hbar\Gamma_k/J=\frac{7z\zeta(\frac{5}{2})}{8(2\pi)^{3/2}S}[e(\mathbf{k})\tau^5]^{1/2}, \tag{6.1c}$$

Regime D: $\tau^{1/3}\ll k\ll 1$

$$\hbar\Gamma_k/J=\frac{3z\zeta(3)}{8\sqrt{2}\pi Se(\mathbf{k})\sqrt{f(\hat{k})}}\tau^3, \tag{6.1d}$$

where $f(\hat{k})$ is a weak function of the direction of the wave vector $\mathbf{k}$.

Since the correlation length diverges with decreasing τ as $\sim\exp(\text{const}/\tau)$, there is a range of wave numbers $k\xi\gg 1$ where the $\Gamma_k(T)$ is much smaller than the energy of the spin-wave excitations. The results of this microscopic calculation are presented in detail in the paper by Tyč and Halperin (1990).

Kopietz (1990a), independently from Tyč and Halperin, has calculated the decaying rates using the Dyson-Maleev boson formalism. In the regime D (which is short wavelengths) his results agree with those of Tyč and Halperin. In the regimes A and B his estimate for the decay rates is $\Gamma_k\sim\tau^2 k$.

Becher and Reiter (1989) have calculated the spin-wave damping by calculating the spin-dynamical structure function $S(\mathbf{k},\omega)$ using the equation-of-motion approach in conjunction with projection-operator methods. They find that, at $T=0$, $\Gamma_k\sim k^2$, which, however, contradicts our expectation that the linear dispersion of the single-magnon excitation at $T=0$ at low k provides no phase space for energy-momentum conservation and makes its decay into multimagnon excitations impossible. Later, Becher and Reiter (1990) located an error in their previous work; their corrected work predicts that, at least to order $1/S$, at $T=0$ and in the long-wavelength limit, the damping of spin waves is zero; at $T=0$, they find that there is no damping of order T^2.

Grempel (1988), in a short comment, has also given Γ for excitations near the antiferromagnetic wave vector and for $k_BT<\hbar\omega$ and $k\xi\ll 1$. He finds that $\Gamma_k\sim\sqrt{\tau ka}/\xi(T)$ and concludes that, at low T where $\xi(T)$ is very large, the relaxation rates are very small. In contrast, Tyč and Halperin find in this regime considerably larger decay rates, which do not depend so strongly on T. In Grempel's calculation, $\Gamma(T)$ has a strong temperature dependence through the temperature dependence of the correlation length, whereas in Tyč and Halperin's calculation Γ depends much more weakly on T.

Similar results were obtained by Kopietz (1990b), who, as explained in Sec. IV.C, carried out exactly the integration over the Brillouin zone for the dynamic structure factor obtained by Auerbach and Arovas (1989), using Schwinger boson mean-field theory. Kopietz pointed out

that this theory gives $\Gamma_k/\omega_k \sim 1/\xi k$, which is the same as the results of Takahashi (1989b) for a quantum ferromagnet and contradicts seriously the results obtained by Tyč and Halperin. Since the correlation length is very large at low T, the decaying rates predicted by Schwinger boson mean-field theory are too small to agree with experimental values of the linewidths. He concludes that the theory of Tyč, Halperin, and Chakravarty (1989) and the calculation of Tyč and Halperin are more accurate than Schwinger boson mean-field theory.

Chakravarty *et al.* (1989) and subsequently Tyč, Halperin, and Chakravarty have used a semiphenomenological approach to calculating the dynamic structure function, based on scaling arguments, hydrodynamics, and the equivalence of the spin-$\frac{1}{2}$ antiferromagnetic Heisenberg model with the nonlinear sigma model. In particular, they used the equivalence of the quantum nonlinear sigma model and the 2D classical nonlinear σ model, with an appropriately renormalized coupling constant defined by Eqs. (4.76) and (4.77), and by simulating the latter model with a molecular dynamics algorithm they were able to predict an empirical form for $S(k,\omega)$ from which they also extracted the decay rate $\Gamma_k(T)$. Tyč and Halperin (1990) also made a connection between the microscopically calculated lifetimes and those predicted by Tyč, Halperin, and Chakravarty. They have shown that if we make the replacement in Eq. (6.1) $\rho_s = JS^2$ and $\hbar c = \sqrt{8}JSa$, which is valid for large S, the resulting formulae are more generally valid on the basis of Tyč-Halperin-Chakravarty model.

VII. COMPARISON WITH EXPERIMENTS

Interesting magnetic properties of the copper-oxygen-based materials are revealed by neutron-scattering experiments performed on undoped single crystals of La_2CuO_4. The $La_2CuO_{4+\delta}$ material has a susceptibility anomaly at a 3D Néel temperature T_N which is sensitive to the value of δ (Yamada *et al.*, 1987). The first neutron-scattering experiments from a single crystal of La_2CuO_4 (Shirane *et al.*, 1987) show that the instantaneous 2D antiferromagnetic correlations exceed 200 Å for $T \sim 200-300$ K, with no average staggered magnetization. The energy scale associated with spin fluctuations above T_N is very large compared to those of other 2D antiferromagnets having the same crystal structure, such as K_2NiF_4 or K_2CoF_4. In addition, the highly correlated but fluctuating spins in La_2CuO_4 do not show the dramatic critical slowing down found in other 2D spin systems. Shirane *et al.* (1987) conjectured that such fluctuations give rise to a new state of the spin system, a quantum "spin-liquid" state. Very quickly it became clear that one needs to understand the model (1.2) in low-dimensional systems and for the smallest-spin case, where the quantum fluctuations are expected to be large. Antiferromagnetic ordering has also been observed by neutron diffraction from powder of YBa_2CuO_6 (Tranquada *et al.*, 1988) with $T_N \sim 500$ K. However, due to difficulties in growing large single crystals of $YBa_2Cu_3O_{7-y}$ to be used for neutron-scattering studies, the studies of the magnetic properties of this material are limited (Sato *et al.*, 1988). In contrast, crystals of La_2CuO_4 close to exact stoichiometry have been more systematically studied, and in this paper the theoretical results are compared only to those obtained on this material.

In this section we first discuss the extent to which the square-lattice spin-$\frac{1}{2}$ antiferromagnetic Heisenberg model can describe the spin dynamics of pure La_2CuO_4. We discuss the role of possible Ising-like anisotropies, antisymmetric terms, and interplanar coupling. We compare the temperature dependence of the theoretically calculated correlation length with that measured on single crystals. The spin-wave excitations and the pair-magnon excitations have been observed by neutron- and Raman-scattering experiments. We compare the experimental and theoretical excitation spectra. Finally, to understand most of the thermodynamic properties of the materials, we need to consider the interplanar coupling. We discuss the role of a Dzyalshinskii-Moriya antisymmetric term, which is responsible for a hidden ferromagnetic-like behavior of the uniform susceptibility below the 3D Néel ordering temperature.

A. Can the isotropic 2D Heisenberg model describe La_2CuO_4?

As we have briefly argued in the Introduction, the spin-$\frac{1}{2}$ antiferromagnetic Heisenberg model arises naturally as an effective low-energy theory to describe spin degrees of freedom in a single copper-oxygen plane. However, in order to establish its relevance, one needs to examine the magnitude of the interplanar coupling and the role of the possible anisotropies that may have to be introduced in order to describe realistically the magnetic properties of La_2CuO_4.

Chakravarty, Halperin, and Nelson (1988) have argued and Thio *et al.* (1988) have found experimentally that the interplanar coupling J' is of the order of $10^{-5}J$. Hence J' has a small effect on the 2D spin correlations above the 3D Néel ordering temperature, and the zero-temperature properties calculated only for an isolated CuO_2 plane will be weakly affected by such a small value of J' (see Chakravarty *et al.*, 1989). The 2D correlation length $\xi(T)$ is very large at room or lower temperatures due to the large in-plane coupling J, and $\xi(T)$ grows exponentially with J/T. As a result, a very small interplanar coupling can still produce a rather high 3D Néel temperature. To understand the behavior of the susceptibility, the intensity of the antiferromagnetic Bragg peak in neutron-scattering experiments at finite temperatures, and other pure 3D effects close to the Néel temperature, one needs to consider the interlayer coupling. Certain 3D effects can be qualitatively included in a simple way, as Thio *et al.* have shown, using a mean-field treatment of the weak plane-plane coupling. For such a treatment, one needs the 2D staggered and uniform susceptibility

calculated from the spin-$\frac{1}{2}$ antiferromagnetic Heisenberg model given in this paper. We shall describe this mean-field theory in Sec. VII.D, where we discuss the behavior of the uniform susceptibility.

We need to discuss the role of other possible terms that one might have to add to the Hamiltonian (1.2) in order to make a meaningful comparison of the results presented here with the experimental results. For example, we need to study the role of Ising-like anisotropies, antisymmetric terms, and further neighbor interactions. Peters *et al.* (1988) have considered a more general neighbor Hamiltonian expressed as

$$H=\sum_{\langle ij\rangle}(J_{aa}S_i^aS_j^a+J_{bb}S_i^bS_j^b+J_{cc}S_i^cS_j^c)\ , \tag{7.1}$$

where $\hat{\mathbf{a}}$, $\hat{\mathbf{c}}$ are the axes on the CuO_2 plane and $\hat{\mathbf{b}}$ is the axis perpendicular to the plane. Here we use the same notation as Peters *et al.* (1988). By measuring the gaps in the excitation spectrum and using the mean-field approximation, they found that $J_{aa}\simeq J_{bb}\simeq J_{cc}\simeq J$ within $<0.01\%$ accuracy. The fact, however, that the staggered magnetization is along the $\hat{\mathbf{c}}$ direction means that there is a very small anisotropy of the three couplings that favors this direction.

Peters *et al.* (1988) and Thio *et al.* (1988) have used an antisymmetric term in the Hamiltonian (1.2) in order to explain hidden ferromagnetism manifesting itself below T_N. Dzyaloshinskii (1958) proposed that weak ferromagnetic behavior could be understood by adding an antisymmetric term of the form $\mathbf{D}\cdot(\mathbf{S}_i\times\mathbf{S}_j)$ in the antiferromagnetic Heisenberg Hamiltonian. Such a term is not forbidden if the symmetry of the crystal is sufficiently low. Later, Moriya (1960) showed that such a term comes from the effect of the spin-orbit coupling on the superexchange interaction; the order of magnitude of $|D|$ is $\Delta g/gJ$, where g is the electron gyromagnetic ratio and Δg is the change in the bare value of g due to spin-orbit coupling. Coffey, Bedell, and Trugman (1990) generalize this Hamiltonian to

$$H_a=\sum_{\langle ij\rangle}\mathbf{D}_{ij}\cdot(\mathbf{S}_i\times\mathbf{S}_j)\ , \tag{7.2}$$

which allows for spatial variation of $\mathbf{D}_{ij}$. This term is responsible for the canting of the spins away from the direction of the staggered magnetization (which lies in the $\hat{\mathbf{c}}$ direction) towards the $\hat{\mathbf{b}}$ axis by a small angle, as observed by Kastner *et al.* (1988) using neutron-scattering experiments. If $\mathbf{D}_{ij}$ is required to be along the positive or negative $\hat{\mathbf{a}}$ direction and change sign from one bond to the next, the term (7.2) in combination with (7.1) can produce the canting of the spins towards the $\hat{\mathbf{b}}$ direction, as shown by Coffey, Bedell, and Trugman. They have also shown that this is consistent with the symmetries of the La_2CuO_4 crystal, taking into account the rotation of the CuO_6 octahedra around the Cu site. This can produce a ferromagnetic moment pointing in the $\hat{\mathbf{b}}$ direction, which can explain the behavior of the uniform susceptibility and the magnetoresistance data of Thio *et al.* (1988). Thio *et al.* considered a uniform $\mathbf{D}_{ij}=J^{bc}\hat{a}$ without the sign alteration; this, however, does not produce a ferromagnetic moment, as pointed out by Coffey *et al.* The analysis of Thio *et al.* (1988) can be easily corrected, however, without affecting the results of their fit. This is discussed in more detail in Sec. VII.D. The coupling $J^{bc}=|\mathbf{D}_{ij}|$, estimated from the angle of the canted spins, was found to be small compared to the antiferromagnetic coupling $J(J^{bc}/J\sim10^{-3})$ and can be neglected in the calculation of the 2D correlation length and staggered magnetization. However, it plays an important role in determining the puzzling ferromagnetic-like behavior of the susceptibility close to the 3D Néel temperature, and we shall return to this point in Sec. VII.D.

The addition of the antisymmetric term (7.2) opens a gap at $\mathbf{k}=(\pi,\pi)$ in the spin-excitation spectrum. Linearizing the equations of motions for the spin operators with respect to small deviations around the classical ground state, Coffey *et al.* (1990) find for a square lattice that $\omega(\mathbf{k})=4SJ[\lambda_D(\lambda_D+\gamma_{\mathbf{k}})(1-\gamma_{\mathbf{k}})]^{1/2}$, with $\lambda_D=[1+(J^{bc}/J)^2]^{1/2}$. Since there is still a continuous symmetry, i.e., global rotation around the direction of $\mathbf{D}$ ($\hat{\mathbf{a}}$ axis), the system is entitled to have a Goldstone mode in the long-wavelength limit and no gap at $k=0$. The Ising-like anisotropies as in Eq. (7.1) open a gap at $\mathbf{k}=0$ [as can be seen by examining Eq. (2.16)] and are responsible for giving a definite direction to the staggered magnetization. The excitation spectrum after the inclusion of both terms has been given by Coffey *et al.* As mentioned before, the gaps in the excitation spectrum of La_2CuO_4 are very small and consistent with small J^{bc}, $|J_{aa}-J_{bb}|$, and $|J_{aa}-J_{cc}|$.

Another possible term that one might need to add to the Hamiltonian (1.2) is a next-nearest-neighbor (NNN) interaction

$$H=J\sum_{\langle ij\rangle}\mathbf{S}_i\cdot\mathbf{S}_j+J_2\sum_{(\mathrm{NNN})}\mathbf{S}_i\cdot\mathbf{S}_k\ , \tag{7.3}$$

where the sum in the second term is over next-nearest-neighbor pairs. Such a term with $\alpha\equiv J_2/J>0$ is expected to frustrate the antiferromagnetic long-range order and lead to a disordered phase for $\alpha>\alpha_c$ (Anderson, 1973, 1987). Classically, this model for $\alpha<\frac{1}{2}$ has Néel order, and for $\alpha>\frac{1}{2}$ the lattice decouples into two Néel sublattices with a highly degenerate ground-state; for $\alpha=\frac{1}{2}$, states having uniform but arbitrary twists are degenerate ground states. This model was also proposed by Inui *et al.* (1988), in a semiphenomenological fashion, to capture the physics of frustration introduced into the system by the addition of holes. Recent calculations (Nori, Gagliano, and Bacci, 1990), however, indicate that frustration in the form of Eq. (7.3) does not properly describe doping.

Doniach *et al.* (1988) studied the model (7.3) using variational theory, and they found that with $\alpha\sim0.07$ the antiferromagnetic long-range order is unstable against a resonating valence bond state. The same model, however, has been studied by Chandra and Doucot (1988) and

Chakravarty *et al.* (1989), using conventional spin-wave theory, and by Dagotto and Moreo (1989a, 1989b), who found that the Néel order is quite robust and a large value of α is necessary to destroy the Néel order. More recently, Kishi and Kubo (1989) have rigorously shown the existence of antiferromagnetic long-range order in the ground state of the Hamiltonian (7.3) on a square lattice for spin values $S \geq 1$ and for $\alpha \leq \alpha_c(S)$. The nature of the magnetically disordered state that appears for $\alpha \geq \alpha_c$ for spin-$\frac{1}{2}$ is controversial. Chandra and Doucot suggested that this state should be a quantum spin liquid. More recently, Gelfand *et al.* (1989), using series-expansion techniques, find that the dimerized state with the "columnar" pattern, suggested by Read and Sachdev (1989), who studied the stability of antiferromagnetic order against quantum fluctuations in a $1/n$ expansion, becomes the new stable state in a certain range of α. In our comparison with the experimental data we shall neglect J_2, even though we do not know its magnitude. The results of the spin-wave theory of Chandra and Doucot and the numerical results of Dagotto and Moreo (1989a, 1989b) and Hirsch and Tang (1989a) suggest that a large magnitude of α is required to have dramatic effects on the antiferromagnetic order. There is no clear experimental evidence or arguments to suggest that J_2 is of a magnitude comparable with J in the real materials.

It has been argued (Aharony *et al.*, 1988) that the addition of holes in La_2CuO_4 introduces a local ferromagnetic exchange coupling between Cu spins. In addition, Aharony *et al.* have suggested that such ferromagnetic defects give rise to the spin-glass phases of $La_{2-x}Sr_xCuO_4$ (Huber and Chin, 1990). Lee and Schlottmann (1990) introduced a single ferromagnetic bond inside the 2D spin-$\frac{1}{2}$ antiferromagnetic Heisenberg model and studied its effect on the antiferromagnetic correlated spins in the neighborhood of the bond, using linear spin-wave theory. They found that the disturbance of the antiferromagnetic order caused by the presence of such a defect is localized within the neighborhood of the ferromagnetic bond and decays as $1/R^3$ far away from it. In addition, the antiferromagnetic moments are rather weakly dependent on the strength of the ferromagnetic coupling, which is required to be comparable to J in order seriously to affect the antiferromagnetic order.

B. Correlation length

Assuming that the isotropic nearest-neighbor spin-$\frac{1}{2}$ antiferromagnetic Heisenberg model can give a realistic description of the spin dynamics in the CuO_2 planes, we proceed to compare the temperature dependence of the correlation length, the spin-wave velocity, the zero-temperature staggered magnetization, and the uniform susceptibility with the experiments. The correlation length is extracted from the static structure factor $S(q)$, which is obtained by integrating the measured spin-dynamic structure function up to the energy of the incident neutron. This integration assumes that the maximum possible energy transfer ω ($\omega \leq E_i$, where E_i is the energy of the incident neutron) is large enough to include the total contribution of relevant spin excitations described by Eq. (1.2). Endoh *et al.* (1988) have approximated the structure function by $S(q) \sim 1/\{q^2 + [1/\xi(T)]^2\}$, and this expression is used to extract an estimate for the 2D correlation length. In Figs. 23 and 24, we plot the inverse correlation length versus T as observed by neutron-scattering experiments (Endoh *et al.*, 1988; Yamada *et al.*, 1989). The solid curves are obtained using the expression $\xi(T) = C_\xi \exp(2\pi\rho_s/T)$, which fits the results obtained from the spin-$\frac{1}{2}$ antiferromagnetic Heisenberg model on a square lattice (or the equivalent nonlinear σ model). The most accurate re-

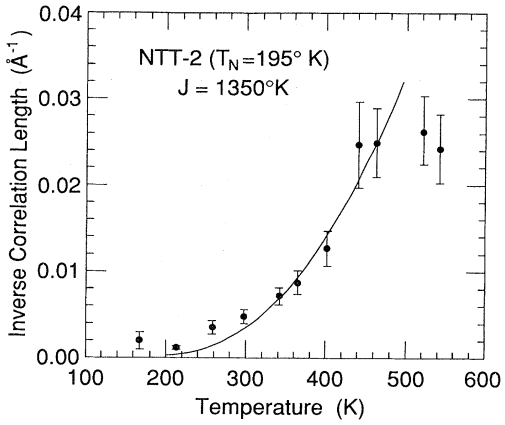

FIG. 23. The data points with error bars are values of the inverse correlation length, as obtained from the neutron-scattering experiments of Endoh *et al.* (1988) done on the NTT-2 crystal with Néel temperature of $T_N = 195$ K. The solid line is obtained using the theoretical form (5.7) obtained from the simulation of the spin-$\frac{1}{2}$ antiferromagnetic Heisenberg model on a square lattice and $J = 1350$ K.

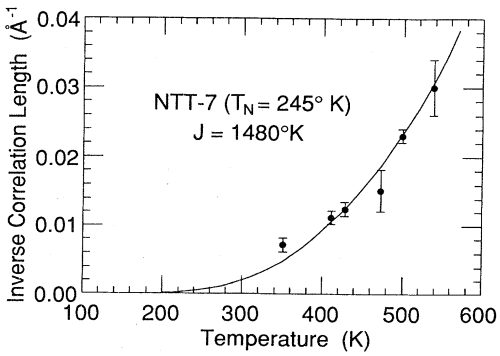

FIG. 24. Similarly to Fig. 23, the results of Yamada *et al.* (1989), obtained on the NTT-7 crystal with $T_N = 245$ K. The solid line was obtained using the theoretical curve (5.7) obtained from the simulation of the spin-$\frac{1}{2}$ antiferromagnetic Heisenberg model on a square lattice and $J = 1480$ K.

sults are $\rho_s = 0.20J$ and $C_\xi = 0.276 a_H$, obtained as explained in Sec. V and given in Table IV. In the plots we used $a_H = 3.8$ Å (the Cu-Cu distance). Different samples require different values of J to obtain a reasonable fit, because they are characterized by somewhat different correlation lengths. In Fig. 23 the solid circles with the error bars are the estimates for the correlation lengths of the NTT-2 crystal of Endoh *et al.* having a Néel temperature $T_N = 195$ K. The solid line represents the theoretical curve obtained with $J = 1350$ K. In Fig. 24 the solid circles with the error bars are the experimental estimates for the $\xi(T)$ extracted for the NTT-7 crystal of Yamada *et al.* (1989) having a Néel temperature $T_N = 245$ K. The solid line is obtained from the same theoretical curve with $J = 1480$ K. The data disagree with the theoretical curves for correlation lengths of the order of 200 Å or larger. The differences and the fact that crystals with higher T_N give somewhat different correlation lengths can be attributed to the high sensitivity of the spin-correlation length to the doping fraction x (hole concentration). For example, Birgeneau *et al.* (1988) have shown that the correlation length is limited by the average hole distance, namely, $\xi(x) \simeq 3.8$ Å$/\sqrt{x}$. A tiny amount of hole concentration, about $x \sim 10^{-4}$, is enough to limit the correlation length to about 200 Å. In $La_2CuO_{4+\delta}$ there is an effective hole concentration $x \sim 2\delta$, and a slight amount of oxygen excess is expected for such as-grown crystals (Yamada *et al.*, 1989). Clearly the sample with $T_N = 195$ K cannot be purely stoichiometric, and the hole impurities reduce the value of the Néel temperature. As the Néel temperature increases, the quality of the crystal is improved, and the value of J increases and approaches the value necessary to give the observed spin-wave velocity discussed next.

C. Spin-wave excitations

The thermal neutron-scattering data provide a lower bound for the spin-wave velocity of approximately $\hbar c \geq 0.6$ eV Å (Birgeneau *et al.*, 1988, Endoh *et al.*, 1988). More recently, however, Aeppli *et al.* (1989), using high-energy inelastic neutron scattering and constant energy transfer ω scans, measured the intensity of the outgoing neutrons as a function of the momentum transfer q [see Fig. 25(a)]. They achieved good enough resolution to measure c accurately (with only about 5% error). Aeppli *et al.* approximated the scattering cross section by the expression suggested by spin-wave theory (Marshall and Lovesey, 1971); in the long-wavelength limit it is given by

$$\frac{\partial^2\sigma}{\partial\Omega\partial\omega} = \frac{k_f}{k_i} A_q [(n(cq)+1)\delta(\omega - cq) + n(cq)\delta(\omega + cq)] , \tag{7.4}$$

where k_i and k_f are the wave vectors of the incident and outgoing neutron, $n(\omega)$ is the Bose-Einstein occupation factor $[\exp(\beta\hbar\omega)-1]^{-1}$, A_q is the square of the matrix

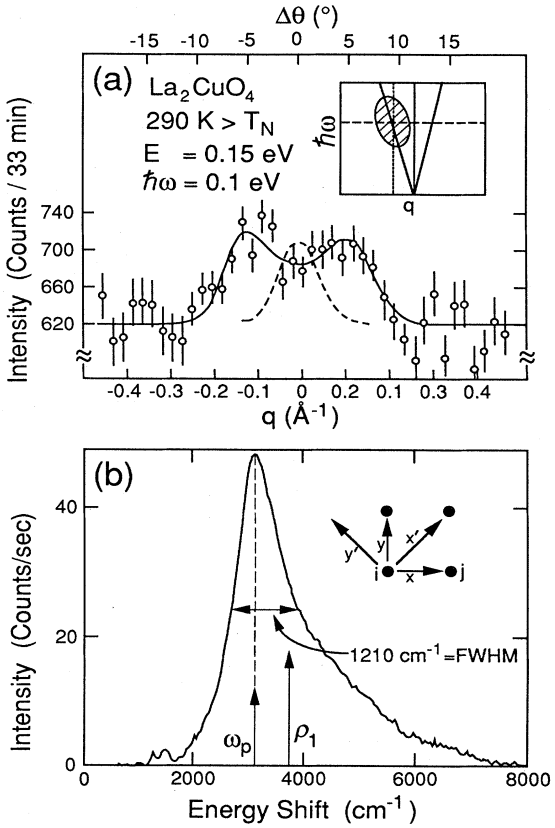

FIG. 25. (a) Constant-energy transfer scan, collected in transverse direction for momentum transfers near (2,0,1), from the neutron-scattering experiment of Aeppli *et al.* (1989); q and $\Delta\theta$ represent deviations from the (2,0,1) in momentum transfer and scattering angle, respectively. The dashed line represents a measure of the experimental resolution. The solid line represents the best fit using the spin-wave expression (7.4) with a spin-wave velocity of $\hbar c = 0.78$ eV −Å and with the delta functions broadened by the instrumental resolution. (b) The Raman-scattering data obtained by Lyons *et al.* (1989) for $\mathbf{E}_1 \| \hat{\mathbf{x}}'$ and $\mathbf{E}_2 \| \hat{\mathbf{y}}'$, where the directions $\hat{x}'$ and $\hat{y}'$ are along the diagonal of the square lattice that connects the coppers in the copper-oxygen plane. In the inset, where the solid circles denote the locations of copper atoms on the copper-oxygen plane, the directions x, y, x', and y' are shown.

element that couples the antiferromagnetic ground state to the spin-wave state, and $A_q \sim 1/q$ for scattering near the antiferromagnetic superlattice reflections. Notice that Eq. (7.4) for positive energy ω is the same as the expression (4.32) given by Arovas and Auerbach. The dashed line in Fig. 25(a) gives the broadening due to instrumental resolution. The solid line gives the fit that Aeppli *et al.* found by broadening the delta function with the experimental resolution and using a spin-wave velocity of $\hbar c = 0.78$ eV Å. Repeating the experiment at different energy transfers, they found that their data in the long-wavelength limit could be explained by the spin-wave expression (7.4) with $\hbar c = 0.85 \pm 0.03$ eV Å and

$A_q \sim 1/q$. Because of the resolution-broadening of the data, it appears very difficult to say something about the thermal broadening and the temperature dependence of the spin-wave lifetime discussed in Sec. VI. In Sec. III we found that $c = Z_c\sqrt{2}Ja$, and the theoretical lines for Z_c obtained with various methods lie in the interval $Z_c \simeq 1.19 \pm 0.05$. Using $Z_c = 1.19 \pm 0.05$ and the value of $c = 0.85$ eV Å inferred from these neutron-scattering studies, we obtain $J \simeq 1540 \pm 60$ K, in excellent agreement with the figure obtained by comparing the correlation lengths for the NTT-7 crystal.

Raman-scattering studies of La_2CuO_4 have revealed (Lyons *et al.*, 1988, 1989; Sugai *et al.*, 1988) a high-frequency peak (at about 3000 cm^{-1}), which has been attributed to scattering from magnon pairs with opposite momenta. The Hamiltonian describing the scattering of light of incident polarization $\mathbf{E}_1$ into a scattered light of polarization $\mathbf{E}_2$ by a magnon pair is given as (Parkinson, 1969)

$$H_R = A \sum_{\langle ij \rangle} (\mathbf{E}_1 \cdot \hat{\mathbf{e}}_{ij})(\mathbf{E}_2 \cdot \hat{\mathbf{e}}_{ij})(\mathbf{S}_i \cdot \mathbf{S}_j) , \tag{7.5}$$

where $\hat{\mathbf{e}}_{ij}$ is the unit vector connecting nearest-neighbor sites. The scattering intensity $I(\omega)$, defined as

$$I(\omega) = \sum_n |\langle n|H_R|0\rangle|^2 \delta(\omega - \omega_{n0}) , \tag{7.6}$$

depends strongly on the light polarization relative to the crystallographic axes, as is clear from Eq. (7.5). The strong two-dimensional nature of the magnetism in La_2CuO_4 is evident from the strong dependence of the peak on the polarization direction of the incident and scattered waves. For example, there is no peak $\mathbf{E}_1 \| \hat{\mathbf{z}}$ and $\mathbf{E}_2 \| \hat{\mathbf{z}}$, with z being the direction perpendicular to the copper-oxygen plane. In Fig. 25(b) we show the data obtained by Lyons *et al.* (1989) for $\mathbf{E}_1 \| \hat{\mathbf{x}}'$ and $\mathbf{E}_2 \| \hat{\mathbf{y}}'$, where the directions $\hat{\mathbf{x}}$ and $\hat{\mathbf{y}}$ are the unit vectors connecting copper atoms on the CuO_2 plane and $\hat{\mathbf{x}}'$ and $\hat{\mathbf{y}}'$ are along the diagonal of the square lattice formed by the copper atoms [see inset of Fig. 25(b)]. An estimate of the antiferromagnetic coupling was initially obtained (Lyons *et al.*, 1988) from the estimate of the two-magnon peak from the Heisenberg model. The peak is expected near the two-magnon energy for magnons near the peak of the single-magnon excitation energy. Lyons *et al.* (1988), by approximately correcting for the energy shift of the peak due to magnon-magnon interaction (Hayes and Loudon, 1978, p. 273), estimated that $J \sim 1500$ K. A better estimate for J can be obtained as follows. We define the moments of the intensity $I(\omega)$ by

$$\rho_n = \langle \omega^n \rangle \equiv \frac{\int \omega^n I(\omega)\, d\omega}{\int I(\omega)\, d\omega} . \tag{7.7}$$

Assuming that the states $|n\rangle$ in Eq. (7.6) are the eigenstates of the spin-$\frac{1}{2}$ antiferromagnetic Heisenberg Hamiltonian H, the numerator and denominator of the right-hand side of Eq. (7.7) can be calculated as follows:

$$\int I(\omega)\, d\omega = \langle 0|H_R^2|0\rangle , \tag{7.8a}$$

$$\int \omega I(\omega)\, d\omega = \langle 0|H_R[H,H_R]|0\rangle , \tag{7.8b}$$

$$\int \omega^2 I(\omega)\, d\omega = -\langle 0|[H,H_R]^2|0\rangle , \tag{7.8c}$$

$$\int \omega^3 I(\omega)\, d\omega = \langle 0|[H,[H,H_R]][H,H_R]|0\rangle , \tag{7.8d}$$

i.e., by calculating the ground-state expectation value of the above commutators of H [Eq. (1.2)] and H_R [Eq. (7.6)]. Singh *et al.* (1989) have estimated ρ_1, ρ_2, and ρ_3 by calculating these expectation values with the series expansion technique explained in Sec. II.C. These moments can be measured by integrating the experimental $I(\omega)$. For example, ρ_1, which is the average frequency of the spectrum, is shown in Fig. 25(b). The value of the antiferromagnetic coupling J can be found so that the theoretical and experimental moments agree. Singh *et al.* found that the spin-$\frac{1}{2}$ antiferromagnetic Heisenberg model with a single value of J close to 1500 K can reproduce the experimental values of the three moments within experimental errors. This is interesting because these three moments are sensitive to different parts of the frequency spectrum. Dagotto and Poilblanc (1990) and Gagliano and Bacci (1990) have calculated the moments ρ_n for $n = 1,2,3$ on a 4×4 lattice using exact diagonalization; their results are close to those obtained by Singh; however, results on different sized lattices are unavailable and this prevents extrapolation to an infinite sized lattice. Liu and Manousakis (1990) have calculated the moments $\rho_1/\rho 0$ and $\rho_2/\rho 0$ of the Raman spectrum using the variational Monte Carlo technique and their results are also close to those obtained by Singh.

D. Uniform susceptibility

Most of the other experimental data require an accurate treatment of the spin-spin interaction introduced by the interlayer coupling J' and by $J^{bc} = |\mathbf{D}_{ij}|$ [Eq. (7.2)]. Here we briefly discuss the mean-field theory developed by Thio *et al.* (1988), which qualitatively explains the puzzling behavior (Fukuda *et al.*, 1987; Yamada *et al.*, 1987) of the uniform susceptibility $\chi(T)$. For instance, if the field H is applied in the direction parallel to the copper-oxygen plane, $\chi(T)$ does not have significant temperature dependence. When H is applied in the orthogonal direction, however, $\chi(T)$ develops a peak at the Néel temperature, as shown in Fig. 26. Thio *et al.* (1988) have shown that this can be qualitatively explained using mean-field theory to calculate the corrections to the uniform susceptibility close to the Néel temperature T_N, which are due to the 3D critical coupling J' in combination with the effect of spin-canting due to the anisotropic (J^{bc}) term (7.2). The following discussion takes into consideration the correction to the Hamiltonian (7.2) pointed out by Coffey *et al.* (1990).

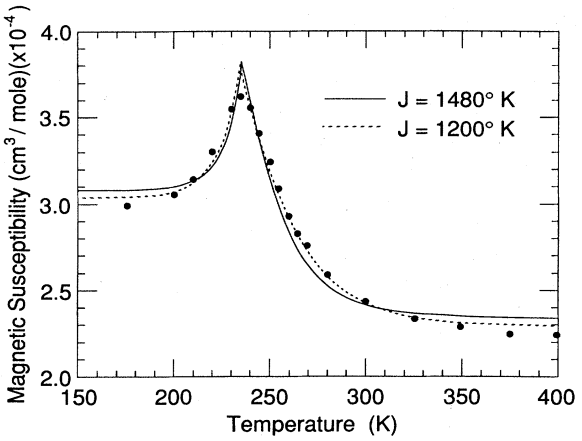

FIG. 26. The uniform susceptibility for the case where the field is in the direction of the b axis (perpendicular to the copper-oxygen planes), using the results of Thio *et al.* (1988). The solid line is a fit using the mean-field expression (7.14) for the staggered magnetization and the theoretical results for the temperature-dependent $2D$ correlation length obtained from the spin-$\frac{1}{2}$ antiferromagnetic Heisenberg model with $J=1480$ K. The dotted line is the best fit to this expression that requires $J=1200$ K.

Let us assume that $m_1^\dagger$ and $m_2^\dagger$ are the staggered magnetizations of two successive $\hat{\mathbf{a}}$-$\hat{\mathbf{c}}$ (copper-oxygen) planes with canted moments alternating in the $\hat{\mathbf{b}}$ direction. Treating the weak plane-plane coupling in mean-field theory, one can write the Landau free-energy density for a pair of layers as

$$f=-\mathbf{m}_1^\dagger\cdot\mathbf{h}_1^\dagger-\mathbf{m}_2^\dagger\cdot\mathbf{h}_2^\dagger+\frac{1}{2\chi_{2D}^\dagger}(m_1^{\dagger 2}+m_2^{\dagger 2}) +\lambda[(m_1^{\dagger 2})^2+(m_2^{\dagger 2})^2]+J'\mathbf{m}_1^\dagger\cdot\mathbf{m}_2^\dagger , \tag{7.9}$$

where $\chi_{2D}^\dagger$ is the staggered susceptibility of the CuO_2 plane and $h_1^\dagger$ and $h_2^\dagger$ are the staggered fields on each plane, with λ an additional parameter. The free energy can be minimized with respect to the order parameters to yield

$$\mathbf{h}_\pm^\dagger=\mathbf{h}_1^\dagger\pm\mathbf{h}_2^\dagger=[(\chi_{2D}^\dagger)^{-1}\pm J']\mathbf{m}_\pm^\dagger +\lambda[(m_+^{\dagger 2}+m_-^{\dagger 2})\mathbf{m}_\pm^\dagger+2(\mathbf{m}_+^\dagger\cdot\mathbf{m}_-^\dagger)\mathbf{m}_\mp^\dagger] , \tag{7.10}$$

where $\mathbf{m}_\pm^\dagger=\mathbf{m}_1^\dagger\pm\mathbf{m}_2^\dagger$ and $\mathbf{h}_\pm^\dagger=\mathbf{h}_1^\dagger\pm\mathbf{h}_2^\dagger$. Removing the external fields, in the ordered phase we find

$$|\mathbf{m}_-^\dagger|^2=\lambda^{-1}[J'-(\chi_{2D}^\dagger)^{-1}] . \tag{7.11}$$

Differentiating Eq. (7.10) with respect to $\mathbf{m}_\pm^\dagger$, we obtain the inverse symmetric and antisymmetric susceptibilities

$$(\chi_\pm^\dagger)^{-1}=\begin{cases}(\chi_{2D}^\dagger)^{-1}\pm J'+3[J'-(\chi_{2D}^\dagger)^{-1}], & T\le T_N ,\\ (\chi_{2D}^\dagger)^{-1}\pm J' , & T\ge T_N ,\end{cases} \tag{7.12}$$

The 3D Néel temperature is determined from the equation $J'\chi_{2D}^\dagger=1$. At low temperatures $\chi_{2D}^\dagger$ can be approximated by

$$\chi_{2D}^\dagger\sim\frac{(\xi_{2D}/a_H)^2}{k_BT} , \tag{7.13}$$

where $\xi_{2D}=C_\xi\exp(2\pi\rho_s/T)$ is the calculated 2D correlation length, with $\rho_s=0.20J$ and $C_\xi=0.276a_H$, as obtained from the spin-$\frac{1}{2}$ antiferromagnetic Heisenberg model. Equation (7.13) approximates $\chi_{2D}^\dagger$ (within a constant numerical factor of order unity) at low temperatures, where $\xi(T)$ is very large.

Next, we shall determine the uniform susceptibility χ. The Hamiltonian (7.2) in the mean-field approximation takes the form $2J^{bc}(m_{1,c}^\dagger M_1^b+m_{2,c}^\dagger M_2^b)$, where M_1^b and M_2^b are the $\hat{\mathbf{b}}$ components of the magnetization in the two neighboring planes, and $m_{1,c}^\dagger$ and $m_{2,c}^\dagger$ are the values of the staggered magnetization of two successive planes which is directed towards the $\hat{\mathbf{c}}$ direction. This is identical to the result of Thio *et al.*; however, it can only be obtained using (7.2) with the alternating directions of $\mathbf{D}_{ij}$ as derived by Coffey *et al.* (1990). Introducing an external field H in the $\hat{\mathbf{b}}$ direction induces a magnetization $M_{1,2}^b=\chi_0 H$, where χ_0 is the uniform (perpendicular) 2D susceptibility of the copper-oxygen plane. This induces a staggered field along the $\hat{\mathbf{c}}$ direction given by $h_+^\dagger=2J^{bc}\chi_0 H$ and a staggered magnetization $m_+^{\dagger c}=2J^{bc}\chi_0 H\chi_+^\dagger$, where $\chi_+^\dagger$ is the symmetric staggered susceptibility. Self-consistency of the mean-field theory provides the susceptibility

$$\chi=\chi_0+\chi_0^2(2J^{bc})^2\chi_+^\dagger . \tag{7.14}$$

In Fig. 26 we show the fits of the experimental results of Thio *et al.* for the uniform susceptibility to the formula (7.14). The experimental results are obtained with the field applied parallel to the $\hat{\mathbf{b}}$ axis. The value of J' is automatically determined from T_N and J as $J'=kT_N/[\xi(T_N)/a_H]^2$. The constant χ_0 is determined from the value of the measured χ at $T\gg T_N$. The solid line is the fit obtained by adjusting χ_0 and J^{bc} and taking $J=1480$ K, the value obtained by fitting the correlation length of the NTT-7 crystal. The results of the fit are $\chi_0=2.3510^{-4}$ cm^3/mol, $J^{bc}\sim 1$ K, and $J'/J=2.8\times10^{-7}$. A better fit is obtained if we allow J to vary as well; we obtain the dotted line with $J=1200$ K, $\chi_0=2.29\times10^{-4}$ cm^3/mol, $J^{bc}=3.4$ K, and $J'/J=6.5\times10^{-6}$. At $H=0$, the layers cant in opposite directions because of the weak antiferromagnetic coupling J'. Thio *et al.* have estimated the magnitude of the angle of the canted spins from the increase in magnetization at the critical field at which the layers cant in the same direction. J^{bc} can be estimated from the value of the angle θ, since in mean-field theory $\theta\simeq J^{bc}/2J$, giving $J^{bc}=6.4$ K, which is of the same magnitude as the value obtained by the fit. The value of χ_0 is of similar magnitude to the value of the perpendicular susceptibility of the $S=\frac{1}{2}$ square-lattice antiferromagnetic Heisenberg model. Using $\chi=(g\mu_B)^2/8J$, $J=1200$ K, we find the

molar value $\chi^{\rm mol}\sim 1.6\times 10^{-4}$ cm^3/mol. The difference may be due to core magnetization or other contributions.

We expect this simple mean-field theory to give us only a qualitative picture; its apparent quantitative success for the susceptibility could be attributed to the fact that we have let the parameters of the model be free to provide the best fit.

E. Staggered magnetization

The antiferromagnetic transition in La_2CuO_4 was first observed in a powder diffraction study by Vaknin *et al.* (1987) who found that the staggered moment at $T=0$ is about $0.5\pm 0.1\mu_B$. The existence of antiferromagnetic long-range order La_2CuO_4 was independently confirmed by muon-spin rotation experiments (Budnick *et al.*, 1987, Uemura *et al.*, 1987). The integrated intensity of the $3D$ antiferromagnetic Bragg peak in neutron-scattering experiments is proportional to the square of the order parameter [i.e., Eq.(3.19a)]. Its behavior differs from the $2D$ Ising-like critical behavior observed in classical antiferromagnets such as K_2NiF_4 (Birgeneau *et al.*, 1971). From the intensity of the Bragg peak, Yamada *et al.* (1987) and Endoh *et al.* (1988) find that the zero-temperature staggered magnetization is strongly dependent on the sample and is strongly correlated to the oxygen content of the sample. For the crystal with the highest $T_N\sim 300$ K, Yamada *et al.* find $m^\dagger\sim 0.6\mu_B$, which is close to the value found in Sec. III for the isotropic spin-$\frac{1}{2}$ antiferromagnetic Heisenberg model on the square lattice. For a crystal with $T_N\sim 200$ K, Endoh *et al.* find $m^\dagger\simeq 0.4\mu_B$. The latter crystal, however, may be slightly oxygen deficient, since T_N is somewhat low.

The mean-field expression (7.11) cannot accurately describe the temperature dependence of the staggered magnetization observed in neutron-scattering experiments (Shirane *et al.*, 1987; Yamada *et al.*, 1987; Endoh *et al.*, 1988) in a broad range of temperatures, as expected. The presence of the rapidly varying function $\chi_{2D}(T)$ forces $m_+^\dagger(T)$ to saturate to its $T=0$ value very quickly. Singh and co-workers (A. Singh *et al.*, 1990; A. Singh, 1990) start from the itinerant description (as in the approach of Schrieffer *et al.*, 1989) and consider corrections to the antiferromagnetic Hartree-Fock state due to the propagation of spin-wave excitations. When they include an interplanar coupling of the same order of magnitude as that discussed previously, they bind a good fit to the data for the temperature dependence of the staggered magnetization away from the critical region (A. Singh *et al.*, 1990).

VIII. CONCLUSIONS

We have attempted to describe the two-dimensional quantum fluctuations and the thermal spin fluctuations of the undoped antiferromagnetic insulator La_2CuO_4 in terms of the spin-$\frac{1}{2}$ quantum Heisenberg antiferromagnet. Despite its simplicity, this model lacks an exact solution in two space dimensions. Its derivation from models that are designed to capture the physics of highly correlated electronic systems, such as the Hubbard model, by taking the strong correlation limit, is only used as an argument for its relevance to the case of copper-oxygen based materials. We expect it to describe the magnetic properties of an isolated copper-oxygen plane on more general grounds.

Despite the low spin and low dimensionality of the model, a number of techniques of analytical, semianalytical, and numerical nature suggest that the ground state possesses antiferromagnetic long-range order. Quantum fluctuations, however, are significant and reduce the value of the staggered magnetization to $m^\dagger=0.62\pm 0.04\mu_B$, i.e., 62% of its classical value. We have analyzed a collection of the most accurate results from several authors and performed finite-size scaling analysis to obtain the value of $m^\dagger$ for the infinite-sized lattice using the scaling form (3.20); we find that the extrapolated values of $m^\dagger$ fall in the above range. The elementary excitations above the ground state are spin waves that are well defined at zero temperature. The various calculations give values for ground-state energy, spin-wave velocity, and perpendicular susceptibility close to those obtained with spin-wave theory. These results are summarized in Tables I–III. There are small differences between them, and it should be the goal of more accurate microscopic calculations to determine these more precisely.

At any nonzero temperature the $2D$ Heisenberg model is prohibited from developing long-range order. At low temperatures ($k_BT/J\ll 1$) the correlation length associated with antiferromagnetic order is large; we find that $\xi(T)=C_\xi e^{2\pi\rho_s/T}$ with $C_\xi\simeq 0.276a_H$ and $\rho_s\simeq 0.20J$ (where a_H is the lattice spacing). At such low temperatures spin-wave excitations with wavelengths short compared to this long correlation length are well defined excitations; their decay rate $\Gamma(k)$ (the width of their spectral-function peak) is very small compared to the energy of the excitation, specifically $\Gamma(k)/\omega(k)\to 0$ when $T\to 0$ and $k\xi(T)\gg 1$.

The only parameter of the model is the antiferromagnetic coupling J, which has been determined from neutron- and Raman-scattering experiments done on the undoped La_2CuO_4. The dispersion relation for spin-wave excitations has been measured by neutron-scattering experiments. Such measurements are consistent with the expectations from spin-wave theory. Using the calculated spin-wave velocity in terms of J, the antiferromagnetic coupling is estimated to be around 1540 ± 60 K. Two-magnon excitations have been observed by Raman-scattering experiments that confirm the two-dimensional nature of the magnetism in the material. The location of a broad high-frequency peak in the scattering intensity is close to the value of the energy of two Brillouin-zone boundary magnon excitations with nearly opposite momenta corrected for magnon-magnon interaction.

The correlation length as a function of T is extracted from neutron-scattering experiments. It is, however, very sensitive to departures from the exact stoichiometry of the La_2CuO_4 because it is limited by the average distance between holes or impurities in the crystal. The single crystals used to measure the correlation length are slightly oxygen deficient, having Néel temperatures $T_N = 195$ K and 245 K. Using the exponential form for $\xi(T)$ given above, one obtains the value for the antiferromagnetic coupling J needed to give a reasonable fit to the measured values of the correlation length, $J = 1350$ K and 1480 K for crystals with Néel temperatures 195 K and 245 K, respectively. We find that the crystal NTT-7, which is closer to the exact stoichiometry of the undoped material, gives a value of J very close to that found by measuring the spin-wave velocity or that determined from the moments of the Raman-scattering intensity.

The semiphenomenological theory of Tyc, Halperin, and Chakravarty (1989) for the dynamic structure factor is in satisfactory agreement with the measurements of Yamada *et al.* (1989). The basic ingredients of this theory are scaling, hydrodynamics, and the equivalence between the quantum nonlinear σ model and the spin-$\frac{1}{2}$ antiferromagnetic Heisenberg model.

The staggered magnetization at $T = 0$ is determined purely by the dynamics of the Cu-O plane. The values extracted from the intensity of the (100) Bragg peak in the neutron-scattering data depend strongly on exact oxygen stiochiometry, as expected due to the sensitivity of the Néel temperature to the Sr or Ba doping fraction x. The highest value reported for a $T_N \sim 300$ K crystal by Yamada *et al.* (1987) is about $0.6\mu_B$, in agreement with the value obtained from the spin-$\frac{1}{2}$ antiferromagnetic Heisenberg model.

Thermodynamic properties of the material, such as specific heat, magnetic susceptibility, and the staggered magnetization at low temperature close to the magnetic-ordering temperature, depend on the value of the $3D$ antiferromagnetic coupling J'. As has been suggested by the experiments of Thio *et al.* (1988) and Kastner *et al.* (1988), these properties also depend on the value of the planar coupling constant J^{bc} of an antisymmetric spin-spin interaction term, arising due to the rotation of the CuO_6 octahedra, which is responsible for the experimental fact that the antiferromagnetically aligned spins on the copper-oxygen plane cant away from the plane towards $\hat{b}$ axis by a small angle. Using a mean-field theory to treat the weakly coupled planes where the response of the planes enters through the "exact" $2D$ staggered susceptibility, one can obtain a qualitative agreement for the observed uniform susceptibility.

This review is an attempt to summarize the initial efforts to understand the spin-$\frac{1}{2}$ antiferromagnetic Heisenberg model on a square lattice and its connection to the physics behind the spin fluctuations in undoped La_2CuO_4. Due to the recent theoretical and experimental effort on the subject, we expect that the subject will be clarified further. For example, more accurate calculations and experiments are needed for the zero-temperature excitations of the model and their lifetime. To treat the weak interlayer antiferromagnetic coupling, we need to go beyond the simple mean-field theoretical treatment to cover a broader range of temperature. Furthermore, studies of hole hopping and pairing in quantum antiferromagnets is a subject of intense current theoretical interest. The instability of the antiferromagnetic state upon a small amount of doping has been suggested by several calculations and is expected from physical arguments. The nature of the new state emerging from the competition of hole-hopping and the antiferromagnetic order remains to be clarified.

When this work was completed, we became aware of a review article by S. Chakravarty (1990) on the "Magnetic Properties of La_2CuO_4." The reader is referred to it for more details about the work of Chakravarty, Halperin, and Nelson (1989) and work on the EPR signal in La_2CuO_4.

ACKNOWLEDGMENTS

I would like to thank A. Aharony, R. Birgeneau, K. Bitar, U. Heller, Z. Liu, D. Pines, R. Shankar, N. Shelton, T. Thio, and Y.-L. Wang for useful discussions and communications. This work is supported in part by the Supercomputer Computations Research Institute of the Florida State University, which partially funded by the U.S. Department of Energy under Contract No. DE-FC05-85ER-250000 and by the U.S. DARPA-sponsored Florida Initiative for Microelectronics and Materials, under Contract No. MDA972-88-J-1006.

APPENDIX: CALCULATION OF TRACES IN HANDSCOMB'S MONTE CARLO METHOD

The trace of any string of Q operators is zero unless the h operators in that string form closed loops. Therefore, for a bipartite lattice, $\Pi(C_r)$ is always non-negative. To give a nonzero trace, any string of operators must satisfy another condition explained below. We define the set of states $S_0 = \{\{\sigma_i\}, i = 1, 2, \ldots, N\}$, where the lattice sites have been ordered. In the following, we give an algorithm for calculating the trace of a particular string of operators, say $C_r = \{Q_{i_r} \ldots Q_{i_2} Q_{i_1}\}$, in this space.

We start from the set S_0 and we apply the operators contained in C_r, one by one and in the same order, to every state contained in the set S_0 to produce the sets $S_1, S_2, \ldots, S_r$, defined as follows. S_n, with $n \leq r$, is the set consisting of all the possible states produced by applying the sequence $C_n = Q_{i_n} \cdots Q_{i_2} Q_{i_1}$ on each state contained in the set S_0 and eliminating those states which are annihilated by the operators in the sequence. After all r operators have been applied, the trace of C_r is simply the number of states contained in the set S_r.

It is convenient to introduce the following vocabulary. A set of lattice sites connected by h or h^2 operators is

called a *cluster*. An isolated site not connected to any other site by h^2 or h is also a cluster (monomer). If C_r is the identity operator, there are N monomers and therefore 2^N possible states giving nonzero contributions to the trace. The presence of operators eliminates some of the states and produces a subset, say, S_r. For example, if C_r contains only one operator, say h_{12}^2, then there are $N-2$ monomers and a dimer, and therefore the set S_1, obtained after the application of h^2, contains states that are the direct products of the 2^{N-2} states of the monomers with the two possible states of the dimer. Hence the subset S_1 includes 2^{N-1} states, in this example. It is now clear that, at the nth step, we only need to keep a record of one representative state from S_n and the clusters. It is also clear that, with our definitions, if there is one state of a cluster giving a nonzero contribution to the trace, there will be one and only one additional state giving a nonzero contribution: the state obtained from the first by flipping all the spins in the cluster simultaneously. Knowing the clusters and the representative state, for each cluster we can construct the entire basis of S_n as the direct product of the two possible states (the one given and the other obtained by flipping all the spins of the cluster). Hence the spins in a given cluster are correlated, and all possible configurations of the lattice can be obtained as direct products of the states of each cluster.

As we have already discussed, the trace can be calculated after the application of the last (rth) operator, and it is given by the total number of states of the set S_r. In practice, we may start from the configuration where all the sites are monomers, selecting the fully ferromagnetic state (all spins up) as the initial representative state, and then apply the operators consecutively. When an h or h^2 operator is applied on the spins of two sites that belong to the same cluster, we obtain zero (nonzero) if the spins of the sites are the same (different). When one of these two operators is applied on two sites that belong to different clusters, we always obtain nonzero; in this case we merge the two clusters into one, and if the current spins on these sites are parallel we change all the spins in one of the clusters. Finally, we perform the operation prescribed by the specific kind of operator of the sequence. If the operator is h we exchange the spins; otherwise, if the operator is h^2, we do not perform any operation.

Having explained how the trace is calculated, we proceed to define a Markov chain that generates a distribution $\Pi(C_r)$ of sequences C_r. Imagine a random walk in the sampling space of sequences C_r; the current state of the random walk C_r is in one-to-one correspondence with S_r, and hence can be specified by the clusters and by giving one state of the two possible states of the cluster. At each step of the random walk we can add or remove any number n_a or n_d of operators, respectively. Let $n_t=n_a+n_d$, the total number of operators we add or delete. Being in the state C_r with r operators, we decide to add or delete an operator with probability f_r and $1-f_r$, respectively. We select a given operator to be added with probability $1/2N_b$ (N_b is the number of bonds) and the specific location in the string with probability $1/(r+1)$. We remove a given operator with probability $1/r$. The acceptance probability for a transition from the state C_r having r operators to the state $C'_{r'}$ having $r'=r+n_a-n_d$ operators, and satisfying the detailed balance, is given by

$$P(C_r\rightarrow C'_{r'})=\min\left[1,\frac{T(C'_{r'}\rightarrow C_r)}{T(C_r\rightarrow C'_{r'})}\frac{\Pi(C'_{r'})}{\Pi(C_r)}\right], \tag{A1}$$

where $T(C_r\rightarrow C'_{r'})$ is the probability of selecting the configuration $C'_{r'}$ starting from C_r. The probability P and the ratio of T's do not depend on the specific path connecting the states C_r and $C'_{r'}$. When $r'>r$, the ratio of T's is equal to

$$\frac{T(C_r\rightarrow C'_{r'})}{T(C'_{r'}\rightarrow C_r)}=\left[\frac{1}{2N_b}\right]^{r'-r}\left[\frac{f_r}{1-f_{r+1}}\right]\left[\frac{f_{r+1}}{1-f_{r+2}}\right]\cdots\left[\frac{f_{r'-1}}{1-f_{r'}}\right]. \tag{A2}$$

The function f_r in the simulation of Manousakis and Salvador is taken as $f_{r\neq 0}=\frac{1}{2}$ and $f_0=1$. For each value of n_t, the detailed balance is satisfied. If n_t is selected from the interval $[1,N_b]$, it guarantees that the Monte Carlo steps cover the entire sample space.

REFERENCES

Aeppli, G., S. M. Hayden, H. A. Mook, Z. Fisk, S.-W. Cheong, D. Rytz, J. P. Remeika, G. P. Espinosa, and A. S. Cooper, 1989, Phys. Rev. Lett. **62**, 2052.

Affleck, I., 1985, Phys. Rev. Lett. **54**, 966.

Affleck, I., 1986, Phys. Rev. Lett. **56**, 408.

Affleck, I., 1988, Phys. Rev. B **37**, 5186.

Affleck, I., T. Kennedy, E. H. Lieb, and H. Tasaki, 1988, Commun. Math. Phys. **115**, 447.

Affleck, I., and J. B. Marston, 1988, Phys. Rev. B **37**, 3774.

Affleck, I., Z. Zou, T. Hsu, and P. W. Anderson, 1988, Phys. Rev. B **38**, 745.

Aharony, A., R. J. Birgeneau, A. Coniglio, M. A. Kastner, and H. E. Stanley, 1988, Phys. Rev. Lett. **60**, 1330.

Amit, D. J. , 1984, *Field Theory, Renormalization Group and Critical Phenomena* (McGraw-Hill, New York).

Anderson, J. B., 1975, J. Chem. Phys. **63**, 1499.

Anderson, J. B., 1981, J. Chem. Phys. **74**, 6307.

Anderson, P. W., 1952, Phys. Rev. **86**, 694.

Anderson, P. W., 1959, Phys. Rev. **115**, 2.

Anderson, P. W., 1973, Mater. Res. Bull. **8**, 153.

Anderson, P. W., 1987, Science **235**, 1196.

Anderson, P. W., 1990, Phys. Rev. Lett. **63**, 1752.
Anderson, P. W., G. Baskaran, Z. Zou, and T. Hsu, 1987, Phys. Rev. Lett. **58**, 2790.
Arovas, D. P., and A. Auerbach, 1988, Phys. Rev. B **38**, 316.
Auerbach, A., and D. P. Arovas, 1988, Phys. Rev. Lett. **61**, 617.
Bardeen, J., L. Cooper, and J. R. Schrieffer, 1957, Phys. Rev. **108**, 1175.
Barnes, T., 1988, Phys. Rev. B **37**, 9405.
Barnes, T., and E. S. Swanson, 1988, Phys. Rev. B **37**, 9405.
Barnes, T., D. Kotchan, and E. S. Swanson, 1989, Phys. Rev. B **39**, 4357.
Bartkowski, R., 1972, Phys. Rev. B **5**, 4536.
Baskaran G., Z. Zou, and P. W. Anderson, 1987, Solid State Commun. **63**, 973.
Baym, G., 1969, *Lectures on Quantum Mechanics* (Benjamin/Cummings).
Bednorz, J. G., and K. A. Müller, 1986, Z. Phys. B **64**, 188.
Becher, T., and G. Reiter, 1989, Phys. Rev. Lett. **63**, 1004.
Becher, T., and G. Reiter, 1990, Phys. Rev. Lett. **64**, 109.
Becker, K. W., H. Won, and P. Fulde, 1989, Z. Phys. B **75**, 335.
Belavin, A. A., and A. M. Polyakov, 1975, JETP Lett. **22**, 245.
Berry, M. V., 1984, Proc. R. Soc. London, Ser. A **392**, 45.
Bethe, H. A., 1931, Z. Phys. **71**, 205.
Bijl, A., 1940, Physica **7**, 869.
Birgeneau, R. J., J. Skalyo, Jr., and G. Shirane, 1971, Phys. Rev. B **3**, 1736.
Birgeneau, R. J., D. R. Gabbe, H. P. Jenssen, M. A. Kastner, P. J. Picone, T. R. Thurston, G. Shirane, Y. Endoh, M. Sato, K. Yamada, Y. Hidaka, M. Oda, Y. Enomoto, M. Suzuki, and T. Murakami, 1988, Phys. Rev. B **38**, 6614.
Bitar, K., and E. Manousakis, 1991, Phys. Rev. B **43**, 2615.
Brézin, E., 1982, J. Phys. (Paris) **43**, 15.
Brézin, E., and J. Zinn-Justin, 1976a, Phys. Rev. Lett. **36**, 691.
Brézin, E., and J. Zinn-Justin, 1976b, Phys. Rev. B **14**, 3110.
Brézin, E., J. C. Le Guillou, J. Zinn-Justin, and B. G. Nickel, 1973, Phys. Lett. A **44**, 227.
Brinkman, W. F., and T. M. Rice, 1970, Phys. Rev. B **2**, 1324.
Budnick, J. I., A. Golnik, C. Niedermayer, E. Recknagel, M. Rossmanith, A. Weidinger, B. Chamberland, M. Filipkowski, and D. P. Yang, 1987, Phys. Lett. A **124**, 103.
Carlson, J., 1989, Phys. Rev. B **40**, 846.
Ceperley, D. M., and B. J. Adler, 1980, Phys. Rev. Lett. **45**, 566.
Ceperley, D. M., and B. J. Adler, 1981, Physica B+C (Amsterdam) **107**, 875.
Chakravarty, S., 1990, in *High-Temperature Superconductivity,* edited by K. S. Bedell, D. Coffey, D. E. Meltzer, D. Pines, and J. R. Schrieffer (Addison-Wesley, Reading, MA), p. 136.
Chakravarty, S., B. I. Halperin, and D. Nelson, 1988, Phys. Rev. Lett. **60**, 1057.
Chakravarty, S., B. I. Halperin, and D. Nelson, 1989, Phys. Rev. B **39**, 2344.
Chandra, P., and B. Doucot, 1988, Phys. Rev. B **38**, 9335.
Chen, C.-X., and H.-B. Schüttler, 1989, Phys. Rev. B **40**, 239.
Chester, G. V., and L. Reatto, 1966, Phys. Lett. **22**, 276.
Chin, S. A., J. W. Negele, and S. E. Koonin, 1984, Ann. Phys. **157**, 140.
Chin, S. A., C. Long, and D. Robson, 1988, Phys. Rev. D **37**, 3001.
Chu, C. W., P. H. Hor, R. L. Meng, L. Gao, Z. J. Huang, and Y. Q. Wang, 1987, Phys. Rev. Lett. **58**, 405.
Coffey D., K. S. Bedell, and S. A. Trugman, 1990, Phys. Rev. B **42**, 6509.
Coleman, S., and E. Weinberg, 1973, Phys. Rev. D **7**, 1888.
Collins, M. F., 1970, Phys. Rev. B **2**, 4552.
Creutz, M., 1983, *Quarks, Gluons and Lattices* (Cambridge University Press, Cambridge, New York).
Dagotto, E., and A. Moreo, 1988, Phys. Rev. B **38**, 5087.
Dagotto, E., and A. Moreo, 1989a, Phys. Rev. B **39**, 4744.
Dagotto, E., and A. Moreo, 1989b, Phys. Rev. Lett. **63**, 2148.
Dagotto, E., A. Moreo, R. Joint, S. Bacci, and E. Gagliano, 1990, Phys. Rev. B **41**, 9049.
Dagotto, E., and D. Poilblanc, 1990, Phys. Rev. B **42**, 7940.
Dalton, N. W., and D. W. Wood, 1967, Proc. Phys. Soc., London **90**, 459.
Dashen, R. F., S.-K. Ma, and R. Rajaraman, 1975, Phys. Rev. D **11**, 1499.
Davis, H. L., 1960, Phys. Rev. **120**, 789.
de Jongh, L. J., and A. R. Miedema, 1974, Adv. Phys. **23**, 1.
de Raedt, H., and A. Lagendijk, 1985, Phys. Rep. **127**, 223.
Ding, H.-Q., and M. Makivic, 1990, Phys. Rev. Lett. **64**, 1449.
Ding, H.-Q. and M. Makivic, 1991, Phys. Rev. B **43**, 3662.
Domb, C., and M. S. Green, 1974, in *Phase Transitions and Critical Phenomena,* Vol. III (Academic, New York).
Dombre, T., and N. Read, 1988, Phys. Rev. B **38**, 7181.
Doniach, S., M. Inui, V. Kalmeyer, and G. Gabay, 1988, Europhys. Lett. **6**, 663.
Dyson, F., 1956a, Phys. Rev. **102**, 1217.
Dyson, F., 1956b, Phys. Rev. **102**, 1230.
Dyson, F., E. H. Lieb, and B. Simon, 1978, J. Stat. Phys. **18**, 335.
Dzyaloshinskii, I. E., 1958, J. Phys. Chem. Solids **4**, 241.
Dzyaloshinskii, I. E., A. M. Polyakov, and P. B. Wiegmann, 1988, Phys. Lett. A **127**, 112.
Endoh, Y., K. Yamada, R. J. Birgeneau, D. R. Gabbe, H. P. Jenssen, M. A. Kastner, C. J. Peters, P. J. Picone, T. R. Thurston, J. M. Tranquada, G. Shirane, Y. Hidaka, M. Oda, Y. Enomoto, M. Suzuki, and T. Murakami, 1988, Phys. Rev. B **37**, 7443.
Feenberg, E., 1969, *Theory of Quantum Fluids* (Academic, New York/London).
Ferer, M., and A. Hamid-Aidinejad, 1986, Phys. Rev. B **34**, 6481.
Feynman, R. P., 1954, Phys. Rev. **94**, 262.
Feynman, R. P., and M. Cohen, 1956, Phys. Rev. **102**, 1189.
Fox, G., R. Gupta, O. Martin, and S. Otto, 1982, Nucl. Phys. B **205** [FS], 188.
Fradkin, E., and M. Stone, 1988, Phys. Rev. B **38**, 7215.
Fukuda, K., M. Sato, S. Shamoto, M. Onoda, and S. Hosoya, 1987, Solid State Commun. **63**, 811.
Gagliano, E., and S. Bacci, 1990, Phys. Rev. B **42**, 8772.
Gelfand, M. P., R. R. P. Singh, and D. A. Huse, 1989, Phys. Rev. B **40**, 10801.
Gomez-Santos, G., J. D. Joannopoulos, and J. W. Negele, 1989, Phys. Rev. B **39**, 4435.
Grempel, D. R., 1988, Phys. Rev. Lett. **61**, 1041.
Gros, C., 1988, Phys. Rev. B **38**, 931.
Gros, C., R. Joynt, and T. M. Rice, 1987, Z. Phys. B **68**, 428.
Gross, M., E. Sánchez-Velasco, and E. Siggia, 1989a, Phys. Rev. B **39**, 2484.
Gross, M., E. Sánchez-Velasco, and E. Siggia, 1989b, Phys. Rev. B **40**, 11328.
Gutzwiller, M. C., 1963, Phys. Rev. Lett. **10**, 159.
Gutzwiller, M. C., 1964, Phys. Rev. **134**, 923A.
Haldane, F. D. M., 1983a, Phys. Lett. A **93**, 464.
Haldane, F. D. M., 1983b, Phys. Rev. Lett. **50**, 1153.
Haldane, F. D. M., 1988 Phys. Rev. Lett. **61**, 1029.
Halperin, B. I., and P. C. Hohenberg, 1969, Phys. Rev. **188**,

898.
Hammel, P. C., M. Takigawa, R. H. Heffner, Z. Fisk, and K. C. Ott, 1989, Phys. Rev. Lett. **63**, 1992.
Handscomb, D. C., 1962, Proc. Camb. Philos. Soc. **58**, 594.
Handscomb, D. C., 1964, Proc. Camb. Philos. Soc. **60**, 115.
Harris, A. B., and R. V. Lange, 1967, Phys. Rev. **157**, 279. See also Hirsch, 1985 and for a simple derivation see Huang and Manousakis, 1987.
Hayes, W., and R. Loudon, 1978, *Scattering of Light by Crystals* (Wiley, New York).
Hertz, J. A., 1976, Phys. Rev. B **14**, 1165.
Heys, D. W., and D. R. Stump, 1983, Phys. Rev. D **28**, 2067.
Hikami, S., and E. Brézin, 1978, Math. Gen. **11**, 1141.
Hirsch, J. E., 1985, Phys. Rev. Lett. **54**, 1317.
Hirsch, J. E., D. J. Scalapino, R. L. Sugar, and R. Blankenbecler, 1981, Phys. Rev. Lett. **47**, 1628.
Hirsch, J. E., R. L. Sugar, D. J. Scalapino, and R. Blankenbecler, 1982, Phys. Rev. B **26**, 5033.
Hirsch, J. E., and S. Tang, 1989a, Phys. Rev. B **39**, 2887.
Hirsch, J. E., and S. Tang, 1989b, Phys. Rev. B **40**, 4769.
Hirsch, J. E., and S. Tang, 1989c, Phys. Rev. B **39**, 2850.
Hohenberg, P. C., and W. F. Brinkman, 1974, Phys. Rev. B **10**, 128.
Holstein, T., and H. Primakoff, 1940, Phys. Rev. **58**, 1098.
Horsch, P., and W. von der Linden, 1988, Z. Phys. B **72**, 181.
Huang, K., and E. Manousakis, 1987, Phys. Rev. B **36**, 8302.
Huber, D. L., and W. L. Chin, 1990, J. Appl. Phys. **67**, 5743.
Hulthén, E., 1938, Ark. Mat. Astron. Fys. **26A**, No. 1.
Huse, D., 1988, Phys. Rev. B **37**, 2380.
Huse, D. A., and V. Elser, 1988, Phys. Rev. Lett. **60**, 2531.
Ioffe, L. B., and A. I. Larkin, 1988, Int. J. Mod. Phys. B **2**, 203.
Inui, M., S. Doniach, and M. Gabay, 1988, Phys. Rev. B **38**, 6631.
Jastrow, R., 1955, Phys. Rev. **98**, 1479.
Kalos, M. H., 1962, Phys. Rev. **128**, 1791.
Kalos, M. H., 1966, J. Comput. Phys. **1**, 257.
Kalos, M. H., 1970, Phys. Rev. A **2**, 250.
Kalos, M. H., M. A. Lee, P. A. Whitlock, and G. V. Chester, 1981, Phys. Rev. B **24**, 115.
Kalos, M. H., D. Levesque, and L. Verlet, 1974 Phys. Rev. A **9**, 2178.
Kane, C. L., P. A. Lee, and N. Read, 1989, Phys. Rev. B **39**, 1989.
Kaplan, T. A., 1990, Phys. Rev. Lett. **63**, 1751.
Kaplan, T. A., P. Horsch, and W. von der Linden, 1989, J. Phys. Soc. Jpn. **58**, 3894.
Kastelijn, P. W., 1952, Physica **18**, 104.
Kastner, M. A., *et al.*, 1988, Phys. Rev. B **38**, 6636.
Kaxiras, E., and E. Manousakis, 1988a, Phys. Rev. B **37**, 656.
Kaxiras, E., and E. Manousakis, 1988b, Phys. Rev. B **38**, 866.
Kennedy, T., E. H. Lieb, and B. S. Shastry, 1988, J. Stat. Phys. **53**, 1019.
Kikuchi, M., and Y. Okabe 1989, J. Phys. Soc. Jpn. **58**, 679.
Kishi, T., and K. Kubo, 1989, J. Phys. Soc. Jpn. **58**, 2547.
Kogut, J., 1983, Rev. Mod. Phys. **55**, 775.
Koonin, S. E., 1981, in *Nuclear Theory 1981,* edited by G. F. Bertsch (World Scientific, Singapore), p. 184.
Kopietz, P., 1990a, Phys. Rev. B **41**, 9228.
Kopietz, P., 1990b, Phys. Rev. Lett. **64**, 2587.
Koterlitz, J., 1974, J. Phys. C **7**, 1046.
Kosterlitz, J., and D. Thouless, 1973, J. Phys. C **6**, 1181.
Kotliar, G., 1988, Phys. Rev. B **37**, 3664.
Kubo, K., 1988, Phys. Rev. Lett. **61**, 110.
Kubo, K., and T. Kishi, 1988, Phys. Rev. Lett. **61**, 2585.
Kubo, R., 1952, Phys. Rev. **87**, 568.
Le Guillou, J. C., and J. Zinn-Justin, 1980, Phys. Rev. B **21**, 3976.
Lee, D. H., J. D. Joannopoulos, and J. W. Negele, 1984, Phys. Rev. B **30**, 1599.
Lee, Kong-Ju-Bock, and P. Schlottmann, 1990, Phys. Rev. B **42**, 4426.
Liang, S., B. Doucot, and P. W. Anderson, 1988, Phys. Rev. Lett. **61**, 365.
Liang, S., 1990, Phys. Rev. B **42**, 6555.
Lieb, E. H., and D. C. Mattis, 1962, J. Math. Phys. **3**, 749.
Lines, M. E., 1970, J. Phys. Chem. Solids **31**, 101.
Liu, Z., and E. Manousakis, 1989, Phys. Rev. B **40**, 11437.
Liu, Z., and E. Manousakis, 1990, Florida State University Preprint, FSU-SCRI-91-06.
Loh, E., Jr., D. J. Scalapino, and D. M. Grant, 1985, Phys. Rev. B **31**, 4712.
Lovesey, S. W., 1984, *Theory of Neutron Scattering from Condensed Matter* (Clarendon, Oxford).
Lyklema, J. W., 1982, Phys. Rev. Lett. **49**, 88.
Lyons, K. B., P. A. Fleury, J. P. Remeika, A. S. Cooper, and T. J. Nergan, 1988, Phys. Rev. B **37**, 2353.
Lyons, K. B., P. E. Sulewski, P. A. Fleury, H. L. Carter, A. S. Cooper, G. P. Espinosa, Z. Fisk, and S.-W. Cheong, 1989, Phys. Rev. B **38**, 9693.
Ma, S. K., 1973, Phys. Rev. A **7**, 2172.
Maeda, H., Y. Tanaka, M. Fukutomi, and T. Asano, 1988, Jpn. J. Appl. Phys. **27**, 574.
Maleev, S. V., 1957, Zh. Eksp. Teor. Fiz. **30**, 1010.
Manousakis, E., 1989, Phys. Rev. B **40**, 4904.
Manousakis, E., and V. R. Pandharipande, 1984, Phys. Rev. B **30**, 5062.
Manousakis, E., V. R. Pandharipande, and Q. N. Usmani, 1985, Phys. Rev. B **31**, 7022.
Manousakis, E., and R. Salvador, 1988, Phys. Rev. Lett. **60**, 840.
Manousakis, E., and R. Salvador, 1989a, Phys. Rev. B **39**, 575.
Manousakis, E., and R. Salvador, 1989b, Phys. Rev. Lett. **61**, 1310.
Manousakis, E., and R. Salvador, 1989c, Phys. Rev. B **40**, 2205.
Marcu, M., 1987, in *Quantum Monte Carlo Methods in Equilibrium and Nonequilibrium Systems,* edited by M. Suzuki (Springer, Berlin), p. 64.
Marshall, W., 1955, Proc. R. Soc. London, Ser. A **232**, 48.
Marshall, W., and S. W. Lovesey, 1971, *Theory of Thermal Neutron Scattering* (Clarendon, Oxford).
Marston, B. J., and I. Affleck, 1989, Phys. Rev. B **39**, 11538.
Matsubara, T., and H. Matsuda, 1956, Prog. Theor. Phys. **16**, 569.
Mattis, D., 1982, *The Theory of Magnetism* (Harper and Row, New York).
Mermin, N. D., and H. Wagner, 1966, Phys. Rev. Lett. **22**, 1133.
Metropolis, N., and S. A. Ulam, 1949, J. Am. Stat. Assoc. **44**, 247.
Mila, F., and T. M. Rice, 1989, Physica C **157**, 561.
Millis, A. J., H. Monien, and D. Pines, 1990, Phys. Rev. B **42**, 167.
Miyashita, S., 1988, J. Phys. Soc. Jpn. **57**, 1934.
Miyashita, S., 1990, in *Quantum Simulations of Condensed Matter Phenomena,* edited by J. D. Doll and J. E. Gubernatis (World Scientific, Singapore), p. 228.
Monien, H., P. Monthoux, and D. Pines, 1991a, Phys. Rev. B **43**, 275.

Monien, H., D. Pines, and C. P. Slichter, 1990, Phys. Rev. B **41**, 11120.
Monien, H., D. Pines, and M. Takigawa, 1991b, Phys. Rev. B **43**, 258.
Moriya, T., 1960, Phys. Rev. **120**, 91.
Moskowitz, J. W., K. E. Schmidt, M. E. Lee, and M. H. Kalos, 1982, J. Chem. Phys. **77**, 349.
Negele, J. W., 1982, in *Time-Dependent Hartree-Fock and Beyond,* edited by K. Goeke and P. G. Reinhardt, Lecture Notes in Physics No. 171 (Springer, Berlin/New York), p. 198.
Nelson, D. R., and R. A. Pelcovits, 1977, Phys. Rev. B **16**, 2191.
Neuberger, H., and T. Ziman, 1989, Phys. Rev. B **39**, 2608.
Neves, E. J., and J. F. Perez, 1986, Phys. Lett. A **114A**, 331.
Nishimori, H., and S. Miyake, 1985, Prog. Theor. Phys. **73**, 18.
Nishimori, H., K. Kubo, Y. Ozeki, Y. Tomika, and T. Kishi, 1989, unpublished.
Nori, F., E. Abrahams, and G. Zimanyi, 1990, Phys. Rev. B **41**, 7277.
Nori, F., E. Gagliano, and S. Bacci, 1990, preprint.
Oguchi, T., 1960, Phys. Rev. **117**, 117.
Oitmaa, J., and D. D. Betts, 1978, Can. J. Phys. **56**, 897.
Okabe, Y., and M. Kikuchi, 1988, J. Phys. Soc. Jpn. **57**, 4351.
Okabe, Y. and M. Kikuchi, 1990, in *Quantum Simulations of Condensed Matter Phenomena,* edited by J. D. Doll and J. E. Gubernatis (World Scientific, Singapore), p. 270.
Okabe, Y., and M. Kikuchi, and A. D. S. Nagi, 1988, Phys. Rev. Lett. **61**, 2971.
Okabe, Y., and M. Oku, 1978, Prog. Theor. Phys. **60**, 1277; **60**, 1287.
Orbach, R. L., 1958, Phys. Rev. **112**, 309.
Pandharipande, V. R., S. C. Pieper, and R. B. Wiringa, 1986, Phys. Rev. B **34**, 4571.
Pandharipande, V. R., J. G. Zabolitzky, S. C. Pieper, R. B. Wiringa, and U. Helmbrecht, 1983, Phys. Rev. Lett. **50**, 1676.
Parrinello, M., and T. Arai, 1974, Phys. Rev. B **10**, 265.
Parisi, G., 1980, Phys. Lett. B **92**, 133.
Parisi, G., 1982, Nucl. Phys. B **205** [FS], 337.
Parkinson, J. B., 1969, J. Phys. C **2**, 2012.
Peters, C. J., R. J. Birgeneau, M. A. Kastner, H. Yoshizawa, Y. Endoh, J. Tranquada, G. Shirane, Y. Hidaka, M. Oda, M. Suzuki,and T. Murakami, 1988, Phys. Rev. B **37**, 9761.
Pikalev, E. M., M. A. Savcenko, and J. Solyom, 1968, Soviet Phys. JETP **28**, 734.
Pines, D., 1990, Physica B **163**, 78.
Pines, D., and P. Nozières, 1966, *The Theory of Quantum Liquids* (Benjamin, New York).
Pitaevskii, L. P., 1959, Sov. Phys. JETP **9**, 1.
Pitaevskii, L. P., 1961, Sov. Phys. JETP **12**, 155.
Polyakov, A. M., 1975, Phys. Lett. B **59**, 79.
Polyakov, A. M., 1988, Mod. Phys. Lett. A **3**, 325.
Reynolds, P. J., D. M. Ceperley, B. J. Adler, and W. A. Lester, 1982, J. Chem. Phys. **77**, 5593.
Read, N., and S. Sachdev, 1989, Phys. Rev. Lett. **62**, 1694.
Reger, J. D., and A. P. Young, 1988, Phys. Rev. B **37**, 5978.
Riera, J. A., and A. P. Young, 1989, Phys. Rev. B **39**, 9697.
Rodriguez, J. P., 1990, Phys. Rev. B **41**, 7326.
Rosenstein, B., B. J. Warr, and S. H. Park, 1990, Nucl. Phys. B **336**. 435.
Ruckenstein, A. E., P. J. Hirschfeld, and J. Appel, 1987, Phys. Rev. B **36**, 857.
Runge, K. J., and R. J. Runge, 1990, in *Quantum Simulations of Condensed Matter Phenomena,* edited by J. D. Doll and J. E. Gubernatis (World Scientific, Singapore), p. 300. The points corresponding to lattices 10×10 and 12 were obtained from private communication.
Rushbrooke, G. S., and P. J. Wood, 1958, Mol. Phys. **1**, 257.
Sato, M., S. Shamoto, J. M. Tranquada, G. Shirane, and B. Keimer, 1988, Phys. Rev. Lett. **61**, 1317.
Scalettar, R. T., D. J. Scalapino, and R. J. Sugar, 1985, Phys. Rev. B **31**, 7316.
Schmidt, K. E., and M. H. Kalos , 1984, in *Applications of the Monte Carlo Method in Statistical Physics,* second ed., edited by K. Binder (Springer, Berlin), p. 125.
Schmitt-Rink, S., C. M. Varma, and A. E. Ruckenstein, 1988, Phys. Rev. Lett. **60**, 2793.
Schrieffer, J. R., X. G. Wen, and S. C. Zhang, 1989, Phys. Rev. B **39**, 11663.
Schwinger, J., 1952, Atomic Energy Commission Report No. NYO-3071. See Mattis, 1982.
Shankar, R., 1989a, private communication.
Shankar, R., 1989b, Phys. Rev. Lett. **63**, 203.
Shankar, R., and G. Murthy, 1989, Phys. Lett. A **137**, 165.
Shastry, B. S., 1989, Phys. Rev. Lett. **63**, 1288.
Sheng, Z. Z., and A. M. Hermann, 1988, Nature (London) **332**, 138.
Shenker, S. H., and J. Tobochnik, 1980, Phys. Rev. B **22**, 4462.
Shirane, G., Y. Endoh, R. J. Birgeneau, M. A. Kastner, Y. Hidaka, M. Oda, M. Suzuki, and T. Murakami, 1987, Phys. Rev. Lett. **59**, 1613.
Shraiman, B., and E. Siggia, 1988, Phys. Rev. Lett. **60**, 740.
Singh, A., 1990, Phys. Rev. B **40**, 7247.
Singh, A., Z. Tesanovic, H. Tang, G. Xiao, C. L. Chien, and J. C. Walker, 1990, Phys. Rev. Lett. **64**, 2571.
Singh, R. R. P., 1989, Phys. Rev. B **39**, 9760.
Singh, R. R. P., P. A. Fleury, K. B. Lyons, and P. E. Sulewski, 1989, Phys. Rev. Lett. **62**, 2736.
Singh, R. R. P., and D. A. Huse, 1989, Phys. Rev. B **40**, 7247.
Slight, A. W., M. A. Subramanian, and C. C. Torardi, 1989, MRS Bulletin XIV, 45.
Solyom, J., 1968, Sov. Phys. JETP **28**, 1251.
Stinchcombe, R. B., 1971, J. Phys. C **4**, L79.
Sugai, S., S. Shamoto, and M. Sato, 1988, Phys. Rev. B **38**, 6436.
Suzuki, M., 1976, Commun. Math. Phys. **51**, 183.
Suzuki, M., 1986, J. Stat. Phys. **43**, 883.
Suzuki, M., and S. Miyashita, 1978, Can. J. Phys. **56**, 902.
Takahashi, M., 1987, Phys. Rev. Lett. **58**, 168.
Takahashi, M., 1989, Phys. Rev. B **40**, 2494.
Takahashi, M., 1990, Phys. Rev. B **42**, 766.
Taketa, H., and T. Nakamura, 1956, J. Phys. Soc. Jpn. **11**, 919.
Tang, S., and J. E. Hirsch, 1989, Phys. Rev. B **39**, 4548.
Tang, S., M. E. Lazzouni, and J. E. Hirsch, 1989, Phys. Rev. B **40**, 500.
Tang, S., and H. Q. Lin, 1988, Phys. Rev. B **38**, 6863.
Thio, T., T. R. Thurston, N. W. Preyer, M. A. Kastner, H. P. Jenssen, D. R. Gabbe, C. Y. Chen, R. J. Birgeneau, and A. Aharony, 1988, Phys. Rev. B **38**, 905.
Tranquada, J. M., D. E. Cox, W. Kunnmann, H. Moudden, G. Shirane, M. Suenaga, P. Zolliker, D. Vaknin, S. K. Sinha, M. S. Alvarez, A. J. Jacobson, and D. C. Johnston, 1988, Phys. Rev. Lett. **60**, 156.
Trivedi, N., and D. M. Ceperley, 1989, Phys. Rev. B **40**, 2747.
Trotter, H. F., 1959, Proc. Am. Math. Soc. **10**, 545.
Tyč, S., and B. I. Halperin, 1990, Phys. Rev. B **42**, 2096.
Tyč, S., B. I. Halperin, and S. Chakravarty, 1989, Phys. Rev. Lett. **62**, 835.
Uemura, Y. J., W. J. Kossler, X. H. Yu, J. R. Kempton, H. E. Schone, D. Opie, C. E. Stronach, D. C. Johnston, M. S. Alverez, and D. P. Goshorn, 1987, Phys. Rev. Lett. **59**, 1045.

Vaknin, D., S. K. Sinha, D. E. Moncton, D. C. Johnston, J. M. Newsam, C. R. Safinya, and H. E. King, Jr., 1987, Phys. Rev. Lett. **58**, 2802.
Walstedt, W., W. Warren, R. F. Bell, G. F. Brennert, G. P. Espinosa, R. J. Cava, L. F. Schneemeyer, and J. V. Waszcak, 1988, Phys. Rev. B **38**, 9299.
Wang, Y. L., S. Shtrikman, and H. Callen, 1966, Phys. Rev. **148**, 419.
Wen, X. G., and A. Zee, 1988, Phys. Rev. Lett. **61**, 1025.
Whitlock, P. A., M. H. Kalos, G. V. Chester, and D. M. Ceperley, 1979, Phys. Rev. B **19**, 5598.
Wiegmann, P. B., 1988, Phys. Rev. Lett. **60**, 821.
Wilson, K. G., and J. Kogut, 1975, Phys. Rep. C **12**, 77.
Yamada, K., K. Kakurai, Y. Endoh, T. R. Thurston, M. A. Kastner, R. J. Birgeneau, G. Shirane, Y. Hidaka, and T. Murakami, 1989, Phys. Rev. B **40**, 4557.
Yamada, K., E. Kudo, Y. Endoh, Y. Hidaka, M. Oda, M. Suzuki, and T. Murakami, 1987, Solid State Commun. **64**, 753.
Yamaji, K., and J. Kondo, 1973, Phys. Lett. A **45**, 317.
Yokoyama, H., and H. Shiba, 1987, J. Phys. Soc. Jpn. **56**, 3570.
Zabolitzky, J. G., and M. H. Kalos, 1981, Nucl. Phys. A **356**, 114.
Zhang, F. C., and T. M. Rice, 1988, Phys. Rev. B **37**, 3759.
Zivkovic, T. P., B. L. Sandleback, T. G. Schmalz, and D. J. Klein, 1990, Phys. Rev. B **41**, 2249.